Chapter 4

Future Climate Change: Modeling and Scenarios for the Arctic

Lead Authors
Vladimir M. Kattsov, Erland Källén

Contributing Authors
Howard Cattle, Jens Christensen, Helge Drange, Inger Hanssen-Bauer, Tómas Jóhannesen, Igor Karol, Jouni Räisänen, Gunilla Svensson, Stanislav Vavulin

Consulting Authors
Deliang Chen, Igor Polyakov, Annette Rinke

Contents

Summary

Increased atmospheric concentrations of greenhouse gases (GHGs) are very likely to have a larger effect on climate in the Arctic than anywhere else on the globe. Physically based, global coupled atmosphere-land-ocean climate models are used to project possible future climate change. Given a change in GHG concentrations, the resulting changes in temperature, precipitation, seasonality, etc. can be projected. Future emissions of GHGs and aerosols can be estimated by making assumptions about future demographic, socioeconomic, and technological changes. The Intergovernmental Panel on Climate Change (IPCC) prepared a set of emissions scenarios for use in projecting future climate change. This assessment uses the A2 and B2 scenarios, which are in the middle of the range of scenarios provided by the IPCC. Projections from the IPCC climate models indicate a global mean temperature increase of 1.4 °C by the mid-21st century compared to the present climate for both the A2 and B2 scenarios (IPCC, 2001). Toward the end of the century, the global mean temperature increase is projected to be 3.5 °C and 2.5 °C for the two scenarios, respectively.

Over the Arctic, the ACIA-designated models project a larger mean temperature increase: for the region north of 60° N, both scenarios result in a 2.5 °C increase by the mid-21st century. By the end of the 21st century, arctic temperature increases are projected to be 7 °C and 5 °C for the A2 and B2 scenarios, respectively, compared to the present climate. By then, in the B2 scenario, the models project temperature increases of around 3 °C for Scandinavia and East Greenland, about 2 °C for Iceland, and up to 5 °C for the Canadian Archipelago and Russian Arctic. The five-model mean warming over the central Arctic Ocean is greatest in autumn and winter (up to 9 °C by the late 21st century in the B2 scenario), as the air temperature reacts strongly to reduced ice cover and thickness. Average autumn and winter temperatures are projected to rise by 3 to 5 °C over most arctic land areas by the end of the 21st century. By contrast, summer temperature increases over the Arctic Ocean are projected to remain below 1 °C throughout the 21st century. The contrast between greater projected warming in autumn and winter and lesser warming in summer also extends to the surrounding land areas but is less pronounced there. In summer, the projected warming over northern Eurasia and northern North America is greater than that over the Arctic Ocean, while in winter the reverse is projected. All of the models suggest substantially smaller temperature increases over the northern North Atlantic sector than in the other parts of the Arctic.

By the late 21st century, projected precipitation increases in the Arctic range from about 5 to 10% in the Atlantic sector to as much as 35% in certain high Arctic locations (for the B2 scenario). As for temperature, the projected increase in precipitation is generally greatest in autumn and winter and smallest in summer.

A slight decrease in pressure in the polar region is projected for throughout the year. While impact studies would benefit from projections of wind characteristics and storm tracks in the Arctic, available analyses in the literature are insufficient to justify firm conclusions about possible changes in the 21st century.

The models also project a substantial decrease in snow and sea-ice cover over most of the Arctic by the end of the 21st century.

The projected increase in arctic temperatures is accompanied by large between-model differences and considerable interdecadal variability. Dividing the average projected temperature change by the magnitude of projected variability suggests that, despite the large warming projected for the Arctic, the signal-to-noise ratio is actually lower in the Arctic than in many other areas.

The Arctic is a region characterized by complex and insufficiently understood climate processes and feedbacks, contributing to the challenge that the Arctic poses from the view of climate modeling. Several weaknesses of the models related to descriptions of high-latitude surface processes have been identified, and these are among the most serious shortcomings of present-day arctic climate modeling.

Local and regional climate features, such as enhanced precipitation close to steep mountains, are not well represented in global climate models due to the limited horizontal resolution of the models. To describe local climate, physical modeling or statistically based empirical links between the large-scale flow and local climate can be used. Despite rapid developments in arctic regional climate modeling, the current status of developments in this field did not allow regional models to be used as principal tools for the ACIA. Therefore, the ACIA used projections from coupled global models, either directly or in combination with statistical downscaling techniques.

A model simulation provides one possible climate scenario. This is not a prediction of future climate change, but a projection based on a prescribed change in the concentration of atmospheric GHGs. A climate shift can be caused by natural variability as well as by changes in GHG concentrations. Natural variability in the Arctic is large and could mask or amplify a change resulting from increased atmospheric GHG concentrations. To assess the relative importance of natural variability versus a prescribed climate forcing, an ensemble of differently formulated climate models should be used. For this assessment, five different models are used to give an indication of simulation uncertainty versus forced changes, although greater numbers of simulations would provide a better estimate of climate change probability distributions, and perhaps allow the estimation of changes in the frequency of winter storms, and temperature and precipitation extremes, etc.

While the level of uncertainty in climate simulations can probably be reduced with improved model formulations,

it will never be certain that all physical processes relevant to climate change have been included in a model simulation. There can still be surprises in the understanding of climate change. The projections presented here are based on the best knowledge available today about climate change; as climate-change science progresses there will always be new results that may change the understanding of how the arctic climate system works.

4.1. Introduction

To assess climate change impacts on societies, ecosystems, and infrastructure, possible changes in physical climate parameters must first be projected. The physical climate change projections must in turn be calculated from changes in external factors that can affect the physical climate. Examples of such factors include atmospheric composition, particularly atmospheric concentrations of GHGs and aerosols, and land-surface changes (e.g., deforestation). This chapter describes the options available to make such projections and their application to the Arctic. The main emphasis is on physically based models of the climate system and the relationship between global climate change and regional effects in the Arctic.

Physically based climate models are used to obtain climate scenarios – plausible representations of future climate that are consistent with assumptions about future emissions of GHGs and other pollutants (i.e., emissions scenarios) and with present understanding of the effects of increased atmospheric concentrations of these components on the climate (IPCC-TGCIA, 1999). Correspondingly, by using a climate change scenario, the difference between the projected future climate and the current climate is described. Being dependent on sets of prior assumptions about future human activities, demographic and technological change, and their impact on atmospheric composition, climate change scenarios are not predictions, but rather plausible, internally consistent descriptions of possible future climates.

In addition to physical climate modeling, there are alternative methods for providing climate scenarios for use in impact assessments. These include synthetic scenarios (also referred to as arbitrary or incremental scenarios) and analogue scenarios. None of the alternatives provide a physically consistent climate change scenario including both atmospheric composition changes and physically coupled changes in temperature, precipitation, and other climate variables. Nevertheless, due to their relative simplicity they can be useful and adequate for some types of impact studies. There are also climate scenarios that do not fall into any of these categories, which primarily employ extrapolation of either ongoing trends in climate, or future regional climate, on the basis of projected global or hemispheric mean climate change. A separate group of scenarios is based on expert judgments. All of the methods have their limitations, but each has some particular advantages (see Mearns et al., 2001; Carter et al., 2001).

Synthetic scenarios are based on incremental changes in climatic variables, particularly air temperature (e.g., +1, +2, +3 ºC) and precipitation (e.g., +5, +10, +15%). Such scenarios often assume a uniform annual change in the variables over the region under consideration; however, some temporal and spatial variability may be introduced as well. Synthetic scenarios provide a framework for conducting sensitivity studies of potential impacts of climate change using impact models. Careful selection of the range and combinations of changes (e.g., using knowledge based on climate model projections), can facilitate "guided" sensitivity analysis, enabling an examination of both the modeled behavior of a system under a plausible range of climatic conditions and the robustness of impact models applied under changed and often unprecedented environmental conditions. Synthetic scenarios can provide a useful context for understanding and evaluating responses to more complex scenarios based on climate model outputs. Transparency to users and limited computational resource requirements, which allow examination of a wide range of potential climate changes (the range is further increased by the possibility of changing individual variables independent of one another), are among the advantages of synthetic scenarios. Their main disadvantage is the lack of internal consistency in applying uniform changes over large and highly variable areas such as the Arctic. Arbitrary changes in different variables may also lead to inconsistencies in synthetic scenarios that can limit their applicability and appropriateness. In addition, synthetic scenarios are not directly related to GHG forcing.

Analogue scenarios of a future climate are of two types: temporal analogue scenarios, which are based on previous warm climate conditions (determined either by instrumental or proxy data), and spatial analogue scenarios, which are based on current climate conditions in warmer regions. The use of historic instrumental records is an apparent advantage of the past climate analogues over other approaches. However, the availability of historic observational data for the Arctic is extremely limited. Proxy climate data, while representing in some cases a physically plausible climate different from the current climate to a degree similar to that of the climate projected for the 21st century, are also not available for many locations. The quality of geological records is often uncertain, and the resolution coarse. Furthermore, the paleoclimate changes are unlikely to have been driven by an increase in GHG concentrations. Spatial analogues are also unrelated to GHG forcing and are often physically implausible. The lack of availability of proper analogues is the major problem for the analogue scenario approach. The IPCC recommends that analogue scenarios are not used, at least not independently of other types of scenario (Carter et al., 1994).

Physical climate models are based on the laws of physics and discrete numerical representations of these laws that allow computer simulations. Trenberth (1992) describes how climate models can be constructed and their underlying physical principles. Of the hierarchy of climate models (Box 4.1), global coupled atmosphere-ocean

general circulation models (AOGCMs) are widely acknowledged as the principal, and most promising rapidly developing tools for simulating the response of the global climate system to increasing GHG concentrations. In its Third Assessment Report, the IPCC (2001) concluded that state-of-the-art AOGCMs in existence at the turn of the century provided "credible simulations of climate, at least down to subcontinental scales and over temporal scales from seasonal to decadal", and as a class were "suitable tools to provide useful projections of the future climate" (McAvaney et al., 2001). The IPCC (2001) identified the following primary sources of uncertainty in climate scenarios based on AOGCM projections: uncertainties in future emissions of GHGs and aerosols (emissions scenarios), and in conversion of the emissions to atmospheric concentrations and to radiative forcing of the climate; uncertainties in the global and regional climate responses to emissions simulated by different AOGCMs; and uncertainties due to inaccurate representation of regional and local climate. A disadvantage of the AOGCMs as a tool for constructing scenarios is their high demand for computational resources, which makes it expensive and time-consuming to carry out calculations for multiple emissions scenarios.

The selection of climate scenarios for impact assessments is always controversial and vulnerable to criticism (Smith et al., 1998). Mearns et al. (2001) suggest that, to be useful for impact assessments and policy makers, climate scenarios should be consistent with global projections at the regional level (i.e., projected changes in regional climate may lie outside the range of global mean changes but should be consistent with theory and model-based results); be physically plausible and realistic; provide a sufficient number of variables and appropriate temporal and spatial scales for impact assessments; be representative, reflecting the potential range of future regional climate change; and be accessible.

Compared to the other methods of constructing climate change scenarios, only AOGCMs (possibly in combination with dynamic or statistical downscaling methods) have the potential to provide spatially and physically consistent estimates of regional climate change due to increased atmospheric GHG concentrations (IPCC-TGCIA, 1999). The AOGCM projections are available for a large number of climate variables, at a variety of temporal scales, and for regular grid points all over the world, which should be sufficient for many impact

Box 4.1. Climate model hierarchy

Climate models have very different levels of complexity with respect to resolution and comprehensiveness. Available computing resources may limit model complexity for practical reasons, but the scientific question to be addressed is the main factor determining the required model complexity. Different levels of reduction (or simplification) create a hierarchy of climate models (McAvaney et al., 2001).

Simple climate models of the energy-balance type, with zero (globally averaged) to two (latitude and height) spatial dimensions, belong to the lowest level of the hierarchy. Based upon parameters derived from more complex climate models, they are useful in studies of climate sensitivity to a particular process over a wide range of parameters (e.g., in a preliminary analysis of climate sensitivity to various emissions scenarios, see section 4.4.1). Simple climate models can also be used as components of integrated assessment models, for example, in analyses of the potential costs of emission reductions or impacts of climate change (see Mearns et al., 2001).

Earth system models of intermediate complexity (EMICs) bridge the gap between the simple models and the comprehensive three-dimensional climate models (see Claussen et al., 2002). These models explicitly simulate interactions between different components of the climate system; however, at least some of the components have a reduced complexity, potentially limiting their applicability. These models are computationally efficient, allow for long-term climate simulations measured in thousands and tens of thousands of years, and are primarily used for studies of particular climate processes and feedbacks that are not believed to be affected by the dynamical simplifications introduced.

Comprehensive three-dimensional coupled atmosphere-ocean general circulation models (AOGCMs) occupy the top level of the hierarchy. The term "general circulation" refers to large-scale flow systems in the atmosphere and oceans, and the associated redistribution of mass and energy in the climate system. General circulation models (GCMs) simulate the behavior of these systems and the interactions between them and with other components of the climate system, such as sea ice, the land surface, and the biosphere. Atmosphere-ocean general circulation models are widely acknowledged as the most sophisticated tool available for global climate simulations, and particularly for projecting future climate states.

Atmosphere-ocean general circulation models were preceded by far less computationally demanding atmospheric GCMs coupled to simple parameterizations of the upper mixed layer of the ocean (AGCM/OUML), which still play an important role in studies of processes and feedbacks in the climate system (see also section 4.2.1) and in paleoclimate simulations.

assessments. Employing an ensemble of different models increases the representativeness of AOGCM-based scenarios. When AOGCMs are used to provide the central scenarios, they can be combined with other types of scenarios (e.g., with synthetic scenarios applied at the regional level, for which the AOGCMs provide a physically plausible range of climate changes).

For this assessment, five AOGCMs (referred to as the ACIA-designated models, see section 4.2.7) were selected for constructing future climate change scenarios for the Arctic (see section 1.3.2). The ACIA-designated models are drawn from the generation of climate models evaluated by the IPCC (2001). This chapter begins with a brief description of the state-of-the-art in AOGCM development at the time of the IPCC assessment (section 4.2), followed by an evaluation of the ACIA-designated models' performance in simulating the current climate of the Arctic (section 4.3). Projections of future climate change in the Arctic using the ACIA-designated models are the central focus of this chapter (section 4.4). An assessment of possible climate change at scales smaller than subcontinental, such as the scale considered by the ACIA, requires the application of a downscaling tech-

nique to the AOGCM output (see Box 4.1). In this assessment, two methods of downscaling AOGCM projections have been considered: regional climate modeling (section 4.5), and statistical downscaling (section 4.6). Finally, section 4.7 presents the outlook for improving AOGCM-based climate change projections for the Arctic.

4.2. Global coupled atmosphere–ocean general circulation models

The atmosphere, oceans, land surface, cryosphere, and associated biology and chemistry form interactively coupled components of the total climate system. Climate models are primary tools for the study of climate, its sensitivity to external and internal forcing factors, and the mechanisms of climate variability and change. These models attempt to take into account the various processes important for climate in the atmosphere, the oceans, the land surface, and the cryosphere, as well as the interactions between them (Fig. 4.1). In addition, models are increasingly incorporating components that describe the role of the biosphere and chemistry in order to provide a comprehensive description of the total earth system.

While the resolution of AOGCMs used for projections of future climate is rapidly improving, it is still insufficient to capture the fine-scale structure of climatic variables in many regions of the world that is necessary for impact assessment studies (Giorgi et al., 2001; Mearns et al., 2001). Hence, a number of techniques exist to enhance the resolution of AOGCM outputs. These techniques fall into three categories:

- High- or variable-resolution stand-alone AGCM simulations initialized using atmospheric and land-surface conditions interpolated from the corresponding AOGCM fields and driven with the sea-surface temperature and sea-ice distributions projected by the AOGCM.

- High-resolution regional (or limited-area) climate models (RCMs) restricted to a domain with simple lateral boundaries, at which they are driven by outputs from GCMs or larger-scale RCMs.

- Statistical downscaling methods that are based on empirically derived relations between observed large-scale climate variables and local variables, and which apply these relations to the large-scale variables simulated by GCMs (or RCMs).

Each of the regionalization techniques is characterized by its own set of advantages and disadvantages. Giorgi et al. (2001) provide details on the high- and variable-resolution AGCMs, while RCMs and statistical downscaling are discussed in sections 4.5 and 4.6.

Climate model hierarchy and downscaling techniques (based on Kattsov and Meleshko, 2004).
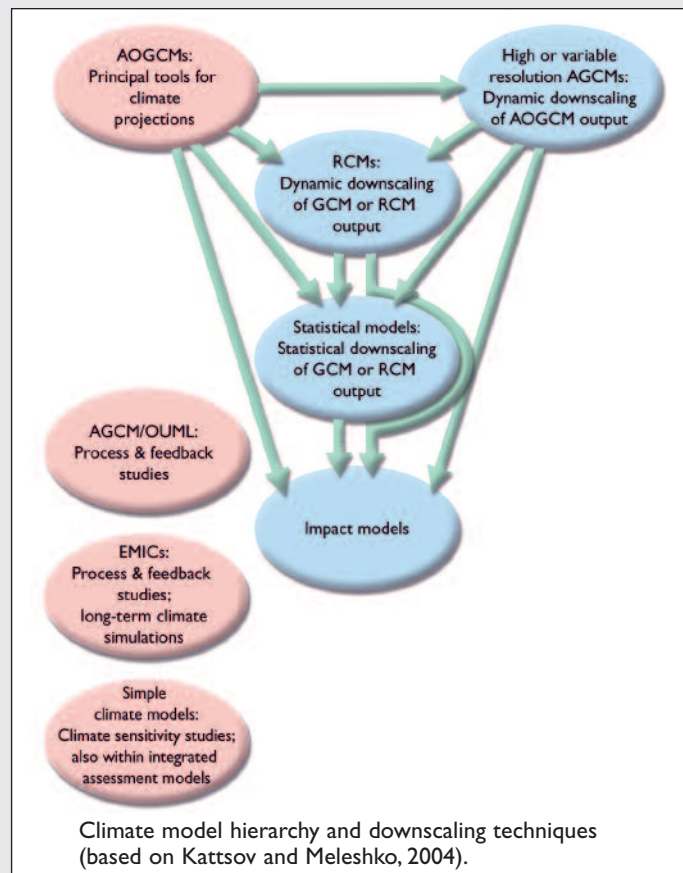
Because physical processes and feedbacks play a key role in the arctic climate system, this section focuses primarily on the physical components of climate models. However, land-surface biology is an important factor in determining the key thermal and radiative properties of the land surface, surface hydrology, turbulent heat and gas exchanges, and other processes. Likewise, the interaction of ocean biology with physical processes is important for air-sea gas exchange, including key processes related to cloud formation such as dimethyl sulfide exchange.

Coupled AOGCMs are made up of component models of the atmosphere, ocean, cryosphere, and land surface that are interactively coupled via exchange of data across the interfaces between them. For example, the ocean component is driven by the atmospheric fluxes of heat, momentum, and freshwater simulated by the atmospheric component. These heat and freshwater fluxes are themselves functions of the sea-surface temperatures simulated by the ocean model. Other driving fluxes for the ocean are produced by the brine rejection that occurs during sea-ice formation, freshwater from sea-ice melt, and freshwater river discharge at the continental boundaries.

Atmosphere-ocean general circulation models are continually evolving. The state-of-the-art climate modeling described in this section refers to the generation of models from the late 1990s and very early 2000s, and is close to that evaluated by the IPCC (2001).

4.2.1. Equilibrium and transient response experiments

Early climate simulations were conducted using atmospheric models coupled to highly simplified representations of the ocean. In these models, only the upper ocean was normally represented and then only as a simple fixed-depth slab of water some tens of meters deep in which the temperature responded directly to changes in atmospheric heat fluxes. Such models are still useful for short sensitivity experiments, such as exploring the impact of new representations of physical processes on climate change in experiments in which the concentration of atmospheric GHGs is instantaneously doubled in the model atmosphere. These models enable a quick assessment of the "equilibrium response" of climate to a given perturbation. The equilibrium response is the change in climate resulting from a perturbation (e.g., a specified increase in effective carbon dioxide (CO_2) concentration) after a period long enough for the climate to reach an equilibrium state. However, such models assume that vertical and horizontal heat transports in the ocean do not change when the climate changes.

Many centers have developed models with full dynamic deep-ocean components over the past decade. The dynamic oceans introduce the long timescales (multi-century to millennia) associated with the equilibration of the abyssal ocean. Such long timescales are absent in the models that represent the ocean as a shallow slab of water. In particular, this development has enabled the
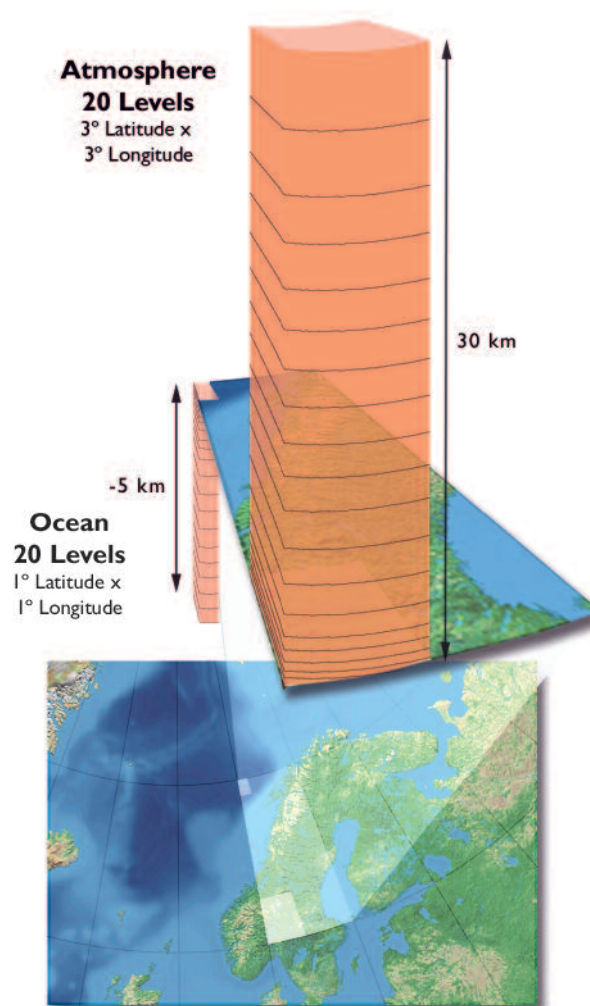
Fig. 4.1. Schematic illustrating the representation of the earth system by a coupled atmosphere-ocean general circulation model. Actual grid size and number of levels may vary.

exploration of the "transient response" of climate to changing concentrations of GHGs, as well as the examination of many aspects of natural climate variability. The transient response is the change over time as the perturbation (e.g., a continuous change in GHG concentrations) is applied. In the case of GHG-induced temperature change, the transient response is smaller than the equilibrium response because the large thermal inertia of the oceans slows the rate of warming.

4.2.2. Initialization and coupling issues

Owing to embodied feedbacks between ocean and atmosphere, an AOGCM-simulated climate is less constrained than climates simulated by stand-alone atmospheric or oceanic general circulation models (GCMs). Upon coupling, an AOGCM-simulated climate typically undergoes a so-called coupling shock (fast drift due to imbalances in the initial conditions between the component models at the time of coupling) and then, after a close-to-balance state between the interacting components of the AOGCM has been achieved, a gradual drift toward the model's equilibrium climatic state. The presence of climate drift, if it is significant, can complicate the study of a possible climate change signal. For example, large

drifts can potentially distort the behavior of various feedback processes present in the climate system and, dependent on the mean state of the model, distort the calculated climatic response to a given change in forcing.

The climate drift problem can introduce many technical considerations into the application of AOGCMs. To limit the influence of climate drift (especially the fast-drift component), careful initialization of AOGCMs is very important. This has led to a relatively wide array of initialization methods (e.g., Stouffer and Dixon, 1998). Initialization techniques often include a sequence of runs of component models separately, and in the coupled mode the components are constrained by observations at their interfaces. This makes it possible to reduce the climate drift and, particularly, the coupling shock.

Until recently, it has been necessary to use so-called "flux adjustments" (or "flux corrections", Sausen et al., 1987) to prevent drift in the climate of the coupled system that arises from inadequacies in the component models and in the simulated fluxes at their interfaces. These adjustments are normally derived as fields of spatially varying "corrections" to the heat and freshwater fluxes between the atmosphere and ocean components of the model. They are often derived during a calibration run of the AOGCM in which the sea-surface temperatures and surface salinities are constrained to observed climatological values of these quantities. The flux adjustments are then applied to succeeding runs of the model to provide improved simulation of the coupled system. In some cases, flux adjustments have also been applied to momentum fluxes. While flux adjustments have not been applied over land, it has in the past been necessary to flux-adjust the fields of sea-ice concentration and thickness. A driver in the development of coupled models has been to improve models to the stage where they can run without flux adjustments, as is now the case for some AOGCMs. In the AOGCMs that continue to use this technique, flux adjustments have become smaller as models have improved. Interestingly, the IPCC did not find systematic differences in the simulation of internal climate variability between flux-adjusted and non-flux adjusted AOGCMs (McAvaney et al., 2001), thus supporting the use of both types of model in the detection and attribution of climate change.

4.2.3. Atmospheric components of AOGCMs

The atmospheric component of AOGCMs enables simulation of the evolution with time of the spatial distributions of the vector wind, temperature, humidity, and surface pressure. This is done by discretization of the basic equations governing the behavior of the atmosphere, and implementation of these discretized equations on an appropriate computer. The equations are time-stepped forward at intervals that typically vary from a few minutes to tens of minutes, depending on the model formulation and resolution, to produce an evolving simulation of the behavior of the atmospheric flow and associated temperature, humidity, and surface-pressure fields.

The model dynamics are usually represented either as periodic functions defined as the sum of several waves (spectral models) or on a grid of points (finite-difference models) covering the globe for various levels of the atmosphere. Typically, the atmospheric components of the generation of climate models evaluated by the IPCC (2001) operated on grids with a horizontal spacing of 200 to 300 km and 10 to 20 vertical levels. Various schemes are available for the specification of vertical coordinates (e.g., Kalnay, 2003).

Simulation of some climatic variables in high latitudes (e.g., atmospheric moisture) using global models presents certain problems. Finite-difference GCMs require undesirable filtering operations in order to avoid computational instability when a reasonable time step is used in regions of converging meridians such as the Arctic. While polar filtering is not needed in spectral models, these models produce fictitious negative moisture amounts in the dry high-latitude atmosphere, thus calling for correction procedures. Both problems are apparently overcome by the application of semi-Lagrangian schemes for moisture advection, which are used in a number of atmospheric general circulation models (AGCMs). However, in semi-Lagrangian schemes, the advantages of large time steps and the absence of spurious negative moisture values are partially offset by the lack of exact moisture conservation. New schemes have recently started to appear that combine the semi-Lagrangian approach with mass conservation (e.g., Zubov et al., 1999), but have other disadvantages. Hopes for improved climate simulations of the polar regions are also associated with spherical geodesic grids, which allow for approximately uniform discretization of the sphere. Such grids are already used in some global numerical weather-prediction models (Majewski et al., 2002).

A key issue is the simulation of the basic physical processes that take place in the atmosphere and determine many of the feedbacks for climate variability and change. Examples include the representation of clouds and radiation; dry and moist convective processes; the formation of precipitation and its deposition on the surface as rain or snow; the interactions between the atmosphere and the land-surface orography (including the drag on the atmosphere caused by breaking gravity waves); and atmospheric boundary-layer processes and their interaction with the surface. Because these processes take place on scales much smaller than the model grid, they must be represented in terms of the large-scale variables in the model (vector wind, temperature, humidity, and surface pressure). Key atmospheric processes from an arctic surface climate perspective include the representations of the planetary boundary layer, clouds, and radiation.

Energy, momentum, and moisture from the free troposphere are transferred via the atmospheric boundary layer (ABL) to the surface and vice versa. Atmospheric general circulation models have difficulty with the proper representation of turbulent mixing processes in general, which

has implications for the representation of boundary-layer clouds (IPCC, 2001). The ABL in the Arctic differs significantly from its mid-latitude counterpart, so parameterizations based on mid-latitude observations tend to perform poorly in the Arctic. Parameterizations of the surface fluxes are usually based on the Monin-Obukhov similarity theory. These parameterizations work reasonably well for cases where the vertical stratification of the atmosphere is weakly stable, but simulate surface fluxes of momentum, heat, and water vapor that are too small in the very stable stratified conditions (Poulus and Burns, 2003) common in the high Arctic. In the very stable cases, turbulence may not be stationary, local, and continuous (Mahrt, 1998) – assumptions used in ABL parameterizations of surface fluxes. In addition, vertical resolution is a critical issue because the very thin stable surface layer is usually shallower than the first vertical model layer. Deviations from observations in the ABL during winter, found in simulations with a regional climate model for the Arctic (section 4.5.1), indicate the necessity of improvements in the atmospheric parameterization that better describe the vertical stratification and atmosphere–surface energy exchange (Dethloff et al., 2001). The mean monthly turbulent heat-flux distribution at the surface strongly depends on different ABL parameterizations and leads to different spatial distributions of temperature, wind, moisture, and other variables throughout the arctic atmosphere. The greatest changes are found in the ABL above the sea-ice edge in January.

Model resolution, both horizontal and vertical, is a problem in simulating the arctic ABL. The vertical discretization of current AGCMs cannot resolve the large temperature gradients and inversions that exist in the arctic ABL. Insufficient resolution gives rise to sensible heat fluxes in the models that tend to be too large. However, simply increasing the resolution will not solve the problem. Even if the very stable ABL can be simulated in finer detail, the fundamental problem of current theories predicting turbulent fluxes that are too small will still remain.

Specific cloud types observed in the arctic ABL present a serious challenge for atmospheric models. Parameterizing low-level arctic clouds is particularly difficult because of complex radiative and turbulent interactions with the surface (e.g., Randall et al., 1998).

The atmospheric components of AOGCMs usually focus on representation of tropospheric processes and the effects of stratospheric processes on the troposphere, while their descriptions of stratospheric processes are less satisfactory. For example, the insufficient vertical resolution in the stratosphere (as compared to that in the troposphere) prevents the atmospheric components of AOGCMs from properly representing important stratospheric phenomena, such as the quasi-biennial oscillation and sudden stratospheric temperature increases (Takahashi, 1999).

Current AOGCMs generally do not include interactive atmospheric chemistry models (Austin et al., 2003). Most of the atmospheric photochemical processes are therefore simulated with chemical transport models (CTMs) that use atmospheric wind velocities and temperature prescribed either from observational data or from GCM simulations. In the latter case, CTMs can be used to project the evolution of the atmospheric content of ozone, other radiatively active gases (e.g., methane and nitrous oxide), and aerosols (Austin et al., 2003; WMO, 2003). Projections of the distributions of tropospheric ozone and aerosols (sulfates, soot, sea salt, and mineral dust collectively known as "arctic haze") are particularly important to climate change projections (IPCC, 2001).

4.2.4. Ocean components of AOGCMs

The oceanic component in AOGCMs has improved substantially over the past decade. These models now include representation of the full dynamics and thermodynamics of the global ocean basins and allow simulation of the full three-dimensional current, temperature, and salinity structure of the ocean and its evolution. Important physical processes are associated with the upper-ocean mixed layer and diffusive processes in the ocean. The freezing, melting, and dynamics of sea ice and ice–ocean interactions are also taken into account. Until recently, because of limitations in available computing power, AOGCMs typically had similar horizontal resolution in the ocean and atmospheric components. Such ocean models poorly represent the large-scale ocean current structure, not only because of the lack of resolution of narrow boundary currents such as the Gulf Stream and the Kuroshio, but also because of the high viscosity coefficients necessary for computational stability (e.g., Bryan et al., 1975). However, as available computing power has increased, the resolution of the ocean component of AOGCMs has increased to roughly one degree of latitude and longitude. Although this resolution does not allow explicit representation of ocean eddies (a resolution of one-third of a degree is considered "eddy permitting", and one-ninth of a degree or better, "eddy-resolving"), it does result in a much-improved representation of ocean current structure.

The Arctic Ocean has always been and still remains one of the weak spots in AOGCMs. This is partly due to specific numerical problems such as the singularity of the longitude-latitude spherical coordinates (converging meridians) at the North Pole (see Randall et al., 1998). Until recently, filtering, or even inserting an artificial island at the North Pole, have been among the usual, but undesirable, ways to overcome the pole problem. Rotating grids or introducing alternative grids, for example, geodesic grids providing approximately uniform discretization of the sphere (e.g., Sadourny et al., 1968) or using curvilinear generalized coordinates (Murray, 1996), are now being pursued in order to eliminate the converging meridian problem. Such features are now starting to appear in oceanic components of AOGCMs (e.g., Furevik et al., 2003). However, a greater challenge is insufficient understanding of some phenomena related to the general circulation of the Arctic Ocean and subarctic seas. In particular, improvement is needed in representing

ocean/atmosphere/sea-ice interaction processes in order to better evaluate their importance within the context of natural variability and anthropogenically forced change in the climate system. A particular problem for the oceanic component of AOGCMs is the treatment of air–ice–ocean interactions and water-mass formation (creation of water bodies with a homogenous distribution of temperature and salinity) over the shallow continental shelves, which requires adequate resolution of shallow water layers, water-mass formation and mixing processes, continental runoff, and ice processes.

4.2.5. Land-surface components of AOGCMs

The land-surface components of climate models include representation of the thermal and soil-moisture storage properties of the land surface through modeling of its upper layers. Key properties include surface roughness and albedo, which are normally specified from global datasets, although models with interactive land-surface properties are now being developed.

Possible changes in vegetation and the effects that these changes may have on future climate are not often taken into account in climate change projections. These effects may be substantial and would be manifested in the local fluxes of water, heat, and momentum controlled by surface roughness, albedo, and surface moisture. The arctic land types have special features that are not well represented in the present generation of climate models (Harding et al., 2001). This is particularly true for winter conditions where snow distribution and its interaction with vegetation are poorly understood and modeled.

The discharge of river water to the ocean, especially to the Arctic Ocean whose freshwater budget is much more influenced by terrestrial water influx than are the budgets of other oceans, is of potential importance to climate change. The land-surface components of AOGCMs usually include river-routing schemes, in which the land surface is represented as a set of watersheds draining the runoff (integrated over their territories at each time step) into the grid boxes of the ocean model closest to the grid points specified as river mouths in the land-surface model. Such schemes are able to provide reasonable annual means of the discharge, but shift and sharpen its seasonal cycle, especially for the Arctic Ocean terrestrial watersheds with their high seasonality of discharge. More comprehensive river-routing schemes (e.g., Hagemann and Dümenil, 1998), allowing for simulations of horizontal transport of the runoff within model watersheds, are usually not used interactively in AOGCMs.

4.2.6. Cryospheric components of AOGCMs

Snow cover and sea ice are the two primary elements of the cryosphere represented interactively in AOGCMs, although some models now incorporate explicit parameterizations of permafrost processes. The large ice sheets are represented, although non-interactively, by land-surface topography and surface albedo (typically fixed at

a value of around 0.8). Likewise, there is usually no explicit representation of glaciers.

The insulating effects and change in surface albedo due to snow cover are of particular importance for climate change projections. AOGCMs demonstrate varying degrees of sophistication in their snow parameterization schemes. For example, some can represent snow density, liquid water storage, and wind-blown snow (see Stocker et al., 2001). Advanced albedo schemes incorporate dependencies on snow age or temperature. However, a major uncertainty exists regarding the ability of AOGCMs to simulate terrestrial snow cover (McAvaney et al., 2001; see also section 6.4), particularly its albedo effects and the masking effects of vegetation that are potentially important in determining the surface energy budget (see section 7.5).

Sea-ice components of AOGCMs usually include parameterizations of the accumulation and melting of snow on the ice, and thermodynamic energy transfers between the ocean and atmosphere through the ice and snow. Most of the AOGCMs evaluated by the IPCC (2001) employed simplistic parameterizations of sea ice. Recent advances in stand-alone sea-ice modeling, including those in modeling sea-ice thermodynamics (e.g., introducing the effects of subgrid-scale parameterizations with multiple thickness categories – the so-called "ice-thickness distribution"), are now being incorporated into AOGCMs. However, understanding is still insufficient for treating some atmosphere–ice–ocean interaction issues (e.g., heat distribution between concurrent lateral and vertical ice melt or accumulation). The primary differences among the various representations relate to treatment of internal stresses in calculating sea-ice model dynamics. An evaluation of the different treatment of sea-ice rheologies (relationships between internal stresses and deformation) was the core task for the Sea-Ice Model Intercomparison Project (SIMIP) initiated in the late 1990s. Having considered a hierarchy of stand-alone sea-ice models with different dynamic parameterizations, SIMIP found the viscous-plastic rheology to provide the best simulation results and adopted it as a starting point for further optimizations (Lemke et al., 1997). Other developments, including the elastic-viscous-plastic rheology (Hunke and Dukowicz, 1997), are helpful in achieving high computational efficiency. However mature the status of stand-alone sea-ice dynamics modeling, some AOGCMs still employ a simple, so-called "free drift" scheme that only allows ice to be advected with ocean currents. There is a large range in the ability of AOGCMs to simulate the position of the ice edge and its seasonal cycle (McAvaney et al., 2001). However, there is no obvious connection between the fidelity of simulated ice extent and the inclusion of an ice-dynamics scheme. This is apparently due to the additional impact of simulated wind-field errors (e.g., Bitz et al., 2002; Walsh et al., 2002), which may offset improvements from the inclusion of more realistic ice dynamics. Conversely, the importance of improved sea-ice dynamics and thermodynamics has become apparent,

and the AOGCM community is responding by including more sophisticated treatments of sea-ice physics.

4.2.7. AOGCMs selected for the ACIA

Selecting AOGCM simulation results to be used in an impact assessment is not a trivial task, given the variety of models. The IPCC (McAvaney et al., 2001) concluded that the varying sets of strengths and weaknesses that AOGCMs display means that, at this time, no single model can be considered "best" and it is important to utilize results from a range of coupled models in assessment studies. The choice of AOGCMs for this assessment used the criteria suggested by Smith et al. (1998): vintage, resolution, validity, representativeness of results, and accessibility of the model outputs.

While models do not necessarily improve with time, later versions (often with higher resolution) are usually preferred to earlier ones. An important criterion for selecting an AOGCM to be used in constructing regional climate scenarios is its validity as evaluated by analyses of its performance in simulating present-day and past climates (the evolution of 20th century climate in particular). The validity is evaluated by comparing the model output with observed climate, and with output from other models for the region of interest and larger scales, to determine the ability of the model to simulate large-scale circulation patterns. Well-established systematic

comparisons of this type are provided by international model intercomparison projects (MIPs, see Box 4.2). Finally, when several AOGCMs are to be selected for use in an impact assessment, the model results should span a representative range of changes in key variables in the region under consideration.

Section 1.4.2 provides details of the procedure for selecting AOGCMs for the ACIA. Initially, a set of the most recent and comprehensive AOGCMs whose outputs were available from the IPCC Data Distribution Center was chosen. This set was later reduced to five AOGCMs (two European and three North American), primarily due to the accessibility of model output, as well as storage and network limitations. By the initial phase of the ACIA, at least one Special Report on Emissions Scenarios (SRES: Nakićenović and Swart, 2000) B2 simulation (see section 4.4.1) extending to 2100 had been generated by each of the ACIA-designated models. All of the models are well documented, participate in major international MIPs, and have had their pre-SRES simulations (see Box 4.2) analyzed for the Arctic and the results published (e.g., Walsh et al., 2002). The five ACIA-designated models listed in Table 4.1, together with information on their formulations, provided the core data for constructing the ACIA climate change scenarios.

Box 4.2. Model intercomparison projects

Model intercomparison projects (MIPs) allow comparison of the ability of different models to simulate current and perturbed climates, in order to identify common deficiencies in the models and thus to stimulate further investigation into possible causes of the deficiencies (Boer, 2000a,b). This is currently the only way to increase the credibility of future climate projections. Participation in MIPs is an important prerequisite for an AOGCM to be employed in constructing climate scenarios (e.g., for the ACIA).

In MIPs, models of the same class (AOGCMs, stand-alone AGCMs or oceanic GCMs, RCMs) are run for the same period using the same forcings. Typically, diagnostic subprojects are established that concentrate upon analyses of specific variables, phenomena, or regions. Occasionally, experimental subprojects are initiated, aimed mainly at answering questions related to model sensitivity.

Of the many international MIPs conducted in the past decade, two are of primary importance for the ACIA: the Atmospheric Model Intercomparison Project (AMIP: Gates, 1992; Gates et al., 1998), and the Coupled Model Intercomparison Project (CMIP: Meehl et al., 2000). Both included subprojects devoted specifically to model performance at high latitudes among their numerous diagnostic subprojects.

Thirty AGCMs were included in the second phase of the AMIP (AMIP-II, concluded in 2002). All of these were forced with the same sea-surface temperatures (SSTs) and sea-ice extents prescribed from observations, and a set of constants, including GHG concentrations. The AMIP-II simulations span the period from 1979 to 1996. AMIP findings related to AGCM performance in the Arctic have been reported since the early 1990s (e.g., Bitz et al., 2002; Frei et al., 2003a; Kattsov et al., 1998, 2000; Tao et al., 1996; Walsh et al., 1998, 2002). Coupled Model Intercomparison Project experiments belong to the class of idealized (e.g., 1% per year increase in CO_2) transient experiments with AOGCMs. Räisänen (2001) discusses some results of the second phase of the CMIP (CMIP2) related to the Arctic (see also section 4.4.5).

The Climate of the 20th Century project was initiated in order to determine to what extent stand-alone AGCMs are able to simulate observed climate variations of the 20th century against a background of natural variability

4.2.8. Summary

Atmosphere-ocean general circulation models are widely acknowledged to be the primary tool for projecting future climate. As understanding of the Earth's climate system increases and computers become more sophisticated, the scope of processes and feedbacks simulated by AOGCMs is steadily increasing. In addition to representing the general circulation of the atmosphere and the ocean, the AOGCMs include interactive components representing the land surface and cryosphere. The biosphere and the carbon and sulfur cycle components of AOGCMs are evolving, while the atmospheric chemistry component is currently being developed off-line. The ability to increase confidence in model projections of arctic climate is limited by the need for further advances in the representation of the arctic climate system in the AOGCMs (see section 4.7).

4.3. Simulation of observed arctic climate with the ACIA-designated models

Model-based scenarios of future climate are only credible if the models simulate the observed climate (present-day and past) realistically – both globally and in the region of interest. While an accurate simulation of the present-day climate does not guarantee a realistic sensitivity to an external forcing (e.g., higher GHG concentrations), a grossly biased present-day simulation may lead to weakening or elimination of key feedbacks in a simulation of change, or conversely may cause key feedbacks to be exaggerated. The ability of the models to reproduce climate states in the past – under external forcings differing from those at present – can therefore help to add to the credibility of their future climate projections.

Boer (2000a) distinguishes three major categories of model evaluation: the morphology of climate, including spatial distributions and structures of means, variances, and other statistics of climate variables; budgets, balances, and cycles in the climate system; and process studies of climate. A comprehensive assessment of recent AOGCM simulations of observed global climate is provided by McAvaney et al. (2001), who, in particular, regarded as well-established the ability of the AOGCMs "to provide credible simulations of both the annual mean climate and the climatological seasonal cycle over broad continental scales for most variables of interest for climate change". In this context, clouds and humidity were mentioned as major sources of uncertainty, in spite of incremental improvements in their modeling.

In this section, the first two categories of model evaluation (Boer, 2000a) are addressed for the five ACIA-designated AOGCM simulations of the observed arctic climate. The primary focus is on the evaluation of representations of surface air temperature and precipitation as

(Folland et al., 2002). In this MIP, the AGCMs are forced with observed SSTs and sea-ice extents and prescribed changes in radiative forcing (GHGs, trace gases, stratospheric and tropospheric ozone, direct and indirect effects of sulfate aerosols, solar variations, and volcanic aerosols).

The outputs of models archived at the IPCC Data Distribution Center provide an additional opportunity for AOGCM intercomparison (IPCC-TGCIA, 1999). The archived outputs have a limited set of variables, but include at least two scenarios (A2 and B2) from the IPCC Special Report on Emissions Scenarios (SRES: Nakićenović and Swart, 2000) and at least two pre-SRES (IS92a) emissions scenarios (GHGs only and GHGs plus sulfate aerosols). The simulation results that are available usually span the 20th and 21st centuries. The selection of these AOGCMs by the IPCC for use in its Third Assessment Report (IPCC, 2001) was an indication that these models provide the most viable basis for climate change assessment.

The foci of the Arctic Regional Climate Model Intercomparison Project (ARCMIP) include the surface energy balance over ocean and land, clouds and precipitation processes, stable planetary boundary layer turbulence, ice-albedo feedback, and sea-ice processes (Curry J. and Lynch, 2002; see also section 4.5.1). Another international effort – the Arctic Ocean Model Intercomparison Project (AOMIP) – aims to identify strengths and weaknesses in Arctic Ocean models using realistic forcing (Proshutinsky et al., 2001; see also section 4.5.2). The major goals of the project are to examine the ability of Arctic Ocean models to simulate variability at seasonal to decadal scales, and to qualitatively and quantitatively understand the behavior of the Arctic Ocean under changing climate forcing.

Other GCM MIPs of relevance to the ACIA include the Ocean Model Intercomparison Project (WCRP, 2002), which is designed to stimulate the development of ocean models for climate research, and the Paleoclimate Modeling Intercomparison Project (Braconnot, 2000), which compares AGCM/OUML models (see Box 4.1) and AOGCMs in simulations of paleoclimate conditions during periods that were significantly different from the present-day climate. There are also a number of MIPs devoted to intercomparison of specific parameterizations employed in GCMs, including the Sea-Ice Model Intercomparison Project (Lemke et al., 1997), the Snow Models Intercomparison Project (Etchevers et al., 2002), and polar clouds (IGPO, 2000).

Table 4.1. Key features of the ACIA-designated AOGCMs

	Atmospheric resolution[a]	Ocean resolution[b]	Land-surface scheme[c]	Sea-ice model[d]	Flux adjustment[e]	Primary reference
CGCM2						
Canadian Centre for Climate Modelling and Analysis, Canada	T32 (3.8° x 3.8°) L10	1.8° x 1.8° L29	M, BB, F, R	T, R	H, W	Flato and Boer (2001)
CSM_1.4						
National Center for Atmospheric Research, United States	T42 (2.8° x 2.8°) L18	2.0° x 2.4° L45	C, F	T, R	-	Boville et al. (2001)
ECHAM4/OPYC3						
Max-Planck Institute for Meteorology, Germany	T42 (2.8° x 2.8°) L19	2.8° x 2.8° L11	M, BB, R	T, R	H*, W*	Roeckner et al. (1996)
GFDL-R30_c						
Geophysical Fluid Dynamics Laboratory, United States	R30 (2.25° x 3.75°) L14	2.25° x 1.875° L18	B, R	T, F	H, W	Delworth et al. (2002)
HadCM3						
Hadley Centre for Climate Prediction and Research, United Kingdom	2.5° x 3.75° L19	1.25° x 1.25° L20	C, F, R	T, F	-	Gordon et al. (2000)

[a]Horizontal resolution is expressed either as degrees latitude by longitude or as a spectral truncation (either triangular (T) or rhomboidal (R)) with a rough translation to degrees latitude and longitude. Vertical resolution (L) is the number of vertical levels; [b]Horizontal resolution is expressed as degrees latitude by longitude, while vertical resolution (L) is the number of vertical levels; [c]B = standard bucket hydrology scheme (single-layer reservoir of soil moisture which changes with the combined action of precipitation (snowmelt) and evaporation, and produces runoff when the water content reaches the prescribed maximum value); BB = modified bucket scheme with spatially varying soil moisture capacity and/or surface resistance; M = multilayer temperature scheme; C = complex land-surface scheme usually including multiple soil layers for temperature and moisture, and an explicit representation of canopy processes; F = soil freezing processes included; R = river routing of the discharge to the ocean (land surface is represented as a set of river drainage basins); [d]T = thermodynamic ice model; F = "free drift" dynamics; R = ice rheology included; [e]H = heat flux; W = freshwater flux; asterisks indicate annual mean flux adjustment only.

reproduced by the AOGCMs for the ACIA climatological baseline period (1981–2000). The evaluation of individual ACIA-designated model simulations compared to historical data is also considered.

In most cases, the area between 60º and 90º N is used as a reference region for model evaluation. In some cases, however, smaller areas are used for consistency with observational data (e.g., precipitation, see section 4.3.1). In cases where a variable was missing from one of the five model outputs, a subset of four models was evaluated for that variable.

4.3.1. Observational data and reanalyses for model evaluation

A considerable number of datasets are available for the Arctic, including remotely sensed and *in situ* data, observations from the arctic buoy program, historical data, and field experiments (see section 2.6). However, for evaluation of three-dimensional AOGCMs, observational data readily available at regularly spaced grid points are the most useful. *In situ* observations are not representative of conditions covering an area the size of an average model grid box, thus a comprehensive analysis is required to match model simulations and observations.

A good opportunity for model evaluation is provided by reanalyses employing numerical weather prediction models to convert irregularly spaced observational data into complete global, gridded, and temporally homogeneous data (presently available for periods of several decades). Reanalyses include both observed (assimilated)

variables (e.g., temperature, geopotential height) and derived fields (e.g., precipitation, cloudiness). For some of the derived fields, direct observations are non-existent (e.g., evaporation). The quality of a reanalysis is not the same for different variables; it may also vary regionally for the same variable, depending on the availability of observations. In areas where observations are sparse, each reanalysis primarily represents the quality of the model's simulation. For variables that are not observed, the reanalysis may not be realistic. Errors in a model's physical parameterizations can also adversely affect the reanalysis. However, despite these problems, reanalyses provide the best gridded, self-consistent datasets available for model evaluation.

It is worthwhile noting that direct point-to-point and time-step-to-time-step comparison of a climate GCM output against observations, reanalyses, or another climate model simulation is not methodologically correct. Only spatial and temporal statistics can be used for the evaluation. For state-of-the-art AOGCMs, spatial averages should be at subcontinental or greater scales, such as the Arctic Ocean; the four ACIA regions (see section 1.1) including their marine parts; or the watersheds of major rivers.

Observational data for validating AOGCM performance in the Arctic (particularly the central Arctic) are characterized by a comparatively high level of uncertainty. Because of the sparsity of direct observations, even the temperature climatology in the Arctic is imperfectly known. Model-simulated surface air temperature and atmospheric pressure have primarily been compared with

Fig. 4.2. Seasonal and annual mean differences in surface air temperature (a) between the NCEP/NCAR reanalysis and the CRU dataset for the period 1961 to 1990 and (b) between the NCEP/NCAR and the ECMWF reanalyses for the period 1979 to 1993.
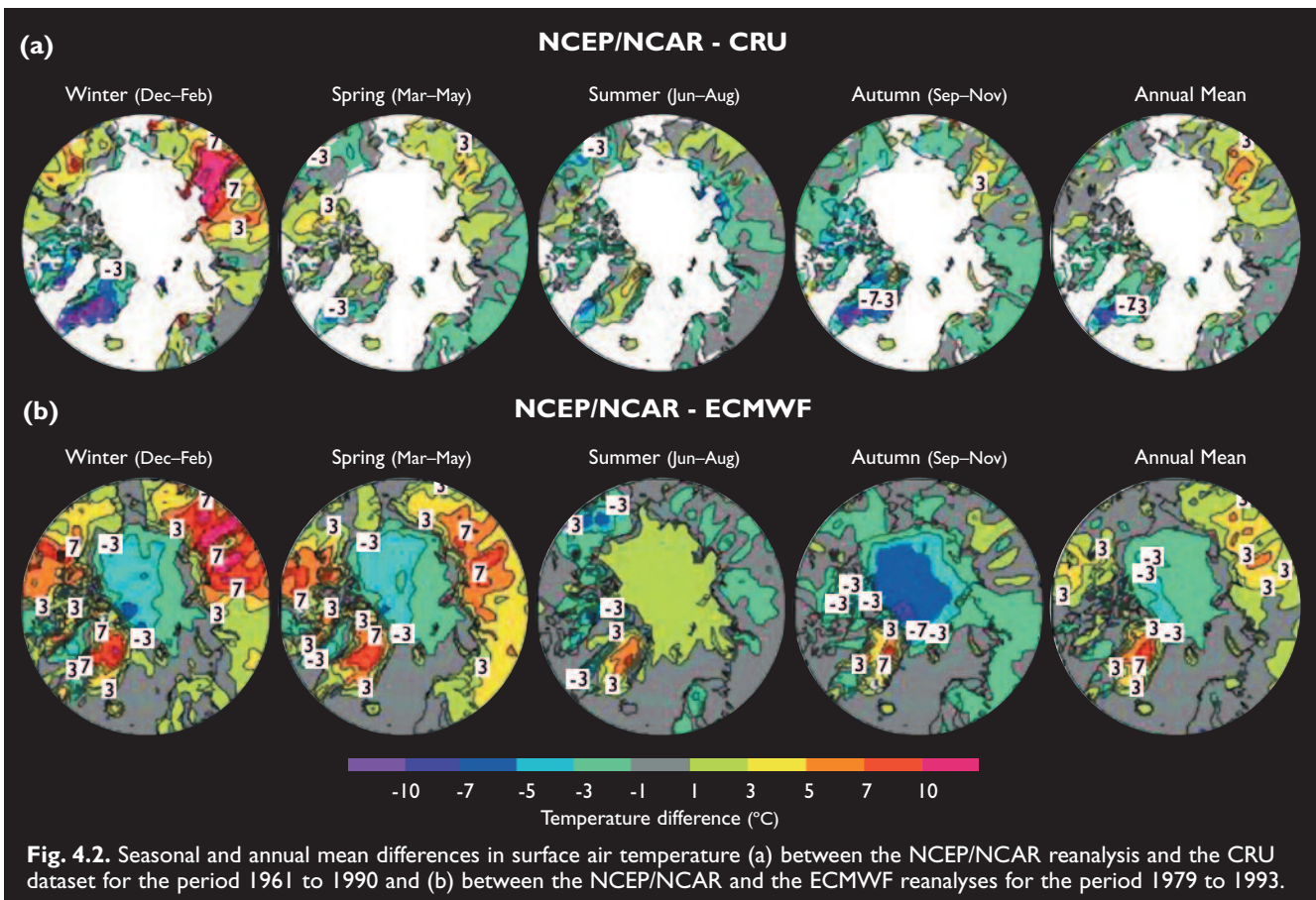
National Center for Atmospheric Research (NCEP/NCAR) reanalysis (Kistler et al., 2001). To estimate the accuracy of the NCEP/NCAR reanalysis, its pattern of surface air temperatures was compared against two other datasets (Fig. 4.2). The first, compiled at the Climatic Research Unit (CRU), University of East Anglia (New et al., 1999, 2000), is based on the interpolation of weather station observations. It is therefore expected to be accurate where the station density is sufficient, but it covers only land areas. The second dataset used for comparison is the European Centre for Medium-Range Weather Forecasts (ECMWF) reanalysis (ERA-15; Gibson et al., 1997). Neither of the two reanalyses should be considered as "truth" but their differences provide some information about the probable magnitude of errors in them. The ECMWF reanalysis is only available for the period since 1979; the difference between the ECMWF and NCEP/NCAR reanalyses shown in Fig. 4.2 was calculated for the overlapping interval (1979–1993).

The differences between the NCEP/NCAR reanalysis and the CRU dataset for the period 1961 to 1990 are smallest in summer (generally within ±1 °C, and almost everywhere within ±3 °C) and largest in winter. In winter, temperatures in the NCEP/NCAR reanalysis are higher than in the CRU dataset over most of northern Siberia and North America, but lower over the northeastern Canadian Archipelago and Greenland. Locally, the differences are as great as 15 °C in northern Siberia (NCEP/NCAR warmer than CRU) and Greenland (NCEP/NCAR colder than CRU). Despite these very

temperatures over the entire arctic land area are in all seasons within 2 °C of each other.

The differences between the NCEP/NCAR and ECMWF reanalyses over land follow the NCEP/NCAR minus CRU differences in most, but not all, respects. Substantial differences also occur between the ECMWF reanalysis and the CRU dataset, most notably in spring when the ECMWF temperatures show a widespread cold bias compared to the CRU dataset. Over the central Arctic Ocean, temperatures in the NCEP/NCAR reanalysis are lower than temperatures in the ECMWF reanalysis throughout most of the year, with the greatest differences (up to 5–7 °C) in autumn. In summer, however, NCEP/NCAR temperatures are slightly higher than ECMWF temperatures.

The quality of precipitation climatologies for high latitudes derived from reanalyses is lower than that for temperature (or, e.g., atmospheric pressure). On the other hand, assessments of simulated precipitation at high latitudes are confounded by the uncertainties in observational estimates, which suffer from errors in gauge measurements of solid precipitation, especially when the solid precipitation occurs under windy conditions. Depending on the partitioning between falling snow (precipitation) and wind-blown snow from the surface, the error can range from a significant "undercatch" to a significant "overcatch". Because different observational climatologies incorporate varying types and degrees of adjustment, there is some variance among the observational esti-

mates, more so in the monthly means than in the annual means (for details see sections 2.6.2.2 and 6.2.1). The primary observational dataset used here is an outgrowth of an arctic climatology originally compiled by Bryazgin (1976), whose monthly mean fields were extended for inclusion in Khrol (1996), and subsequently updated and enhanced by additional corrections. This compilation includes data from the Russian drifting ice stations and high-latitude land-surface stations, and it is gridded over the 65° to 90° N domain. Additional precipitation climatologies used in this assessment are Legates and Willmott (1990) and Xie and Arkin (1998). Both the Bryazgin and Legates-Willmott climatologies are based on gauge-corrected *in situ* data only. The two climatologies are multi-year averages over periods that do not coincide with each other or with the ACIA climatological baseline (see section 4.3.2). The Xie and Arkin climatology is a blend of *in situ* and satellite data, and reanalysis where *in situ* and satellite data are not available. It differs significantly from the other two not only in spatial distributions, but also in areal averages. The Xie and Arkin dataset provides monthly means for individual years over a period that includes the ACIA baseline.

4.3.2. Specifying the ACIA climatological baseline

A climatological baseline is a period of years representing the current climate in terms of the mean and variability over the period. To satisfy widely adopted IPCC (1994) criteria, a baseline period should:

- be representative of the present-day or recent average climate in the region considered;
- be of sufficient duration to encompass a range of climatic variations;
- cover a period for which data on all major climatological variables are abundant, adequately distributed in space, and readily available;
- include data of sufficiently high quality for use in evaluating impacts; and should
- be consistent or readily comparable with baseline climatologies used in other impact assessments.

Until recently, the most widely used baseline period has been the "classical" 30-year period defined by the World Meteorological Organization (WMO). Usually the period 1961 to 1990 is used (as was the case for the first three IPCC Assessment Reports). In some cases, an earlier period (1951–1980) was used. It is expected that the IPCC Fourth Assessment Report will use the climatological baseline 1971–2000 (IPCC-TGCIA, 1999).

The 20-year period 1981–2000 was selected as the ACIA climatological baseline. While shorter than the 30-year WMO standard, the ACIA baseline is linked to the period of high-quality (satellite) observations of sea-ice extent and concentration (important climatological variables for the Arctic), which have been available only since the late 1970s (IPCC, 2001; see also section 6.3). The precise coincidence of the baseline duration with

the ACIA future time slices (also 20 years, see section 1.4.2) is also methodologically consistent. Another technical reason for selecting the 1981–2000 baseline period, rather than 1971–2000, was the availability of the former (but not the latter) in the outputs of all five B2 simulations stored in the ACIA archive.

A serious concern is that the ACIA baseline duration is insufficient to reflect natural climatic variability on a multi-decadal timescale. Indeed, the ACIA climatological baseline includes at least ten of the warmest years globally since the mid-19th century when the instrumental record began (IPCC-TGCIA, 1999). However, considering the large interdecadal variability of arctic climate during the entire period of the instrumental record (e.g., Bengtsson et al., 2003; Polyakov and Johnson, 2000; Polyakov et al., 2002a,b), any particular 30-year (or even longer) period of the 20th century could exhibit a similar limitation.

Following the recommendations of the IPCC Task Group on Scenarios for Climate and Impact Assessment, the ACIA climatological baseline (1981–2000) was compared with the standard 1961–1990 baseline, using surface air temperature and precipitation data from the NCEP/NCAR reanalysis (Kistler et al., 2001). Table 4.2 provides seasonal and annual multi-year means of the atmospheric variables for the two baseline periods.

The differences in the global means between the two baseline periods are systematic, but small. Globally, the ACIA baseline period is warmer by 0.1 to 0.2 °C in all seasons. The differences in global precipitation are negligible. For the polar region (60°–90° N), the differences between the two baselines are larger. The difference in the surface air temperature is at a maximum in winter

Table 4.2. Multi-year means of surface air temperature and precipitation derived from the NCEP/NCAR reanalysis and averaged over the WMO standard (1961–1990) and ACIA (1981–2000) climatological baselines (Kattsov et al., 2003).

	Global		60°–90° N	
	Surface air temperature (°C)	Precipitation (mm/d)	Surface air temperature (°C)	Precipitation (mm/d)
Winter (Dec–Feb)				
WMO	12.3	2.69	-22.1	1.10
ACIA	12.4	2.70	-21.5	1.12
Spring (Mar–May)				
WMO	13.7	2.71	-11.6	1.03
ACIA	13.8	2.72	-10.9	1.05
Summer (Jun–Aug)				
WMO	15.3	2.91	5.5	1.65
ACIA	15.5	2.89	5.7	1.67
Autumn (Sep–Nov)				
WMO	13.8	2.69	-9.1	1.31
ACIA	13.9	2.69	-8.6	1.31
Annual				
WMO	13.8	2.75	-9.3	1.28
ACIA	13.9	2.75	-8.8	1.28

Fig. 4.3. Differences in seasonal and annual multi-year mean surface air temperature in the northern polar region (60°–90° N) between the ACIA (1981–2000) and the standard WMO (1961–1990) climatological baselines, obtained from the NCEP/NCAR reanalysis.

(0.6 °C) and is smallest in summer (0.2 °C). The ACIA baseline annual mean precipitation is the same as the 1961–1990 mean.

Geographically, the differences between the two baseline periods in the NCEP/NCAR reanalysis are more pronounced (Fig. 4.3). The Arctic is generally warmer during the ACIA baseline period, especially in autumn. The strongest warming is evidently associated with the marginal sea-ice zone, particularly along the east coast of Greenland. Mean sea-level pressure (SLP) is generally lower (by up to about 1.5 hPa) over the central Arctic and northern North Atlantic in the ACIA baseline period compared to the 1961–1990 baseline period.

Because 1961–1990 is expected to be superseded in the near future by 1971–2000 as the new standard 30-year averaging period, it is worth comparing the ACIA climatological baseline against the latter. Figure 4.4 shows the spatial distributions of seasonal and annual differences in surface air temperature between the 1981–2000 and 1971–2000 periods.

In summary, for surface air temperature, precipitation, and atmospheric pressure, the ACIA baseline period has systematic but generally small differences in comparison with the WMO standard baseline (1961–1990). The differences can easily be taken into account when a comparison between climate change scenarios employing the

different baselines is required. An advantage of the ACIA climatological baseline period is that it is more "current" than the 1961–1990 period. The duration of the ACIA baseline period is exactly the same as that adopted for the ACIA future time slices. There are only minor geographical differences in seasonal temperature means between the ACIA baseline and the new standard baseline (1971–2000). While the ACIA climatological baseline period (1981–2000) satisfies the IPCC (1994) selection criteria, its relative shortness (compared to the standard 30-year period) may not provide an adequate representation of the probability of extreme events.

4.3.3. Surface air temperature

The seasonal cycle of the simulated and analyzed air temperatures at the 2 m height (1.5 m height for HadCM3) for the period 1981 to 2000 is illustrated in Fig. 4.5a, which shows means for the entire area north of 65° N. While there are differences between the five-model mean and the NCEP/NCAR reanalysis, these are relatively small compared with the range of model results. In particular, the area mean temperatures during the greater part of the year differ by about 5 °C between the models simulating the highest and lowest temperatures, and local differences are even larger. In late winter (February–March), all the models simulate slightly lower temperatures than those in the NCEP/NCAR reanalysis. It should be noted that the 1.5 and 2 m temperatures in

Fig. 4.4. Differences in seasonal and annual multi-year mean surface air temperature in the northern polar region (60°–90° N) between the ACIA (1981–2000) and the new standard (1971–2000) climatological baselines, obtained from the NCEP/NCAR reanalysis.

Surface air temperature (°C)

Precipitation (mm/day)
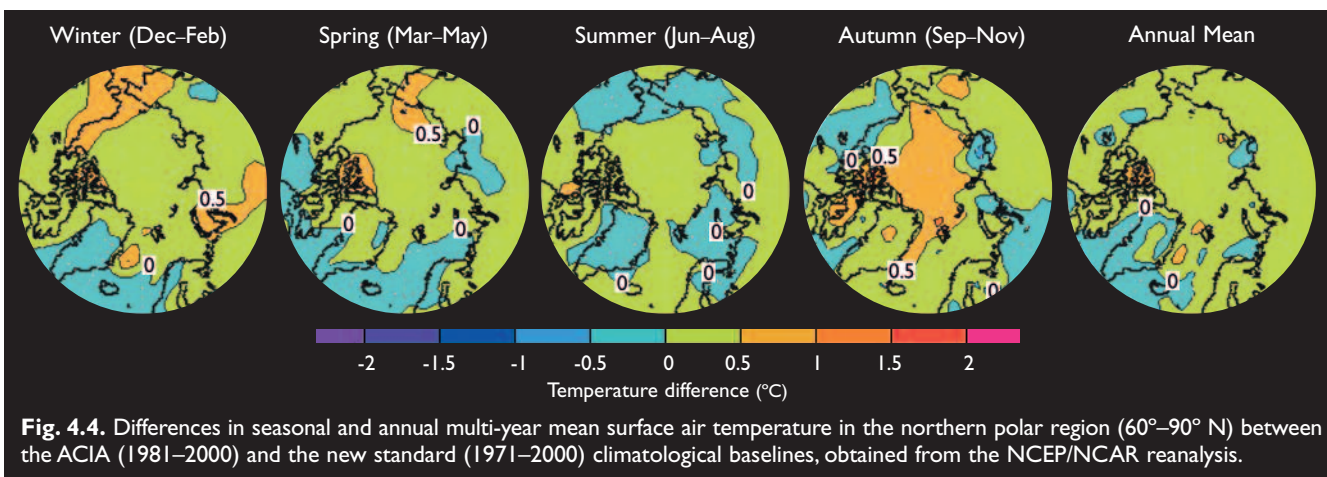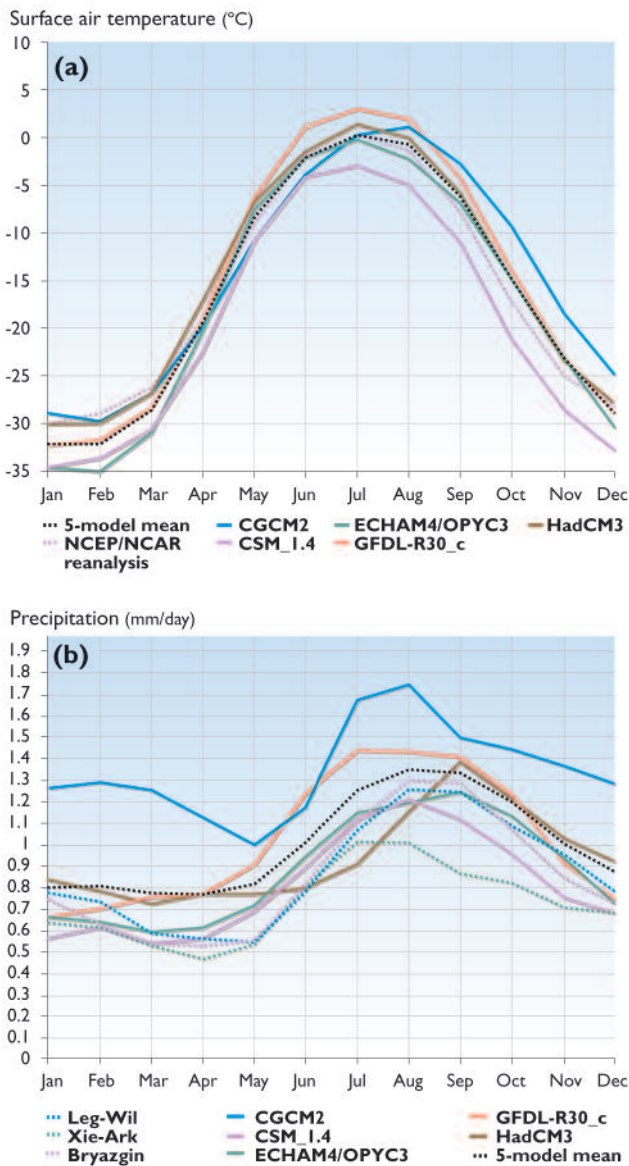
Fig. 4.5. Seasonal cycles of (a) surface air temperature and (b) precipitation simulated by the five ACIA-designated models for the period 1981–2000 and averaged over the area 65°–90° N. For comparison, data for the same area are included in (a) from the NCEP/NCAR reanalysis for the same time period and in (b) from three climatologies: Bryazgin (1936–1990), Legates-Willmott (1920–1980), and Xie-Arkin (1981–2000) (Khrol, 1996; Legates and Willmott, 1990; Xie and Arkin, 1998).

the models are not prognostic variables – they are derived from the prognostic temperatures at the lowest model level (typically a few tens of meters) using the models' ABL parameterizations; as a result, the biases may be partly due to the diagnostic schemes. In addition, surface elevation differences between the models and the reanalysis, as a result of differences in spatial resolution, could be contributing to the apparent biases.

The large-scale spatial distribution of annual mean temperature in the Arctic is, on average, reasonably well reproduced by the ACIA-designated models. The simulations tend to be slightly colder than the NCEP/NCAR reanalysis in northern Eurasia and somewhat warmer over the western Arctic Ocean and northern North

America (Fig. 4.6). A sharp local maximum in the five-model bias (Fig. 4.6c) in southern Greenland probably reflects the relatively smooth model topographies. However, the biases vary substantially between the individual models. Figure 4.6d shows the number of the five models that simulate lower mean annual temperatures than those in the NCEP/NCAR reanalysis. There are a few areas in the western Arctic where all five models simulate higher mean annual temperatures than those in the NCEP reanalysis and a few areas in the eastern Arctic where all five models simulate lower mean annual temperatures. The seasonal distribution of the biases in the five-model mean temperature is shown in Fig. 4.6e-h. The cold bias in northern Eurasia is most pronounced in winter and spring, whereas the warm bias in northern North America persists for most of the year and is largest in autumn. The simulated temperatures in the central Arctic Ocean tend to exceed the NCEP/NCAR reanalysis estimate in spring and especially in autumn. The five-model mean simulated summer temperatures in the central Arctic are lower than in the NCEP/NCAR reanalysis and the model-to-model variation is relatively small.

The ability of AOGCMs to provide credible projections of future climates is strongly supported by their ability to simulate the evolution of the climate during past centuries. One of the five-member ensemble 20th century simulations with the GFDL-R30_c model driven by historical changes in GHG and sulfate aerosol concentrations demonstrated an impressive resemblance to the observed warming that occurred in two distinct periods in the first and second halves of the 20th century with a pronounced maximum in the Arctic (Delworth and Knutson, 2000). The early 20th-century warming was not obtained in the other simulations of the GFDL-R30_c ensemble, which highlights the role of internal variability in the climate evolution, and therefore proves the necessity of ensemble simulations, rather than single runs, in order to better delineate the associated uncertainties. In the HadCM3 model, a good fit to 20th century observations was only obtained when natural (varying) forcing from solar and volcanic activity was also included (Stott et al., 2000; Stott, 2003; Tett et al., 2000; see also IPCC, 2001a).

4.3.4. Precipitation

More so than with temperature, there are major systematic differences between precipitation in the ACIA 1981–2000 simulations and in observational datasets. The five-model mean seasonal cycle of precipitation in the area 65° to 90° N is in qualitative agreement with the climatologies (Fig. 4.5b). While the range between the individual simulations is substantial throughout the year, it is noteworthy that the observational climatologies demonstrate a comparable scatter, at least in summer and autumn.

As shown in Fig. 4.7a-d, the average simulated annual precipitation generally exceeds the Bryazgin estimate

Fig. 4.6. Comparison of surface air temperature simulated by the ACIA-designated models for 1981–2000 and the NCEP/NCAR reanalysis temperature for the same period. The top row shows (a) the simulated annual mean temperature averaged over the five ACIA-designated models; (b) the NCEP/NCAR reanalysis for 1981–2000; (c) the difference between (a) and (b); and (d) the number of models (out of five) in which the simulated annual mean temperature is lower than that of the NCEP/NCAR reanalysis. The bottom row shows seasonal differences between the five-model mean and the NCEP/NCAR reanalysis for (e) winter; (f) spring; (g) summer; and (h) autumn.

in some areas by a factor of two. The reverse is true, however, in the northeastern North Atlantic and parts of northwestern Eurasia, probably because simulated cyclone activity in this area tends to be too weak (see section 4.3.5). The same geographical pattern of biases persists throughout the year, although the magnitude of these biases varies with season. The positive biases relative to the Bryazgin climatology are generally greatest in spring and smallest in summer (Fig. 4.7e-h).

The differences between the simulated precipitation and the observational estimates may be partly due to measurement errors that lead to underestimation of the actual precipitation, particularly when it falls in solid form. However, this clearly cannot explain all the differences in the spatial and seasonal distributions of precipitation. For example, the difference between the five-model area mean and the observational estimates is substantially larger in spring than in winter, in contrast to what might be expected from measurement errors alone.

The ability of AOGCMs (including three of the ACIA-designated models: HadCM3, ECHAM4/OPYC3, and CGCM2) to reproduce the 20th century increase in arctic precipitation has been demonstrated (e.g., Kattsov

trends in 20th century arctic precipitation agree with available observational estimates (see section 2.6.2.2).

Further details on the evaluation of the five ACIA-designated models with respect to simulation of precipitation and other components of arctic hydrology and climatology can be found in Chapter 6.

4.3.5. Other climatic variables

The distribution of the 1981–2000 mean SLP is qualitatively similar between the mean of four of the ACIA-designated models (for GFDL-R30_c, only surface pressure fields were available) and the NCEP/NCAR reanalysis, but there are important differences in details (Fig. 4.8). Surface pressure is the prognostic variable in GCMs, while SLP is diagnosed using different reduction schemes. Some of the variations in SLP between the different models, and between the models and the reanalysis, may be due to the use of different SLP reduction schemes.

The models simulate the main lobes of the annual mean Icelandic and Aleutian lows quite well, but the simulated extension of the Icelandic low towards the Barents Sea is too weak. The positive pressure bias over the eastern

Fig. 4.7. Comparison of precipitation simulated by the ACIA-designated models for 1981–2000 and precipitation from the Bryazgin climatology (Khrol, 1996) for 1936–1990. The top row shows (a) the simulated annual mean precipitation averaged over the five ACIA-designated models; (b) the Bryazgin climatology for 1936–1990; (c) the percentage difference between (a) and (b); and (d) the number of models (out of five) in which the simulated annual mean precipitation exceeds that of the Bryazgin climatology. The bottom row shows seasonal percentage differences between the five-model mean and the Bryazgin climatology for (e) winter; (f) spring; (g) summer; and (h) autumn.

Arctic Ocean and the negative bias in western Eurasia (Fig. 4.8c) suggest that the path of cyclone activity is too far south in the simulations. There also tends to be a slight negative pressure bias in the western Canadian Arctic, which suggests that the simulated cyclone activity is too strong in that region. Winter pressure biases make the greatest contribution to the four-model annual mean pressure biases. However, the positive bias over the eastern Arctic Ocean persists throughout the year. As with temperature and precipitation, the pressure biases also vary between the individual models. The shift of the arctic air mass relative to observations is a well-known feature of both AOGCMs and stand-alone AGCMs (e.g., AMIP; see Box 4.2). The pressure biases contribute to significant differences in wind forcing of sea ice between the AOGCM simulations and the real world, and lead to distortions in simulated spatial distributions of sea ice (see Bitz et al., 2002; Walsh, in press; Walsh et al., 2002).

Cloudiness and the radiative properties of clouds, particularly in the Arctic, remain a major challenge to simulate. Figure 4.9 shows the dramatic scatter between the total cloud amounts simulated by four of the ACIA-designated models (the results from CGCM2 were not available) over

the Arctic Ocean between 70º and 90º N. Two observational estimates, one based primarily on Television and Infrared Observation Satellite Operational Vertical Sounder (TOVS) data (Schweiger et al., 1999) and the other obtained primarily from surface-based observations (Hahn et al., 1995), diverge substantially in late summer and early autumn, but give an idea of the seasonality of arctic cloud cover. While the inter-model scatter is quite large (e.g., the difference between the highest (CSM_1.4) and lowest (GFDL-R30_c) simulations approaches 60% in winter), the four-model mean underestimates cloudiness in the warm season and overestimates it in winter. Of the four ACIA-designated models, only the HadCM3 simulation shows some qualitative agreement with the observed seasonality of arctic cloud cover.

Surface radiative fluxes also vary widely between the models. Figure 4.10 shows the seasonal variation in incident solar radiation as simulated by four of the ACIA-designated models (ECHAM4/OPYC3 data were not available) for the Arctic Ocean between 70º and 90º N and the lone observational estimate obtained from the Langley Atmospheric Sciences Data Center. The four-model mean seasonal cycle is close to the observed one.
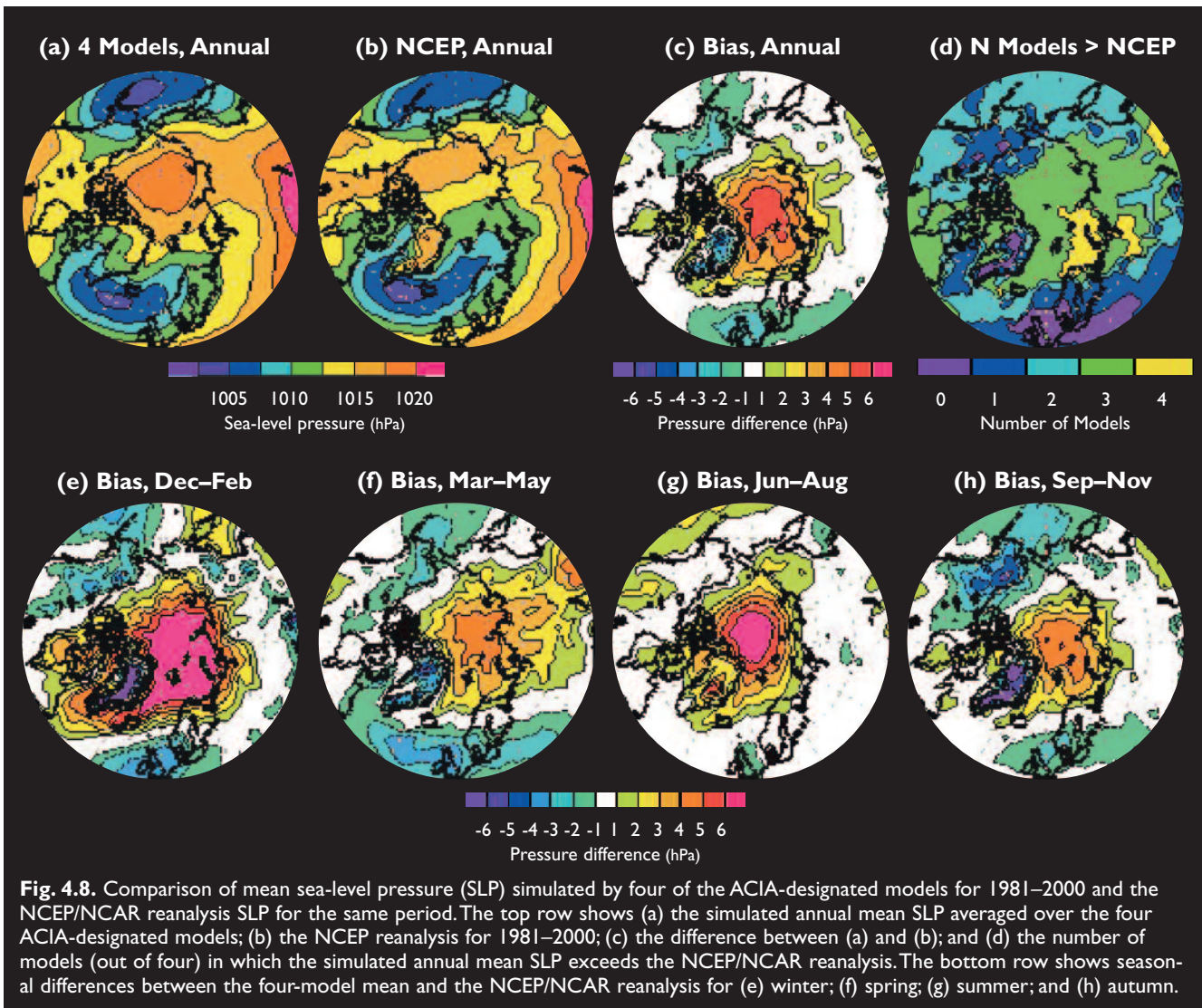
Fig. 4.8. Comparison of mean sea-level pressure (SLP) simulated by four of the ACIA-designated models for 1981–2000 and the NCEP/NCAR reanalysis SLP for the same period. The top row shows (a) the simulated annual mean SLP averaged over the four ACIA-designated models; (b) the NCEP reanalysis for 1981–2000; (c) the difference between (a) and (b); and (d) the number of models (out of four) in which the simulated annual mean SLP exceeds the NCEP/NCAR reanalysis. The bottom row shows seasonal differences between the four-model mean and the NCEP/NCAR reanalysis for (e) winter; (f) spring; (g) summer; and (h) autumn.

In summer, however, the difference between the highest and lowest simulated values (CGCM2 and CSM_1.4, respectively) reaches a maximum of up to 125 W/m^2.

The large inter-model scatter in the ACIA-designated model simulations of baseline (1981–2000) sea-ice and terrestrial snow-cover distributions reflects problems in modeling the cryosphere as discussed in sections 4.2.5 and 4.2.6. Figure 4.11 presents an integrated picture of sea-ice distributions in the Northern Hemisphere as simulated by the five ACIA-designated models for March (maximum observed sea-ice extent) and September (minimum extent). The distribution is represented by the number of models simulating sea ice in each of the 2.5° x 2.5° grid cells. For each model, sea ice is defined as present in a grid cell if its quantity exceeds one of the *ad hoc* critical values (depending on what variable is available from the model output): 5 cm thickness, 45 kg/m^2 mass, or 10% areal coverage. For the greater part of the Arctic Ocean, all five models simulate sea ice in both March and September; however, major differences between the models occur along the margins of the ice cover.

A detailed evaluation of the five ACIA-designated models with respect to simulation of the baseline sea-ice and terrestrial snow-cover distributions in the Northern Hemisphere is provided in sections 6.3.3 and 6.4.3.

4.3.6. Summary

A key characteristic of the simulations of the arctic climate from the ACIA-designated models is their large inter-model scatter. Biases in surface air temperature and SLP spatial distributions and simulation of excessive arctic precipitation are among the most important systematic errors. Significant uncertainty is introduced by the simulated cloudiness – one of the key variables in climate system feedbacks (this is also a problem in the current generation of AOGCMs outside of the Arctic). The large inter-model scatter in reproducing sea-ice and terrestrial snow-cover extent limits the credibility of future climate projections obtained with the models. Conversely, compared to the five individual simulations, the five-model ensemble means show reasonable agreement with available observations, at least for the area averages. The evaluation of the ability of the ACIA-designated AOGCM ensemble to simulate observed climate conditions supports use of the ensemble for constructing 21st-century climate change scenarios for the Arctic. This suitability is further supported by the ability
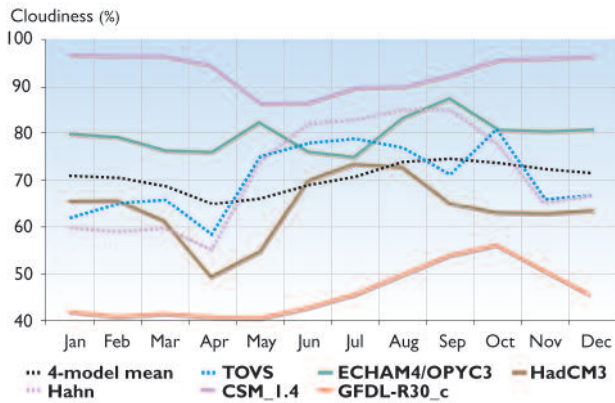
Fig. 4.9. Annual cycle of monthly mean cloudiness over the Arctic Ocean (70°–90° N) for 1981–2000 simulated by four of the ACIA-designated models, and observational estimates from TOVS satellite data and surface observations (Hahn et al., 1995).
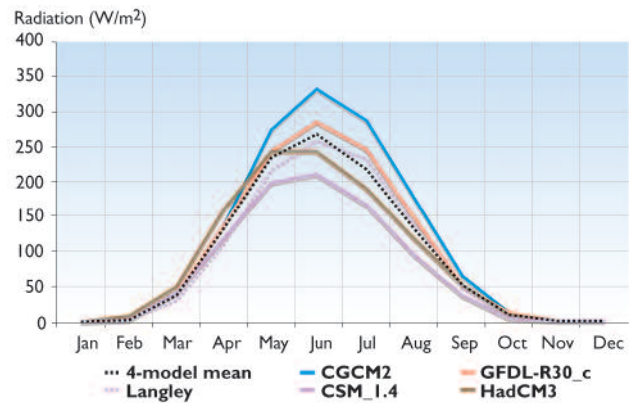
Fig. 4.10. Annual cycle of incident solar radiation at the surface of the Arctic Ocean (70°–90° N) for 1981–2000 simulated by four of the ACIA-designated models, and the observationally based estimate obtained using data from the Langley Atmospheric Sciences Data Center (1983–1991).

of some of the ACIA-designated models, when driven by estimates of historical radiative forcing, to satisfactorily emulate the observed evolution of arctic surface air temperature and precipitation throughout the 20th century, which enhances the credibility of future arctic climate change projected by these models.

As a consequence of the biases and inter-model scatter in AOGCM simulations of the present-day arctic climate, the ACIA has chosen to append (add or subtract) the simulated changes to observed baseline climates as was done, for example, by the National Assessment Synthesis Team (NAST, 2001) rather than to use the model-simulated climates directly in impact studies. The climate changes should be expressed either as absolute differences (e.g., temperature), or as ratios (e.g., precipitation).

4.4. Arctic climate change scenarios for the 21st century projected by the ACIA-designated models

The IPCC Third Assessment Report (IPCC, 2001), based on a set of AOGCM projections, has provided the following global context for the ACIA. For the last three decades of the 21st century (2071–2100), the IPCC (2001) projects a mean increase in globally averaged surface air temperature, relative to the period 1961–1990,

of 3.0 °C (with a range of 1.3–4.5 °C derived from the nine models used by the IPCC) for the A2 emissions scenario and 2.2 °C (with a range of 0.9–3.4 °C) for the B2 emissions scenario. Most of the spatial patterns of the AOGCM-projected responses to the SRES emissions scenarios are similar to other emissions scenarios, including the idealized 1% per year CO_2 increase. The following list summarizes the key projections of climate change over the 21st century by the AOGCMs used in the IPCC (2001) assessment.

- It is very likely that nearly all land areas will warm more rapidly than the global average, particularly during the cold season in northern high latitudes.
- Models project a decrease in the diurnal temperature range in many areas, with nighttime lows increasing more than daytime highs.
- Models project a decrease in Northern Hemisphere snow cover and sea-ice extent, and continued retreat of glaciers and ice caps.
- Projected increases in mean precipitation are likely to lead to increases in interannual precipitation variability.
- Increases in the lowest daily minimum temperatures are projected to occur over nearly all land areas and are generally greatest in areas where snow and ice retreat.
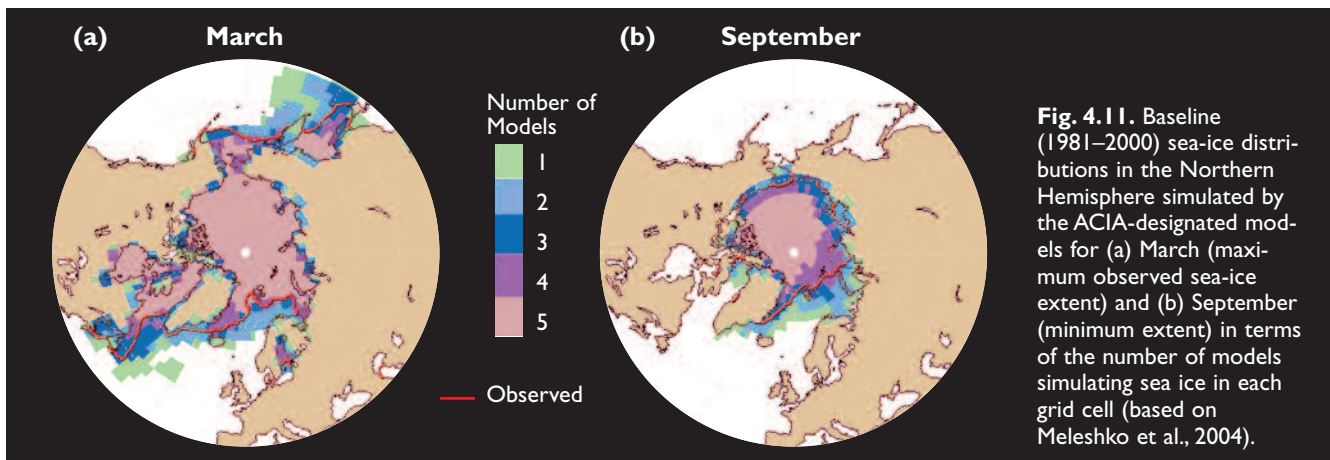
Fig. 4.11. Baseline (1981–2000) sea-ice distributions in the Northern Hemisphere simulated by the ACIA-designated models for (a) March (maximum observed sea-ice extent) and (b) September (minimum extent) in terms of the number of models simulating sea ice in each grid cell (based on Meleshko et al., 2004).

Box 4.3. Uncertainties in climate change scenarios based on AOGCM simulations

Uncertainties in future GHG and aerosol emissions, their conversion to atmospheric concentrations, and their contribution to radiative forcing of the climate. Different assumptions about future social and economic development, and hence future GHG and aerosol emissions, comprise one of the major uncertainties in the climate change scenarios. For example, the IPCC Special Report on Emissions Scenarios (Nakićenović and Swart, 2000; see also section 4.4.1) presents 40 different emissions scenarios. Uncertainty is also associated with the conversion of emissions into atmospheric GHG and aerosol concentrations. Additional uncertainty arises from the calculation of radiative forcing associated with given concentrations, which occurs implicitly within AOGCMs, but is problematic in particular for aerosols.

Uncertainties in the global and regional climate responses to a radiative forcing from different AOGCM simulations. Due to different representations of processes and feedbacks in the climate system (e.g., Stocker et al., 2001), or by excluding some of them, AOGCMs differ in their sensitivity to the same radiative forcing. Sometimes, the difference in AOGCM sensitivity manifests itself only in projected regional climate change patterns, while the magnitudes of projected global mean changes remain similar between models. At long timescales, the forcing uncertainty (differences between emissions scenarios) and model uncertainty are of approximately equal importance.

Uncertainties due to insufficient AOGCM resolution and different methods of regionalizing (downscaling) AOGCM results. Insufficient AOGCM resolution limits direct use of their outputs in impact assessments. In most cases, a climate scenario for a certain region requires a combination of the simulated variables and observed data, which may be accomplished with different methods. In addition, observational data often fail to capture the full range of decadal-scale natural variability. Finally, gridding the observational data in order to create baseline climatologies can introduce errors. Employing regional climate models to enhance the spatial and temporal resolution of AOGCM outputs introduces further uncertainties arising from individual features of the RCMs. In principle, by employing a range of downscaling methods, quantification of this class of uncertainties is possible, but this is seldom done (Mearns et al., 2001).

Uncertainties due to forced and unforced natural variability. In addition to anthropogenic forcing, climate change in the real world is affected by largely unpredictable natural variability. Part of the natural variability is thought to be due to variations in solar and volcanic activity, but a substantial part is unforced, resulting from the internal dynamics of the climate system. Climate models also simulate unforced natural variability, such that, when the same model is run with the same forcing scenario but different initial conditions, there are non-negligible differences in the results, particularly in regional details that are affected by internal variability much more than global means. When different models are run using the same forcing scenario, some of the differences in their results arise from different realizations of natural variability.

- Frost days and cold waves are very likely to become fewer.
- High extremes of precipitation are projected to increase more than the mean, and the intensity of precipitation events is projected to increase.
- The frequency of extreme precipitation events is projected to increase almost everywhere.
- For some other extreme phenomena, many of which may have important impacts on the environment and society, the confidence in model projections and understanding is currently inadequate to make firm projections.
- No clear consensus has been reached about how extratropical cyclones are likely to change, as the results differ between the relatively few studies that have been conducted.
- Most AOGCMs project a weakening of the Northern Hemisphere thermohaline circulation, which would contribute to a reduction of surface warming in the subarctic North Atlantic.
- There is no clear agreement on likely changes in the probability distribution or structure of natural modes of variability, like the North Atlantic Oscillation (NAO) or the Arctic Oscillation (AO),

whose magnitude and character changes vary across the models.

Box 4.3 reviews some of the major uncertainties associated with AOGCM projections.

In this section, the Arctic is considered in the context of the 21st-century global climate change projections listed previously, focusing on surface air temperature and precipitation in the Arctic and the inter-model differences for the A2 and B2 emissions scenarios. All changes are compared to the ACIA climatological baseline (1981–2000). A wider context of climate change simulations is provided by comparing the behavior of the five ACIA-designated AOGCMs in Phase 2 of the Coupled Model Intercomparison Project (CMIP2: Meehl et al., 2000) with the other 14 models included in that project.

4.4.1. Emissions scenarios

Emissions scenarios are plausible representations of the future development of emissions of radiatively active substances (GHGs, aerosols), based on a coherent and internally consistent set of assumptions about demo-
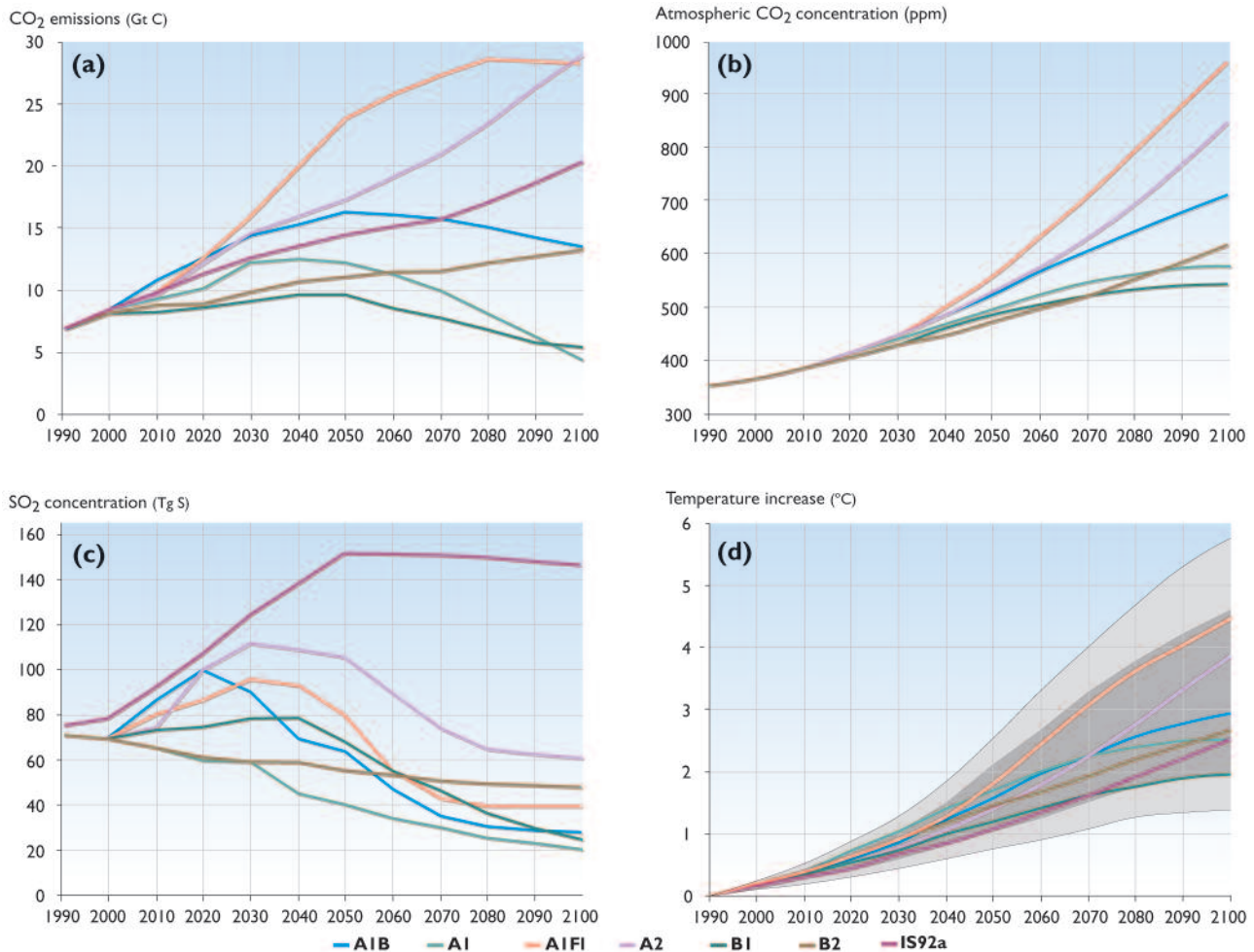
Fig. 4.12. Comparison of the six SRES marker scenarios and the IS92a scenario showing (a) CO_2 emissions; (b) the resulting atmospheric CO_2 concentrations; (c) sulfur dioxide (SO_2) emissions; and (d) projections of global mean temperature increases relative to 1990. In (d), the projected temperature increase for each emissions scenario is an average of the results of the seven climate models used by IPCC (2001). The dark shading represents the range of average warming across all 40 SRES scenarios, and the light shading the range across all scenarios and models (based on IPCC, 2001).

graphic, socioeconomic, and technological changes and their key relationships in the future. Emissions scenarios are converted into concentration scenarios that are used as input for climate model projections.

In idealized transient experiments (e.g., CMIP2, see Box 4.2), the atmospheric CO_2 concentration increases gradually, usually at a rate of 1% (compound) per year, which results in a doubling of its concentration in 70 years. The 1% idealized scenario lies at the high end of the SRES scenarios.

In transient experiments with a detailed forcing scenario, the concentrations of CO_2 and other GHGs such as methane and nitrous oxide are prescribed as a function of time, based on an emissions scenario for these gases. Frequently, sulfate aerosols are also included. Examples of the scenarios used in model simulations include the IPCC IS92 scenarios (Leggett et al., 1992) and the more recent SRES scenarios (Nakićenović and Swart, 2000).

The SRES emissions scenarios were built around four narrative storylines that describe the evolution of the world in the 21st century. Altogether, 40 different emis-

sions scenarios were constructed. Six of these (A1B, A1T, A1FI, A2, B1, and B2) were chosen by the IPCC as illustrative "marker" scenarios. The SRES scenarios include no additional mitigation initiatives, which means that no scenarios are included that explicitly assume the implementation of the United Nations Framework Convention on Climate Change or the emission targets of the Kyoto Protocol.

The greatest difference between the SRES scenarios and the earlier IS92 scenarios relates to sulfur emissions and hence sulfate aerosol concentrations. The commonly adopted intermediate IS92 scenario (IS92a) assumed a doubling of anthropogenic sulfur emissions between 1990 and 2050, and little change in emissions thereafter. In contrast, all six illustrative SRES scenarios project lower sulfur emissions in 2100 than at present, although some include an increase over the next few decades. The lower sulfur emissions together with higher GHG emissions in some of the SRES scenarios are the main reason for the upward shift in the IPCC projections of the increase in global mean temperature between 1990 and 2100 from 1.0 to 3.5 °C in the Second Assessment Report (IPCC, 1996) to 1.4 to 5.8 °C in the Third

Assessment Report (IPCC, 2001). The CO_2 emissions and the derived atmospheric CO_2 concentrations, the sulfur dioxide (SO_2) emissions, and projections of global mean temperature increases for the SRES marker scenarios and for the IS92a scenario are shown in Fig. 4.12.

No probabilities are assigned to the various SRES scenarios. During the initial stage of the ACIA process, to stay coordinated with current IPCC efforts, it was agreed that the ACIA projections would be based on the IPCC SRES scenarios (Källén et al., 2001). By that time, most of the available (and expected to be shortly available) AOGCM simulations to be relied upon had been forced by two emissions scenarios: A2 and B2 (Cubasch et al., 2001). Globally, the model mean transient climate responses to the A2 and B2 emissions scenarios are close to each other for each of the different models through the first half of the 21st century and only diverge significantly after that. Given the schedule for producing this assessment and the limits of resources for data storage, the B2 emissions scenario was chosen as the primary scenario for use in ACIA impact analyses.

In a number of studies (e.g., Carter et al., 2000; Ruosteenoja et al., 2003), a "pattern-scaling" technique is applied to represent a wider range of possible future forcings than are available from AOGCM simulations alone. In particular, Ruosteenoja et al. (2003) extrapolated available A2 and B2 AOGCM projections of temperature and precipitation for the SRES B1 and A1FI scenarios over 32 world regions, including the Arctic. The application of this technique is based on the assumption that the spatial pattern of the response is independent of the forcing, while the amplitude of the response at each location is linearly proportional to the global mean change in surface air temperature. The global mean temperature changes for the entire range of SRES scenarios (as shown by shading in Fig. 4.12d) were calculated using a simple climate model system (Box 4.1) calibrated to be consistent with each AOGCM being emulated. Additional assumptions of this approach, first suggested by Santer et al. (1990), are that the patterns of the climate response to anthropogenic forcing can be adequately defined from AOGCM simulations and that they are stable through time and across a representative range of possible anthropogenic forcings. Uncertainties due to scaling climate response patterns increase for scenarios that include substantial, regionally differentiated aerosol forcings and in regions where there is an enhanced response, for example, near sea-ice and snow margins (Carter et al., 2000).

Box 4.4 discusses specific issues related to the use of the ACIA-designated model projections as a basis for local scenarios.

4.4.2. Changes in surface air temperature

Figure 4.13 displays the evolution of arctic annual mean temperature during the 21st century projected by the five ACIA-designated model simulations using the B2 emissions scenario. The projections for the 60° to 90° N polar region are shown along with the range of global mean temperature changes projected by the same simulations. In the five ACIA-designated model projections, by the late 21st century (2071–2090), the global mean temperature increase (from the 1981–2000 baseline) varies from 1.4 °C (CSM_1.4) to 2.1 °C (ECHAM4/OPYC3 and CGCM2), with a five-model average of 1.9 °C. In the Arctic, the increase in mean annual temperature projected by the five models is significantly larger, reaching 3.7 °C (twice the increase in the global mean) for the area north of 60° N. The projected temperature change varies by about ±25% about the mean of the five models. For the Arctic north of 60° N, the projected area mean temperature increase by 2071–2090 ranges from 2.8 °C (CSM_1.4) to 4.6 °C (ECHAM4/OPYC3), with the other models within the 3.7 to 4.0 °C range (Table 4.3). The projected arctic mean temperature increase exceeds the projected global mean temperature increase in all of the models.

In Fig. 4.14, spatial patterns of projected increases in the annual mean temperature in the Arctic are put in a global perspective for the three 21st-century time slices. On average, the models project a greater temperature increase at high northern latitudes than anywhere else in the world (Fig. 4.14, left column). By 2071–2090, the five-model average projected increase in the mean annual temperature in the central Arctic is more than 5 °C (about three times the global mean). By that time, the mean annual temperature is projected to increase by around 3 °C in Scandinavia and East Greenland, about 2 °C in Iceland, and up to 5 °C in the Canadian Archipelago and Russian Arctic. However, the variation in projected temperature change between the individual models is also generally much larger over the Arctic than for most other regions of the globe (Fig. 4.14, middle column). The standard deviation of the mean temperature change averaged over the five models also varies substantially across the Arctic, but these variations are difficult to interpret because there are only five models in the sample. The relative agreement between the different projections is measured by the ratio between the

Table 4.3. Increases in mean annual surface air temperature in the Arctic (60°–90° N) compared to the 1981–2000 baseline, as projected by the five ACIA-designated models forced with the B2 emissions scenario (Kattsov et al., 2003).

|	CGCM2	CSM_1.4	ECHAM4/OPYC3	GFDL-R30_c	HadCM3	Five-model mean
			Temperature change (°C)			
2011–2030	1.2	1.5	1.3	1.0	1.1	1.2
2041–2060	2.5	2.2	3.2	2.5	2.2	2.5
2071–2090	3.7	2.8	4.6	3.8	4.0	3.7

Box 4.4. Specific issues related to the use of ACIA-designated AOGCM projections as a basis for local scenarios

There are two basic approaches for applying climate change projections in impact studies: deterministic and probabilistic. In the deterministic approach, a single best-guess projection of climate change is used for impact modeling. The simplest way of making a best-guess projection, which is based on the assumption that all models give equally likely results, is to use the arithmetic mean of all available model results (such as the mean of the five ACIA simulations). In the probabilistic approach, in contrast, the projections from different climate models are treated as giving a probability distribution of future climate changes (Giorgi and Mearns, 2003; Palmer and Räisänen, 2002; Räisänen and Palmer, 2001). With this approach, each climate model projection is used separately in an impact analysis. If averaging of different scenarios is performed, it is done in the last phase: the calculated impacts, rather than the climate change projections, are averaged. Because the impacts may depend nonlinearly on changes in climate, the average impact scenario derived by the probabilistic method may differ from the impact scenario obtained by using the average climate change projection. For this reason and because information on uncertainty of the impacts is also important, the probabilistic approach is, in principle, preferable to the deterministic approach. However, it is also more demanding in terms of the computations required.

The simplest variants of both deterministic and probabilistic methods assume that all available climate model results are equally likely. In some situations, this simple assumption may be questionable. For example, when models have serious problems in their control climates, it may be best to exclude them from the calculations. Furthermore, for some situations different models may give such widely divergent results that a deterministic averaging may be misleading. Examples of situations in which local scenario construction requires special care include the following.

- Climate changes in the North Atlantic depend to a high degree on the state of the ocean circulation. Some models project a significantly reduced thermohaline circulation as a consequence of climate change, while oth-

five-model mean change and the inter-projection standard deviation (Fig. 4.14, right column). Because the large standard deviations compensate for the large average warming, this signal-to-noise ratio in the Arctic is not exceptional. Very high relative agreement (mean exceeding the standard deviation by a factor of six) occurs by 2071–2090 in some (but not all) arctic regions, but this is also the case in lower latitudes where both the mean and the standard deviation are smaller.
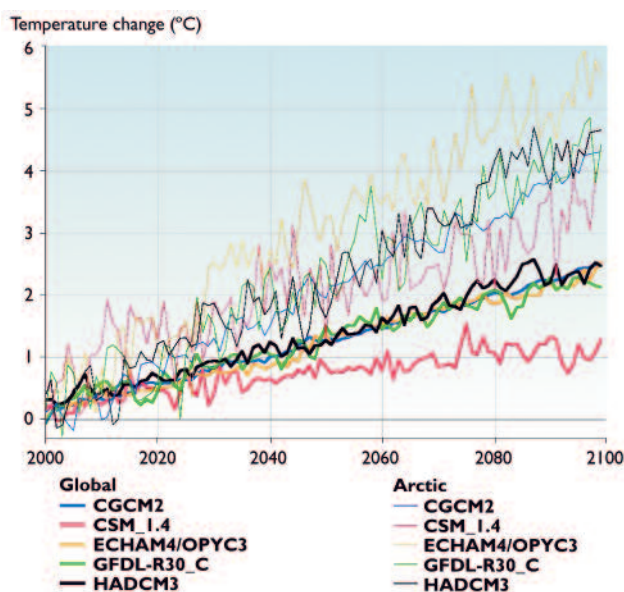
Fig. 4.13. Global and arctic (60°–90° N) changes in annual mean surface air temperature relative to the baseline period 1981–2000 as projected by the five ACIA-designated models forced with the B2 emissions scenario.

The differences in temperature change between the five ACIA-designated simulations are caused primarily by model differences and by noise associated with internal variability. To investigate the role of the latter factor alone, the five-model mean temperature changes were compared with the variability of 20-year mean temperatures generated in CMIP2 control simulations. The signal-to-noise ratio that was estimated by dividing the average warming by $\sqrt{2}$ times the standard deviation of 20-year means is shown in Fig. 4.15. The ratios are generally higher than those in Fig. 4.14, because internal variability does not cause all differences between the ACIA-designated simulations. Importantly, however, the ratio is still relatively low (<2) in some parts of the Arctic in the period 2011–2030. Because a ratio of two defines the lower limit of statistical significance, this suggests that, at least in some parts of the Arctic, the GHG-induced temperature increase may remain difficult to differentiate from natural variability over the next few decades. Indeed, the real signal-to-noise ratio might be even lower than calculated here, because the CMIP2 simulations exclude external sources of natural variability. Later in the 21st century, the signal-to-noise ratio increases, but remains generally lower in the Arctic than at low latitudes, where the internal variability is much smaller. Thus, despite the large average warming suggested by these simulations, the Arctic might not be the area where anthropogenic climate changes are easiest to detect.

Together, the results in Figs. 4.14 and 4.15 emphasize the importance of improving understanding of how best to interpret the relatively large arctic warming in the

ers do not. It is currently not possible to determine which scenario is most likely. In this case, arithmetic averaging of the ACIA-designated model simulations may not be meaningful. It makes more sense to consider all or at least two scenarios separately: one with and one without a significantly reduced thermohaline circulation (see also Box 4.5).

• The Barents Sea is currently ice-free throughout the year, mainly as a result of the northward flow of warm Atlantic water into the region. Models that simulate an ice-covered Barents Sea for the present-day climate and near ice-free conditions in a climate change scenario will therefore highly overestimate the amplitude of local warming in the region. In this situation, only model realizations with a realistic sea-ice distribution in the baseline simulation should be used for a scenario of future climate change.

• Sea ice is generally not well handled by AOGCMs, and this is also the case for the ACIA-designated models. Specifically, problems relate to their simulation of major polynyas and differences in larger-scale ice cover. For these areas, future climate change cannot be projected using any specific model or a combination of models. Given the present state of modeling, expert judgment has to be used in combination with the model projections.

• Snow cover during winter is reasonably well represented in the Arctic in all of the ACIA-designated models. However, in both of the transition seasons, as well as during summer, some models exhibit an unrealistically extensive snow pack for the present-day climate, and then complete absence of snow for some regions in a climate change scenario. As a consequence, these simulations project temperature increases that are too large in these regions. In this situation, only model realizations with a realistic seasonal distribution of snow cover in the baseline simulation should be used for scenarios of future climate change.

light of simulation and projection uncertainties. This issue is discussed further in section 4.7.

Figure 4.16 displays spatial distributions of seasonal temperature changes in the Arctic for the three 21st-century time slices. The five-model mean projected temperature

Fig. 4.14. Changes in annual mean temperature projected by the ACIA-designated models for the early (top row), middle (center row), and late (bottom row) 21st century, as compared to the ACIA baseline (1981–2000). From left to right: five-model mean change; the inter-projection standard deviation; and the ratio between the mean and the standard deviation.

Fig. 4.15. The ratio between the ACIA five-model average projected change in mean annual temperature and √2 times the standard deviation of 20-year mean temperatures in the CMIP2 control simulations.

Fig. 4.16. Seasonal changes in surface air temperature averaged over the five ACIA-designated B2 projections. Top: 2011–2030; middle: 2041-2060; bottom: 2071-2090.

Ocean in summer remain below 1 ºC, because the temperature is held close to the freezing point by the presence of melting ice in both the control and the climate change simulations. The contrast between larger temperature increases in autumn and winter and smaller temperature increases in summer also extends to the surrounding land areas, but is less pronounced there. In summer, projected temperature increases over northern Eurasia and northern North America are larger than over the Arctic Ocean, while in winter the reverse is projected.

The spatial patterns of projected climate change within the Arctic also differ markedly between the individual models, so that, at any single location, the scatter of the model results is larger than it is for change in the arctic

increase over the central Arctic Ocean is greatest in autumn (up to 9 ºC by 2071–2090), when the air temperature reacts strongly to reduced sea-ice cover and thickness. Average autumn and winter temperatures are projected to rise by 3 to 5 ºC over most arctic land areas. By contrast, projected temperature increases over the Arctic

Fig. 4.17. Projected changes in mean annual surface air temperature in the Arctic (60°–90° N) for the A2 and B2 emissions scenarios, relative to 1981–2000. A binomial approximation is used to smooth the original mean of the four ACIA-designated model projections (CGCM2, ECHAM/OPYC3, GFDL-R30_c, and HadCM3) for each emissions scenario.

Fig. 4.18. Global and arctic (60°–90° N) percentage change in mean annual precipitation relative to the baseline period (1981–2000) projected by the five ACIA-designated models forced with the B2 emissions scenario.

Box 4.5. The Atlantic meridional overturning circulation in the 21st century

Evidence from paleoclimate records indicates that the Earth underwent large and rapid climate changes during the last glacial and early postglacial periods. The origin of the abrupt changes is being closely studied. A number of studies suggest that the Atlantic meridional overturning circulation (MOC), as part of the global thermohaline circulation, played an active and important role in these rapid climate transitions (e.g., Broecker, 1997; Ganopolski and Rahmstorf, 2001). Furthermore, modeling studies agree that the Atlantic surface freshwater balance is a key control parameter for the strength and variability of the Atlantic MOC. A common finding from idealized models and AOGCMs is that the strength of the Atlantic MOC decreases if the net flux of freshwater to the high northern latitudes increases (Manabe and Stouffer, 1997; Otterå et al., 2003; Rind et al., 2001; Schiller et al., 1997; Vellinga et al., 2002).

Increased precipitation at high northern latitudes is commonly projected by AOGCM simulations forced with increasing GHG concentrations (e.g., Räisänen, 2001). There is also recent observational evidence of intensification of the hydrological cycle at high northern latitudes (Curry R. et al., 2003; Dickson et al., 2002; Peterson et al., 2002). This raises questions about whether the Atlantic MOC will weaken in the 21st century, and what the likelihood is of a full shutdown of the Atlantic MOC.

Most AOGCMs forced with prescribed scenarios of the major GHG concentrations and aerosol particle distributions project a weakening of the MOC. The projected changes in the maximum strength of the Atlantic MOC by the end of the 21st century range from about zero to a reduction of 30 to 50% (Cubasch et al., 2001). The projected changes, if any, typically start around 2000 and show a quasi-linear trend thereafter. Irrespective of model differences in the sensitivity of the simulated Atlantic MOC to global climate change, no AOGCM has yet projected a shutdown of the Atlantic MOC by 2100 (Cubasch et al., 2001).

The present generation of AOGCMs used for these simulations does not include freshwater runoff from melting ice sheets and glaciers; therefore, it is possible that the model MOC sensitivity to global climate change is too weak. However, sensitivity experiments with freshwater artificially added to high northern latitudes indicate that fluxes corresponding to several times the present-day freshwater input are required to significantly alter the Atlantic MOC (Manabe and Stouffer, 1997; Otterå et al., 2003; Schiller et al., 1997; Vellinga et al., 2002), so this shortcoming may not be significant. As a result, the IPCC Third Assessment Report (Cubasch et al., 2001) concluded that it is unlikely that the Atlantic MOC will experience a shutdown in the 21st century. It is also likely that the major part of the North Atlantic–Nordic Seas region will experience warming throughout the 21st century, even with a weakened Atlantic MOC.

area mean temperature. However, all of the models project substantially smaller temperature increases over the northern North Atlantic sector than for other parts of the Arctic. In this area of the sinking branch of the Atlantic thermohaline circulation, the ocean is well mixed to a great depth. Therefore, much of the GHG-induced heating is devoted to warming the deeper ocean, rather than to warming the surface water. The warming is further reduced because the thermohaline circulation weakens in most of the model projections, transporting less warm water from the subtropical regions to the northern North Atlantic. The different degree of projected weakening of the thermohaline circulation in the models presents a special problem for scenario development for the North Atlantic area (see Boxes 4.4 and 4.5).

A comparison between changes in mean annual surface air temperature in the area north of 60º N projected by four of the ACIA-designated models (CGCM2, ECHAM4/OPYC3, GFDL-R30_C, and HadCM3) for the A2 and B2 emissions scenarios is shown in Fig. 4.17. The difference between the two scenarios is not dramatic during the first half of the 21st century, but becomes more systematic and significant during the second half of the century. These differences between the projected A2 and B2 arctic area-averaged temperature increases do not exceed the differences between the highest and lowest projections from the different ACIA-designated AOGCMs.

4.4.3. Changes in precipitation

Table 4.4. Percentage increases in mean annual precipitation in the Arctic (60°–90° N) compared to the 1981–2000 baseline, as projected by the five ACIA-designated models forced with the B2 emissions scenario (from Kattsov et al., 2003).

	Precipitation increase (%)					
	CGCM2	CSM_1.4	ECHAM4/OPYC3	GFDL-R30_c	HadCM3	Five-model mean
2011–2030	2.3	8.3	5.1	3.0	4.0	4.3
2041–2060	4.6	8.3	12.3	7.4	7.3	7.9
2071–2090	7.5	14.0	18.1	11.9	12.9	12.3

Fig. 4.19. Changes in mean annual precipitation projected by the ACIA-designated models for the early (top), middle (center), and late (bottom) 21st century, as a percentage of baseline (1981–2000) values. From left to right: five-model mean change; the inter-projection standard deviation; and the ratio between the mean and the standard deviation.
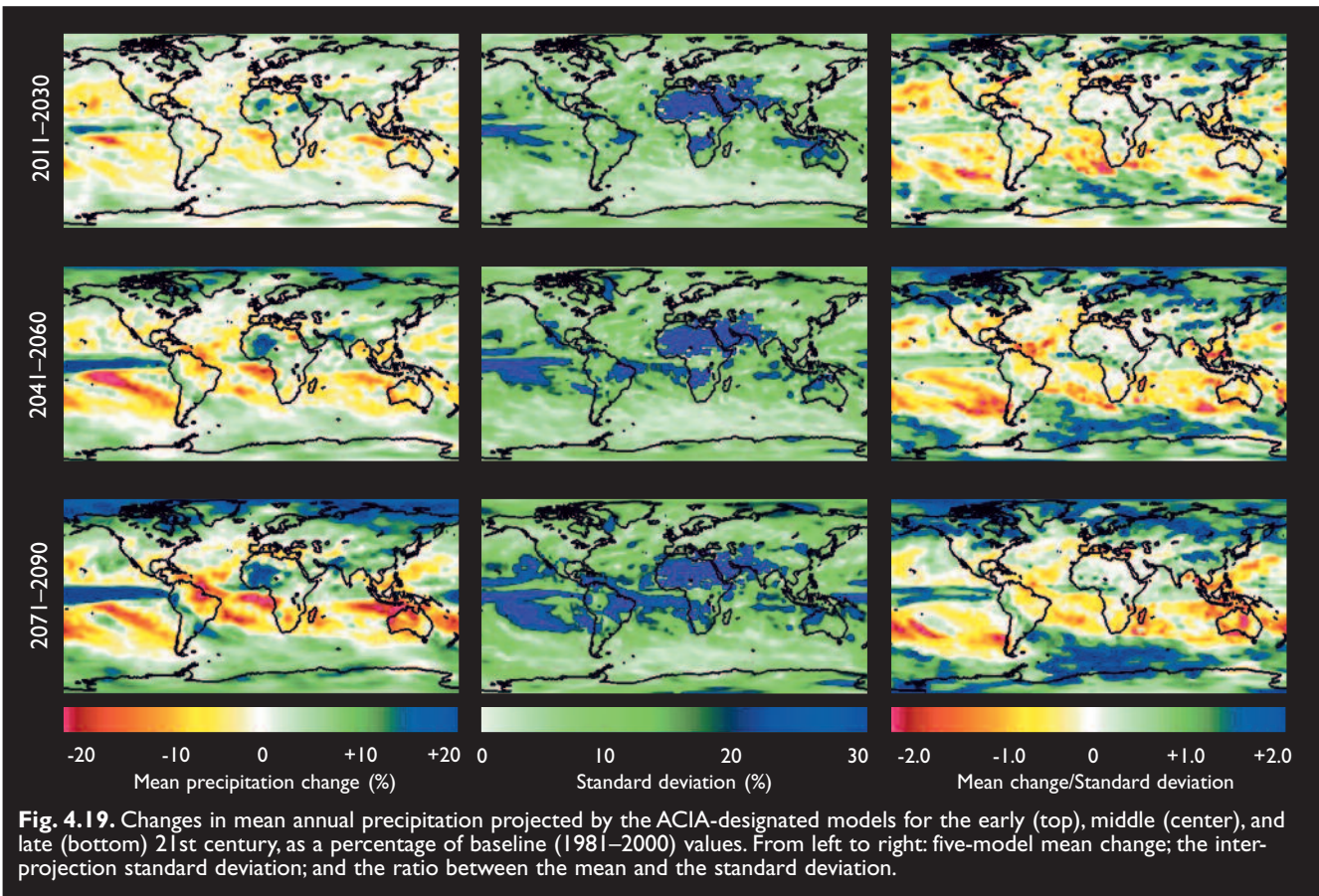
Increases in arctic and global mean annual precipitation over the 21st century projected by the five ACIA-designated models forced with the B2 emissions scenario are displayed in Fig. 4.18. By the end of the 21st century (2071–2090), the projected change in global mean precipitation varies from 1.4% (ECHAM4/OPYC3) to 4.7% (GFDL-R30_C), with a mean of 2.5%. The Arctic Ocean and terrestrial arctic regions of North America and

Eurasia are among the areas with the greatest projected percentage increase in precipitation. The general increase in high-latitude precipitation is a robust and qualitatively well-understood result from climate change experiments. With increasing temperature, the ability of the atmospheric circulation to transport moisture from lower to higher latitudes increases, leading to an increase in precipitation in the polar areas where the local evaporation is relatively small (e.g., Manabe and Wetherald, 1975).

For the area north of 60º N, all five models simulate an increase in annual precipitation by 2071–2090, which varies from 7.5% (CGCM2) to 18.1% (ECHAM4/OPYC3), and from 12 to 14% in the other models (Table 4.4). The differences between the models increase rapidly as the spatial domain becomes smaller.

The spatial distribution of the projected mean annual precipitation changes (five-model average) is shown in the left column of Fig. 4.19. By 2071–2090, projected precipitation increases in the Arctic vary from about 5 to 10% in the Atlantic sector to up to 35% locally in the high Arctic. Most of the projected increase in precipitation is due to increasing atmospheric water vapor convergence, which apparently results from the ability of a warmer atmosphere to transport more water vapor from lower to higher latitudes. The increased water vapor convergence is particularly important for precipitation in the high Arctic, where the local evaporation is small (see section 6.2). Although evaporation is projected to increase slightly in most of the Arctic, the change is near zero (or

Fig. 4.20. Seasonal percentage changes in precipitation averaged over the five ACIA-designated B2 projections. Top: 2011–2030; middle: 2041–2060; bottom: 2071–2090.
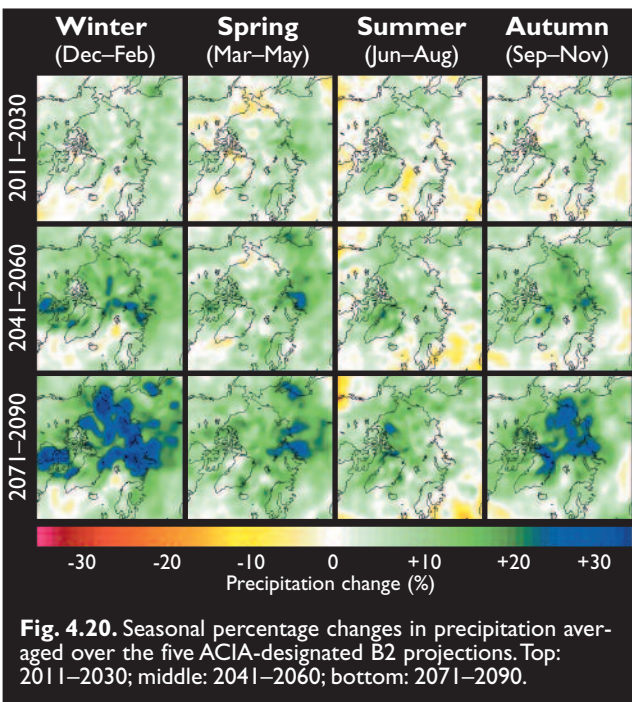
even negative) in the Atlantic sector, where the change in sea-surface temperature is small. Unlike surface air temperature, the ratio between the five-model mean precipitation change and the inter-model standard deviation (middle column) is larger in the Arctic than almost anywhere else (right column), with comparable agreement only at high southern latitudes. Nevertheless, the relative agreement between models is worse for precipitation than temperature changes.

Similar to projected temperature increases, the projected increase in precipitation is generally greatest in autumn and winter and smallest in summer (Fig. 4.20), but the summer minimum is less pronounced than that of temperature change.

The four-model projected changes in mean annual precipitation for the area north of 60° N (Fig. 4.21) behave similarly to temperature. The difference between the A2 and B2 scenarios is small in the first half of the 21st century. Later in the century, the difference increases and is systematic (i.e., shown in all models), but does not exceed the inter-model scatter.

4.4.4. Changes in other variables

The average projected changes in mean seasonal and annual sea-level pressure are shown in Fig. 4.22. Throughout the year, there is a slight projected decrease in pressure in the polar region, suggesting a shift toward the positive phase of the AO. However, the changes are small. Even in winter, when the projected decrease in sea-level pressure over the central Arctic is greatest, this amounts to only 4 hPa. The changes projected by individual models are larger, but vary widely, especially in winter. While many impact studies would benefit from projections of wind characteristics and storm tracks in the Arctic, the available analyses in the literature are
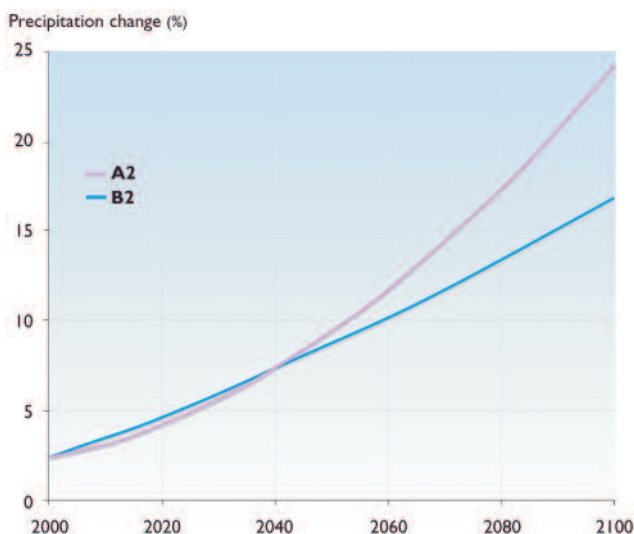
insufficient to justify any firm conclusions about their possible changes in the 21st century.

Changes in cloud cover over the Arctic are small but systematic. By 2071–2090, the five-model average projects an increase in mean annual cloud cover. This is accompanied by a projected decrease (four-model average) in the mean incident short wave radiation. In summer, this flux is projected to decrease across the Arctic by more than $10\,W/m^2$ by 2071–2090 compared to the baseline (1981–2000).

The ACIA-designated models agree in their projections of decreases in sea-ice and terrestrial snow extents during the 21st century, as well as general increases both in precipitation minus evaporation over the marine Arctic and in river discharge to the Arctic Ocean from the surrounding terrestrial watersheds. The projected cryospheric and hydrological changes are quantified and discussed in detail in Chapter 6.

4.4.5. ACIA-designated models in the CMIP2 exercise

The five ACIA-designated models also participated in the CMIP2 intercomparison (Meehl et al., 2000), together with 14 other models. The model versions used in the CMIP2 simulations are in two cases (CGCM and CSM) slightly different from the ACIA-designated model versions, but this is unlikely to have any substantial influence on the comparison. The CMIP2 intercomparison helps to place the ACIA-designated model results in the broader context of model behavior. The climate changes in the CMIP2 simulations (Table 4.5) are examined for the 20-year period centered on the year when atmo-

Fig. 4.21. Projected percentage changes in mean annual precipitation in the Arctic (60°–90° N) for the A2 and B2 emissions scenarios, relative to 1981–2000. A binomial approximation has been applied to the original mean of the four ACIA-designated model projections (CGCM2, ECHAM/OPYC3, GFDL-R30_c, and HadCM3) for each emissions scenario
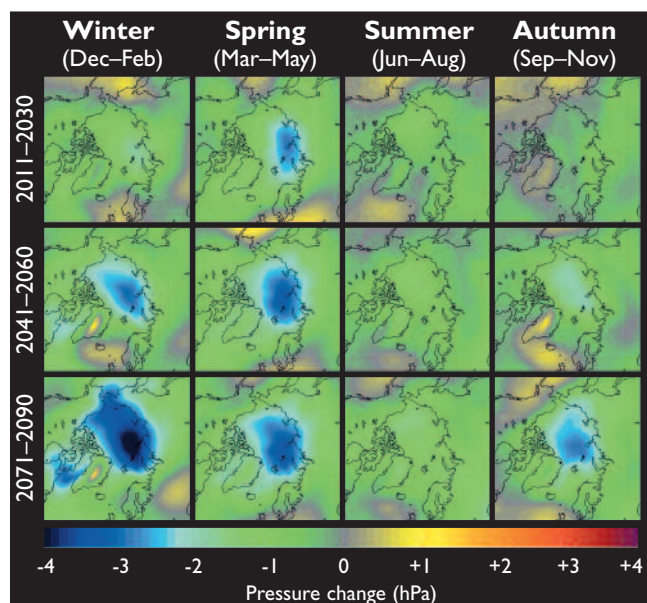

Fig. 4.22. Seasonal changes in mean sea-level pressure averaged over the five ACIA-designated B2 projections. For GFDL-R30_c, the variable used is surface pressure change, rather than sea-level pressure.

Table 4.5. The 19 models participating in the CMIP2 intercomparison, with the five ACIA models shown in bold. The first column provides the symbol used in Figure 4.23.

	Model acronym	Institution	Reference
A	BMRC	Bureau of Meteorology Research Center	Power et al., 1993
B	**CCCma[a]**	**Canadian Centre for Climate Modelling and Analysis**	**Flato et al., 2000**
C	CCSR1	Center for Climate System Research	Emori et al., 1999
D	CCSR2	Center for Climate System Research	Nozawa et al., 2000
E	CERFACS	Centre Européen de Reserche et de Formation Avancée en Calcul Scientifique	Barthelet et al., 1998
F	CSIRO	Commonwealth Scientific and Industrial Research Organization	Hirst et al., 2000
G	ECHAM3	Max-Planck Institute for Meteorology	Voss et al., 1998
H	**ECHAM4/OPYC3**	**Max-Planck Institute for Meteorology**	**Roeckner et al., 1999**
I	GFDL-R15	Geophysical Fluid Dynamics Laboratory	Manabe et al., 1991
J	**GFDL-R30_c**	**Geophysical Fluid Dynamics Laboratory**	**Knutson et al., 1999**
K	GISS	Goddard Institute for Space Studies	Russell and Rind, 1999
L	HadCM2	Hadley Centre for Climate Prediction and Research	Johns et al., 1997
M	**HadCM3**	**Hadley Centre for Climate Prediction and Research**	**Gordon et al., 2000**
N	IAP/LASG	Institute of Atmospheric Physics, Chinese Academy of Sciences	Zhang et al., 2000
O	LMD/IPSL	Laboratoire de Météorologie Dynamique, Institut Pierre Simon Laplace	Braconnot et al., 1997
P	MRI1	Meteorological Research Institute	Tokioka et al., 1995
Q	MRI2	Meteorological Research Institute	Yukimoto et al., 2000
R	**NCAR-CSM[a]**	**National Center for Atmospheric Research**	**Boville and Gent, 1998**
S	NCAR/DOE-PCM	National Center for Atmospheric Research/ Department of Energy	Washington et al., 2000

[a]An earlier model version than that used by the ACIA participated in the CMIP2 intercomparison.

spheric CO_2 doubles in the simulations, which takes 70 years in these idealized experiments.

Figure 4.23a shows the global and arctic (60º–90º N) mean temperature changes in the CMIP2 simulations. Models located above the diagonal dashed line project greater temperature increases in the Arctic than globally, while models below the dashed line project the reverse. The global temperature increase varies from 1.1 ºC (MRI2) to 3.1 ºC (CCSR2), with a mean of 1.75 ºC. The mean value for the five ACIA-designated models is very similar but the spread is smaller, 1.4 to 2.0 ºC. The 19-model average projected increase in mean annual temperature in the Arctic (60º–90º N) is 3.4 ºC (twice the global mean), and for the five ACIA-designated models the projected arctic temperature increase is 3.6 ºC. Again, the range of the five ACIA-designated model projections (3.1–4.1 ºC) is much smaller than the total range (1.5–7.6 ºC) of all 19 CMIP2 simulations. However, individual outliers contribute substantially to the large range in the CMIP2 results.

Similar conclusions are valid for the projected change in arctic mean precipitation (Fig. 4.23b). The full range of projected precipitation change in the 19 models (4–24%) is wider than the range in the five ACIA-designated models (8–15%), but the 5-model and the 19-model means are both 11%. The larger set of models
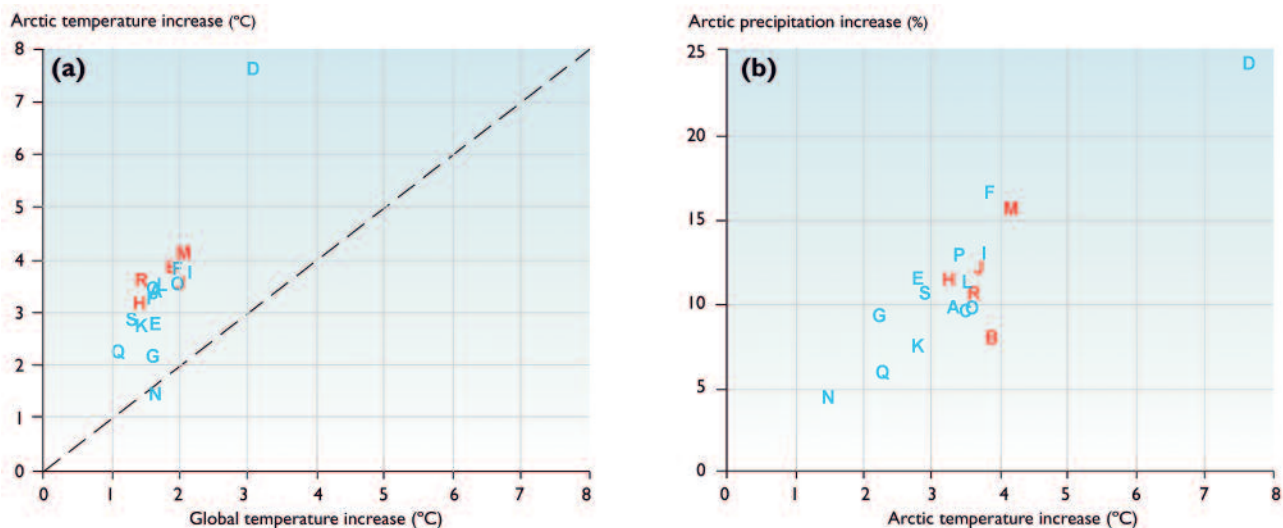
Fig. 4.23. Projections from the 19 CMIP2 models of (a) changes in global mean annual temperature (horizontal axis) and arctic (60º–90º N) mean annual temperature (vertical axis) and (b) changes in arctic mean annual temperature (horizontal axis) and precipitation (vertical axis). Table 4.5 lists the model associated with each letter. The five ACIA-designated models are shown in red and the others in blue.

Fig. 4.24. Projected increase in mean annual temperature (°C) for a doubling of atmospheric CO_2 concentration averaged over (a) the 19 CMIP2 models, and (b) the 5 ACIA-designated models.

Fig. 4.25. Projected increase in mean annual precipitation (%) for a doubling of atmospheric CO_2 concentration averaged over (a) the 19 CMIP2 models, and (b) the 5 ACIA-designated models.
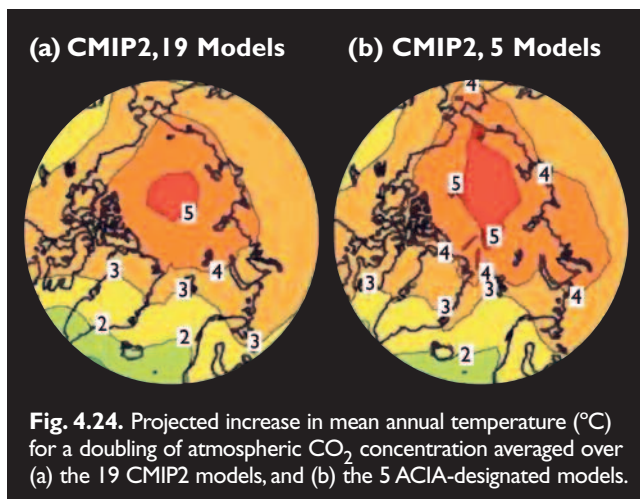
shows an expected tendency for the projected precipitation change to be greatest for the models with the greatest projected temperature increase, which is not visible in the results from the five ACIA-designated models alone. The same tendency is seen in a comparison of projected global mean temperature and precipitation change (see Cubasch et al., 2001).

Figure 4.24 shows the spatial distribution of the projected change in mean annual temperature from the CMIP2 experiments, as averaged over all 19 models and over the five ACIA-designated models. The basic patterns are very similar, with the greatest temperature increases over the central Arctic in both cases. A similar comparison of projected precipitation changes (Fig. 4.25) also indicates broad agreement between the 19-model mean and the 5-model mean. However, some of the spatial details in the 5-model mean, such as the maxima over northeastern Greenland and eastern Siberia, are smoothed out when the change is averaged over all 19 models.

4.4.6. Summary

Projections of arctic climate change in the 21st century from all of the ACIA-designated AOGCMs are qualitatively consistent and in line with the IPCC conclusions listed at the beginning of section 4.4. The across-model scatter of the arctic climate change scenarios is significant, but smaller than the scatter between the climates simulated by the different models for the baseline period. Even the difference between the two single-model projections driven with both the A2 and B2 emissions scenarios is comparable to the range of corresponding changes projected by the five ACIA-designated models forced with the B2 scenario.

In summary, the five ACIA-designated AOGCMs appear to be a representative sample of climate models, at least in terms of the average response of arctic temperature and precipitation to the B2 emissions scenario. However, this set of projections does not capture the full range of uncertainty associated with model and emissions scenario differences, at least in the second half of the 21st century.

4.5. Regional modeling of the Arctic

An improved understanding of the arctic climate system is necessary to provide better quantitative assessments of the magnitude of potential global change and to clarify the role of the Arctic in the global climate s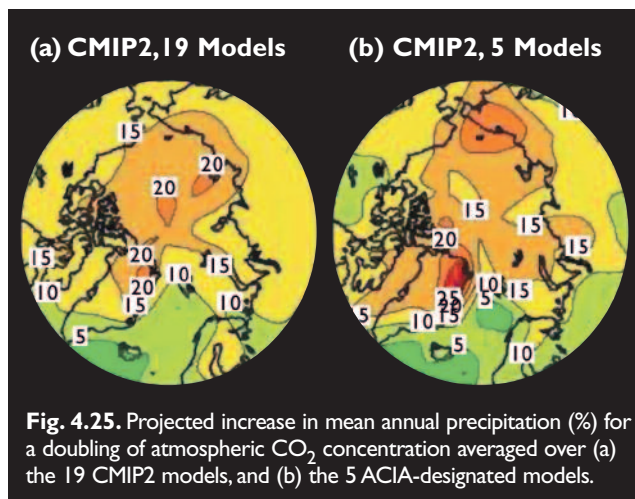ystem. The deficiencies of AOGCMs in describing arctic climate are partly due to inadequate parameterizations of physical processes. Equally important, AOGCMs are characterized by a rather coarse horizontal resolution, which fails to capture atmospheric mesoscale features caused by coastlines, ice sheets, sea-ice margins, and mountains. To some extent, this failure is overcome when the resolution is increased (Giorgi et al., 2001). The most obvious step – to simply increase resolution in AOGCMs – has until now been impractical due to the computational capacities required. Experience with high- or variable-resolution AGCMs has been limited and no results are available that focus on the performance of these models for the Arctic.

Another approach to obtaining enhanced regional details is the use of a nested limited-area model. This technique has garnered considerable interest in recent years because it requires less computational capacity than a global model with comparable resolution. These models can be used for process studies and for model validation studies using lateral boundaries from observation-based analysis (e.g., Giorgi and Mearns, 1999; Giorgi et al., 2001). However, the technique can also be used as the basis for dynamic downscaling of AOGCM simulations. Models used in this way are often referred to as regional climate models (RCMs; see Box 4.1).

4.5.1. Regional climate models of the arctic atmosphere

4.5.1.1. General

Regional models show considerable skill in short-term (few hour to few day) weather forecasting and are used worldwide for this purpose. This application is basically an initial-value problem, and most of the success of this approach can be ascribed to the high resolution of the models and the use of very recent observations.

Likewise, at timescales of a few years to decades and beyond, regional models have shown their strength in comparison with coarse-resolution global models, as they are capable of capturing the fine-scale details of climatic processes – such as the presence of complex topography and small-scale weather features such as tropical cyclones and even polar lows – much more realistically than global models (Giorgi et al., 2001). Moreover, it has been shown that the statistics of extreme precipitation are realistically simulated by high-resolution regional models (Frei et al., 2003b) and that they show skill even at their grid scale (Huntingford et al., 2003). This is a boundary-value problem and the assessment of the skill of the model is based on statistics of model performance over long time periods (several years or more).

Regional model projections are limited by the quality of the global model projections used for the lateral boundary conditions. In this respect, a potential problem is the mismatch between scales in the coarse-resolution global model and the high-resolution regional model. Recently, this has been demonstrated not to be a fundamental problem if proper boundary condition procedures are used (Denis et al., 2002). In fact, it has been demonstrated that, when driven by realistic (observed) boundary conditions, regional climate models are capable of capturing the overall observed regional climatic evolution and can add realistic spatial and temporal information to the information provided by the driving model (Dethloff et al., 2002; Frei et al., 2003b; Giorgi et al., 2001). When nested within a GCM, it is important, however, to stress that the large scale circulation is imposed by the lateral boundaries. The regional model is not able to, nor is it intended to, correct the large-scale errors made by the global model. The role of the regional model is instead to add regional detail and fine spatial and temporal scales to the simulation, not to improve the large-scale simulation.

Atmospheric regional modeling systems for the Arctic have been developed by Lynch et al. (1995) and Dethloff et al. (1996). Dethloff et al. (1996) applied the regional atmospheric climate model HIRHAM (Christensen J. et al., 1996) to the entire Arctic north of 65° N. This model has so far been the only RCM used with a circumpolar focus for climate simulations, although the recent Arctic Regional Model Intercomparison Project (ARCMIP; see section 4.5.1.2) initiative has increased the interest in arctic RCMs. Many other groups have developed RCMs, but mostly with a more southerly region of interest, although in some cases parts of the Arctic have been included in simulations performed with these models. For example, several models have been applied over most of the European continent including the Scandinavian Peninsula and parts of the North Atlantic Ocean extending all the way to the ice margins; even parts of Greenland have been included in such simulations (Christensen J. et al., 1997; Rummukainen et al., 2001). Likewise, experiments with a Canadian RCM have been applied to the whole of Canada (Laprise et al., 1998) including a fair proportion of the Arctic. The

development of these models continues, but limited results with an arctic focus have been published.

Giorgi et al. (2001) documented how much insight has been provided into fundamental issues concerning the nested regional modeling technique. For example, multi-year to multi-decadal simulations must be used for climate change studies to provide meaningful climate statistics, to identify significant systematic model errors and climate changes relative to internal model and observed climate variability, and to allow the atmospheric model to equilibrate with the land surface conditions (e.g., Christensen O., 1999; Jones et al., 1997; Machenhauer et al., 1998; McGregor et al., 1999). In addition, the choice of domain size is not a trivial question. The influence of the boundary forcing is reduced as region size increases (Jacob and Podzun, 1997; Jones et al., 1995) and may be dominated by the internal model physics for certain variables and seasons (Noguer et al., 1998). This can lead to the RCM solution significantly departing from the driving data, which can make the interpretation of downscaled regional climate changes more difficult (Jones et al., 1997). For most experiments with very high resolution, the domain size is limited by practical considerations and the large-scale flow is, therefore, constrained substantially by the driving model (Christensen J. and Kuhry, 2000). Denis et al. (2002) demonstrated that when the discrepancy in resolution between the model providing the lateral boundary conditions and the nested RCM does not exceed a factor of 10, the RCM is able to generate added value high-resolution information. With this limitation, they also showed that for a typically sized domain, the RCM does not introduce any spurious developments due to the nesting technique, and is fully capable of a consistent development within the model domain.

Configurations of RCM model physics are derived either from a pre-existing (and well-tested) limited-area model system with modifications suitable for climate applications or are implemented directly from a GCM (see Giorgi et al., 2001). In the first approach, each set of parameterizations is developed and optimized for the respective model resolutions. However, this makes interpreting differences between the nested model and the driving GCM more difficult, as these will result from more than just changes in resolution. Also, the different model physics schemes may result in inconsistencies near the boundaries (Machenhauer et al., 1998; Rummukainen et al., 2001). The second approach maximizes compatibility between the models. However, physics schemes developed for coarse-resolution GCMs may not always be adequate for the high resolutions used in nested regional models and may at a minimum require recalibration. Overall, both strategies have shown performance of similar quality and either is acceptable (Giorgi and Mearns, 1999).

4.5.1.2. Simulations of present-day climate with regional climate models

Regional climate models have been used for a wide variety of research worldwide, and have generated a sizeable research community. However, very few groups have focused on the Arctic to date, although several new initiatives have recently been undertaken. Intercomparison projects entailing participation of different international research groups have been conducted or are currently underway (Christensen J. et al. 1997, 2002; Machenhauer et al., 1998; Takle et al., 1999; Rinke et al., 2000; www:awi-potsdam.de/www-pot/atmo/ glimpse/index.html). This section describes the existing applications of RCMs for simulating present-day arctic climate conditions.

Advances in regional climate modeling must be based on an analysis of physical processes and comparison with observations. In data-poor regions such as the Arctic, this procedure may be complemented by a community-based approach (i.e., through collaborative analysis by several research groups). To illustrate this approach, simulations of the Arctic Basin north of 65° N have been performed and planned with different RCMs, driven at their lateral boundaries by observationally based analyses (Rinke et al., 2000). Motivated by this, an international intercomparison of regional model simulations for the Arctic, ARCMIP, has been organized under the auspices of the World Climate Research Programme. The foci of the evaluation include the surface energy balance over ocean

Table 4.6. Comparison of observed changes in net accumulation rates for the north Greenland Ice Sheet (76°–79° N) with simulations by a general circulation model (ECHAM4/OPYC3) and a regional climate model (HIRHAM). Model uncertainties are estimated as one standard deviation of the 30-year inter-annual variability in the simulation.

	Change in net accumulation rate (mm/yr)	
	27°–30° W	60°–65° W
ECHAM4/OPYC3[a]	170±40	-1390±560
HIRHAM[a]	75±24	-223±189
Observed[b]	97±84	-310±107

[a] 1961–1990 (Kiilsholm et al., 2003)
[b] 1954–1995 (Paterson and Reeh, 2001)

and land, clouds and precipitation processes, stable planetary boundary layer turbulence, ice-albedo feedback, and sea-ice processes. The preliminary results from this project indicate that the participating regional models are able to reproduce reasonably well the main features of the large-scale flow and the surface parameters in the Arctic. However, in order to reach definitive conclusions in an RCM intercomparison, ensemble simulations with adequate spin-up (time for regional model processes to equilibrate with prescribed external forcings) and equivalent initialization of surface fields are required (Rinke et al., 2000). Several aspects of the intercomparison are difficult due to the lack of adequate data for model validation. However, some aspects of the models, such as the hydrological cycle, compare well with each other (see Rinke et al., 2000).

Determining the primary causes of model biases, deficiencies, and uncertainties in atmosphere-only and coupled atmosphere-ice-ocean climate models for the Arctic is of vital importance in order to model the arctic climate adequately. Participants in the ARCMIP project are seeking to improve model representations through an intercomparison of simulations by different models and comparison with observations made during the Surface Heat Budget of the Arctic Ocean field-experiment year (October 1997 to October 1998).

For the Arctic, only very limited multi-year RCM experiments have been conducted. For example, Kiilsholm et al. (2003) assessed the uncertainty in regional accumulation rates for the Greenland Ice Sheet due to model resolution. They used the HIRHAM RCM (50 km resolution) with boundary conditions from a 30-year control simulation with the ECHAM4/OPYC3 model (~300 km horizontal resolution; Roeckner et al., 1996). Figure 4.26 compares the resulting accumulation and ablation zones as simulated by the RCM and the GCM. Table 4.6 illustrates the ability of the models to simulate present regional (northern Greenland) changes in accumulation rates. It appears that the RCM simulation is in better agreement with the observational evidence than the GCM simulation.

Fig. 4.26. Net mass balance of the Greenland Ice Sheet over the period 1961–1990 simulated by (a) the ECHAM4/OPYC3 general circulation model and (b) the HIRHAM regional climate model. Model-designated elevation contours shown for every 500 m (Kiilsholm et al., 2003).

Non-arctic applications have shown that regional models may have significant potential for use as dynamic interpolators, yielding useful data for a wide range of times and

Fig. 4.27. Net accumulation rates over the Greenland Ice Sheet (a) estimated from observations and (b) four years of HIRHAM simulation (from Dethloff et al., 2002).

4.5.1.3. Time-slice projections from atmospheric RCMs

In IPCC (2001), the concept of using RCMs for climate change projections was considered at some length. The IPCC (2001) considered the concept of using RCMs for climate change projections at some length, and concluded that it is essential that information from a transient AOGCM simulation be available. In such studies, the RCM is used to provide a reinterpretation of the overall AOGCM behavior, including its response to external forcing (from GHGs and aerosols). Sometimes ocean modeling is also done as part of the regional model simulation (Räisänen et al., 2003). In a typical experiment (Christensen J. et al., 2002; Jones et al., 1995; Kiilsholm et al., 2003; Machenhauer et al., 1996; Räisänen et al., 1999; Rummukainen et al., 2001), two time slices (e.g., 1961–1990 and 2071–2100) are selected from a transient AOGCM simulation. The RCM simulations include prescribed time-dependent GHG and aerosol concentrations for the corresponding periods of the AOGCM run. The time-dependent sea-surface temperatures and sea-ice distributions simulated by the AOGCM are also prescribed as lower boundary conditions, although some models also incorporate an interactive ocean/sea-ice model (Räisänen et al., 2003). The RCM simulations are typically initialized using atmospheric and land-surface conditions interpolated from the corresponding AOGCM fields, and there may be a considerable spin-up period before the actual simulation is started (e.g., Christensen O., 1999).

Only a few studies of this type have been conducted for time slices of durations long enough to encompass the large interannual variability in Arctic. Only two sets of experiments exist to date that cover the entire Arctic (Dorn et al., 2003; Kiilsholm et al., 2003), while Haugen et al. (2000) report simulations that only cover the Atlantic sector, with the main focus of the experiment being Norwegian land territories (mainland Norway and Svalbard). Kiilsholm et al. (2003) and Dorn et al. (2003) have conducted a set of such experiments using information from transient simulations with the ECHAM4/OPYC3 model (Stendel et al., 2000).

This section highlights the experiments conducted by Kiilsholm et al. (2003) using the HIRHAM4 model forced with the B2 emissions scenario, as they are the only ones with complete multi-year integrations that are generally consistent with the characteristics of the ACIA scenarios. In this study, the AOGCM had a resolution of approximately 300 km, while the resolution of the RCM was approximately 50 km. This discussion focuses on differences in the climate projections of the RCM and the driving AOGCM.

Figure 4.28 depicts the winter temperature change as simulated by the AOGCM and the RCM. In general, the patterns of warming as well as their amplitude are quite similar. However, the RCM depicts some regional patterns that can be ascribed to the higher resolution. Along the ice

locations where *in situ* observations are not available. As regional models become increasingly accurate, they could become valuable tools for glaciological research. A primary application in glaciology is the investigation of mass balance changes in continental ice sheets. Determining the climatic conditions affecting ice sheets is important because major changes in ice-sheet dimensions affect climate and sea level throughout the world. Much recent work has gone into the validation of RCM simulations (Bromwich et al., 2001; Cassano et al., 2001) using observational data analyses (Hanna and Valdes, 2001) for the Greenland Ice Sheet. Dethloff et al. (2002) carried out a detailed RCM validation study on the basis of multi-year ensemble simulations, selected annual simulations, and derived results for the mass balance of the Greenland Ice Sheet. Figure 4.27 illustrates net accumulation rates from the HIRHAM simulations. Compared with available results from earlier work, these results indicate a high degree of skill in spatial representation.

Another promising application was identified by Christensen J. and Kuhry (2000), who analyzed the ability of an RCM to simulate permafrost zonation at very high spatial resolution. Based on a simple permafrost index (Nelson and Outcalt, 1987), but applied to the subsurface model layers rather than near-surface air temperatures, they documented that at sufficiently high resolution the permafrost zonation in complex regions can be quite accurately modeled.
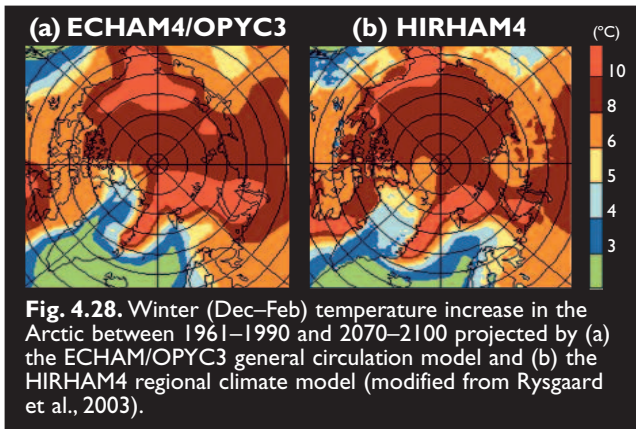
Fig. 4.28. Winter (Dec–Feb) temperature increase in the Arctic between 1961–1990 and 2070–2100 projected by (a) the ECHAM/OPYC3 general circulation model and (b) the HIRHAM4 regional climate model (modified from Rysgaard et al., 2003).

margin in the Greenland Sea and the Barents Sea, where sea ice retreats in the simulations (sea ice in the RCM is interpolated from the AOGCM), the RCM shows greater temperature increases. This is due to a stronger response to sea-ice changes resulting from a better description of the nonlinear energy cascade connected with mesoscale weather developments (e.g., stronger cyclonic developments) in the RCM than in the AOGCM. Conversely, temperature increases projected by the RCM tend to be lower over most of the central Arctic and all of Siberia, particularly during summer. This is due to a more realistic simulation of the present-day snow pack by the RCM than by the AOGCM (see Box 4.4).

Figure 4.29 shows the winter change in simulated precipitation minus evaporation. As with temperature, the large-scale agreement is striking. However, regional details are evident along the North Atlantic storm track and close to complex topography. In general, the RCM shows a stronger increase in precipitation minus evaporation upwind of major topographical obstacles and a corresponding decrease in precipitation minus evapotranspiration downwind (e.g., Scandinavia, the Rocky Mountains, and Siberia). This is partly explained by the increased topographical gradients due to the higher resolution of the model.

These apparently small differences may have substantial effects on the assessment of future changes in various geophysical systems, such as the mass balance of glaciers and the Greenland Ice Sheet in particular (Kiilsholm et
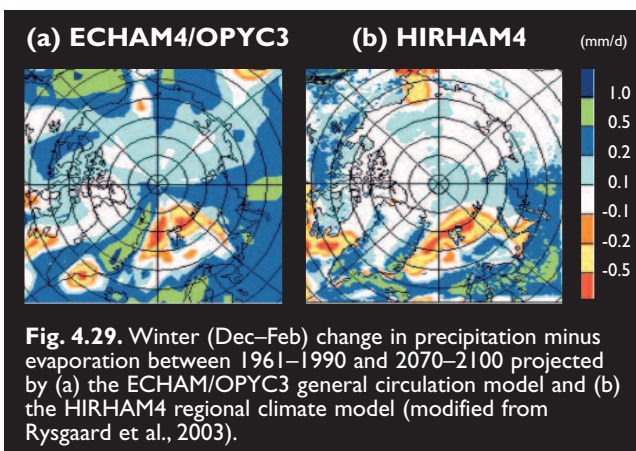
al., 2003) and the depth of the permafrost active layer (Walsh, in press; see also section 6.6). The RCM is better suited for simulating climate change at the regional level, particularly for areas with complex topography and coastlines. This has been confirmed in multiple applications of the model outside of the Arctic (e.g., Giorgi et al., 2001; Christensen J. and Christensen O., 2003; Huntingford et al., 2003).

Projected changes in arctic climate due to anthropogenic GHG emissions will occur together with natural dynamic processes in the climate system. In order to improve projections of the evolution of arctic climate, the effects of natural climate variability and in particular their regional dimensions must be taken into account. One major phenomenon contributing to the natural variability of the climate of the Northern Hemisphere is the NAO, which is also associated with the AO, and is described in more detail in section 2.2.2. In general, the influence of the NAO on arctic temperatures is directly opposed in the western and eastern Arctic, and is stronger over land areas than over ocean areas or sea ice. Dorn et al. (2003) investigated the combined effects of varying phases of the NAO and increasing GHG and aerosol concentrations on arctic winter temperatures (Fig. 4.30). In this study, different phases o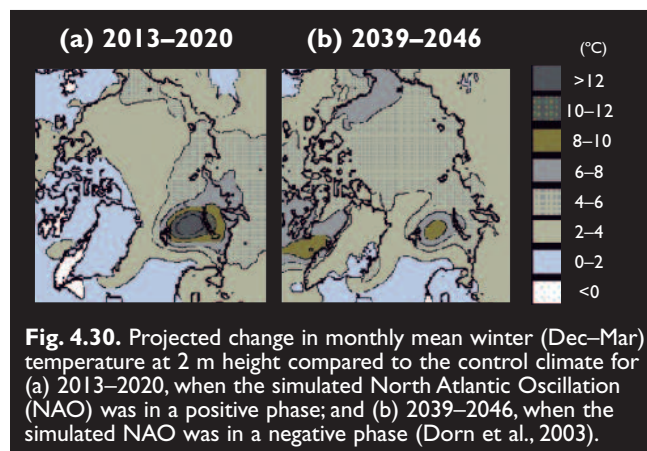f the NAO in a transient coupled AOGCM simulation were considered in time slice simulations using an RCM. Two future periods, 2013–2020 and 2039–2046, representing a positive and a negative phase of the NAO, respectively, were analyzed. The level of GHGs and aerosols in the simulation is higher during the negative NAO phase (2039–2046) than during the positive phase (2013–2020). Although mean arctic winter temperatures are projected to be approximately 1.3 °C higher during the negative phase compared to the positive phase, regions of warming and cooling between the two periods can be observed in Figs. 4.30a and 4.30b. Subsequent to the positive phase, a strong warming of more than 6 °C is simulated over some areas of Alaska, the Labrador Sea, and Baffin Island, whereas a similar strong cooling is simulated only over the northern Barents Sea. The temperature effect of the NAO is altered by the general temperature increase resulting from enhanced GHG and aerosol concentrations, but the influence of the NAO is still clearly evident at the regional scale. Although the statistical signifi-

Fig. 4.29. Winter (Dec–Feb) change in precipitation minus evaporation between 1961–1990 and 2070–2100 projected by (a) the ECHAM/OPYC3 general circulation model and (b) the HIRHAM4 regional climate model (modified from Rysgaard et al., 2003).

Fig. 4.30. Projected change in monthly mean winter (Dec–Mar) temperature at 2 m height compared to the control climate for (a) 2013–2020, when the simulated North Atlantic Oscillation (NAO) was in a positive phase; and (b) 2039–2046, when the simulated NAO was in a negative phase (Dorn et al., 2003).

cance of these differences has not been assessed, the results clearly show that regional changes in the Arctic at decadal timescales may, at least for several more decades, be dominated by changes in the overall atmospheric flow rather than by the temperature increases due to rising GHG concentrations.

Circulation in an RCM is determined by the boundary conditions provided by the driving AOGCM. As noted in section 4.3, simulations from different global models can be very different in terms of circulation patterns, and the small-scale response in a regional model can amplify such differences. An example is given in Fig. 4.31. Here, the Rossby Centre regional model (RCAO: Rummukainen et al., 2001) is driven by 30-year global climate simulations from the HadAM3H and ECHAM4/OPYC3 global climate models forced with the A2 and B2 emissions scenarios. Both regional simulations driven by the HadAM3H scenarios (Fig. 4.31a,b) show only moderate increases in precipitation while both ECHAM4/OPYC3 simulations (Fig. 4.31c,d) show dramatic precipitation increases, particularly on the western side of the Scandinavian mountains. The differ-

ence between the A2 and B2 emissions scenarios is quite small relative to the inter-model differences, which are due to a clear difference in the circulation regime change simulated by the two AOGCMs. The HadAM3H model projects a relatively small change in the north-south pressure gradient across the Nordic region, in sharp contrast to the ECHAM4/OPYC3 model, which projects a substantial strengthening of the north-south pressure gradient. This difference is in turn connected with a difference in the projected shifts in the main storm track regions over the North Atlantic. The physical reason behind the different responses in storm track regions for the two global models is at present unclear. Keeping in mind the results of Dorn et al. (2003), a plausible explanation is that part of the difference may be due to different simulations of decadal variability in the NAO by the two AOGCMs.
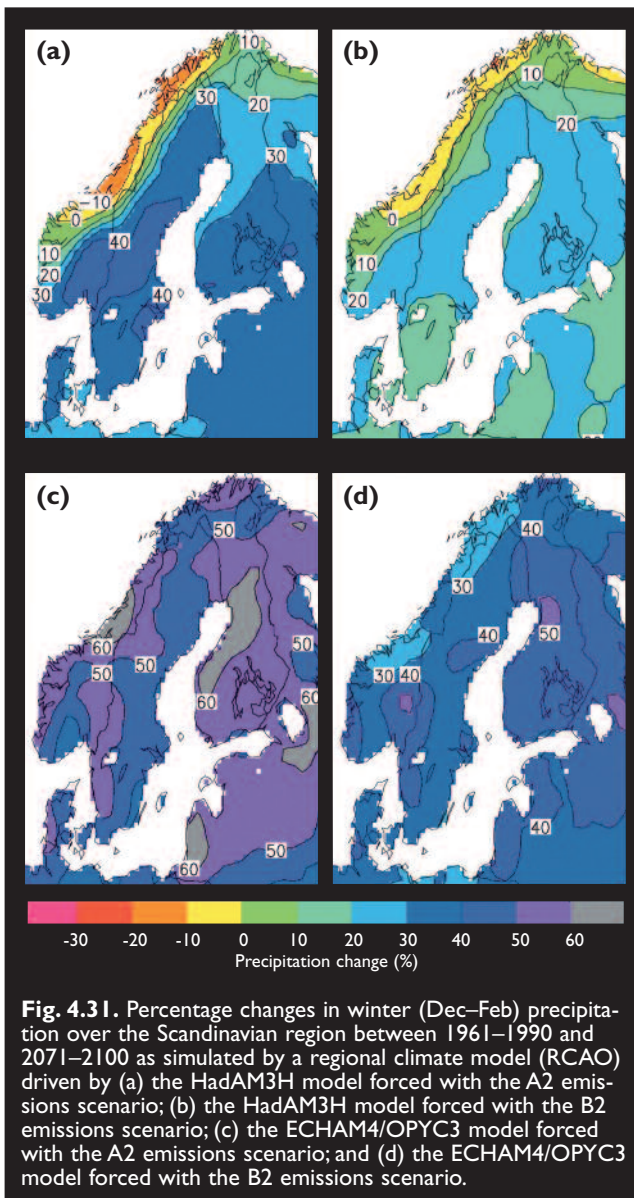
The lack of experiments with different RCMs using boundary conditions from more than one GCM so far prevents the practical use of RCM information for general impacts work. This is also the situation even for better-studied regions, such as continental Europe, due to a lack of appropriate coordination of these efforts; however, see Christensen J. et al. (2002) for an update on recent progress.

4.5.2. Regional Arctic Ocean models

Proper treatment of the Arctic Ocean requires a spatial resolution high enough to account for reduced Rossby length scales (the smallest scale at which the rotation of the Earth has a dominating influence on flow dynamics); to permit the important flows through Bering Strait and the Canadian Archipelago; and to accurately represent the complex bottom topography steering the currents, as well as the continental slopes and the large continental shelves where the thermohaline, wind-driven, and tidal dynamics interact.

Currently, about a dozen Arctic Ocean models exist, most of which are participating in the Arctic Ocean Model Intercomparison Project (AOMIP: Proshutinsky et al., 2001; see also Box 4.2). Most of the Arctic Ocean models are derived from global oceanic GCMs – in many cases from the Geophysical Fluid Dynamics Laboratory (GFDL) Modular Ocean Model (MOM: Pacanowski and Griffies, 1999). The Arctic Ocean models represent a wide spectrum of numerical approaches, employing either finite-difference (in most cases) or finite-element approximations, and three types of vertical coordinates: z (constant geopotential surfaces), sigma (bathymetry-following), and isopycnal (constant potential density referenced to a given pressure). The models differ in their spatial resolution (from 40–50 km down to 16–20 km in the horizontal and typically 25–30 levels in the vertical); specifications of surface and lateral fluxes; and formulations of the surface mixed and bottom boundary layers. Regional models of the Arctic Ocean are usually coupled to comprehensive sea-ice models,

Fig. 4.31. Percentage changes in winter (Dec–Feb) precipitation over the Scandinavian region between 1961–1990 and 2071–2100 as simulated by a regional climate model (RCAO) driven by (a) the HadAM3H model forced with the A2 emissions scenario; (b) the HadAM3H model forced with the B2 emissions scenario; (c) the ECHAM4/OPYC3 model forced with the A2 emissions scenario; and (d) the ECHAM4/OPYC3 model forced with the B2 emissions scenario.

although these often differ in their treatment of dynamics and thermodynamics.

To ensure a degree of fidelity to the simulations, an artificial constraint known as "climate restoring" (i.e., relaxation to the observed climate) based on the surface salinity is often introduced. This constraint prevents a model from drifting significantly from observations. Restoring time constants vary across models from several months (strong restoring) to several years (weak restoring). Some models do not employ restoring at all. However, the biases in simulations monotonically increase with the value of the restoring constant, reaching their highest levels in the models without restoring (Proshutinsky et al., 2001). This emphasizes that there are some processes and feedbacks crucial for representing the Arctic Ocean general circulation that are still neither sufficiently understood nor properly represented in the regional models, just as is the case for the global models.

From the viewpoint of their employment in downscaling AOGCM outputs or in constructing scenarios of future climate change, regional ocean models lag behind the atmospheric RCMs.

4.5.3. Coupled arctic regional climate models

The construction of coupled RCMs is a recent development. These models couple atmospheric RCMs to other models of climate system components, such as lake, ocean/sea-ice, chemistry/aerosol, and land biosphere/hydrology models (Bailey and Lynch, 2000a,b; Bailey et al., 1997; Hostetler et al., 1994; Lynch et al., 1995, 1997, 1998; Mabuchi et al., 2000; Maslanik et al., 2000; Qian and Giorgi, 1999; Rinke et al., 2003; Roed et al., 2000; Rummukainen et al., 2001; Small et al., 1999a,b; Tsvetsinskaya et al., 2000; Weisse et al., 2000). These initial efforts provide a path toward the development of coupled "regional climate system models". For some parts of the Arctic, coupled mesoscale atmosphere-ice-ocean models already exist, although they are restricted to small domains and short integration times (e.g., Lynch et al., 1997, 2001; Roed et al., 2000; Schrum et al., 2001).

For the circumpolar Arctic, Maslanik et al. (2000) presented the first results of a coupled atmosphere-ice-ocean RCM called ARCSyM. The oceanic component in this RCM was a simple mixed layer model. Rinke et al. (2003) present a more complex coupled RCM (i.e., a fully coupled atmosphere-ice-ocean circulation model system) called HIRHAM-MOM. The ability to simulate conditions over the Arctic Ocean during April to September 1990, a period of anomalous atmospheric circulation and sea-ice conditions, was investigated with both models. A common result was found: neither model was able to correctly reproduce the large retreat of sea ice in the eastern Eurasian Basin and the adjacent shelf sea observed during the summer of 1990 (Maslanik et al., 1996). The sea ice in the Chukchi and East Siberian Seas does not retreat as completely in the

model simulations as it does in observations inferred from satellite data.

The HIRHAM-MOM coupled model (Rinke et al., 2003) reproduced the general sea-level pressure patterns for the summer of 1990, based on a comparison with ECMWF analyses. However, discrepancies appeared in late summer that significantly affected variables such as wind flow and sea-ice transport. Similar to the ARCSyM results (Maslanik et al., 2000), HIRHAM-MOM simulated too much sea ice in the Bering, Chukchi, and East Siberian Seas during the summer of 1990. This is also the case for the ocean/sea-ice models driven by ECMWF atmospheric data.

The results from both coupled models highlight the importance of regional atmospheric circulation in driving interannual variations in arctic sea-ice extent, and illustrate the level of model performance required to simulate such variations. Such studies are valuable because they indicate improvements needed in the models by evaluating the results against observations, and the roles of key processes and feedbacks by comparing the results to those of the uncoupled atmospheric model. While results for the Baltic Sea imply improved model performance when an ocean model is coupled to the RCM (Räisänen et al., 2003), high-resolution coupled model systems for the Arctic have not provided improved performance to date.

4.5.4. Summary

The current status of arctic regional climate modeling did not allow RCMs to be employed as principal tools for the ACIA. Present scenarios of future arctic climate change are therefore based on results from global AOGCMs. However, presently available global coupled models have a coarse spatial resolution that limits their ability to capture many important aspects of climate change. In particular, intense storms, the effects of topography, and fundamental aspects of regional ocean circulation cannot be represented adequately. To improve the modeling of such phenomena, development of regional coupled ocean-ice-atmosphere climate models should receive a high priority in the efforts of the climate modeling community. Such developments should go hand in hand with developments in global modeling, in particular development of high-resolution AOGCMs.

4.6. Statistical downscaling approach and downscaling of AOGCM climate change projections

Statistical downscaling (also called empirical downscaling) is a tool for downscaling climate information from coarse spatial scales to finer scales. It may be applied as an alternative, or as a supplement, to dynamic downscaling (i.e., regional modeling). The underlying concept is that local climate is conditioned by large-scale climate and by local physiographical features such as topography, distance to a coast, and vegetation (von Storch, 1999). At

a specific location, therefore, links should exist between large-scale and local climatic conditions. Statistical downscaling consists of identifying empirical links between large-scale patterns of climate elements (predictors) and local climate (predictand), and applying them to output from global or regional models. Successful statistical downscaling is thus dependent on long reliable series of predictors and predictands. Giorgi et al. (2001) provide a survey of statistical downscaling studies with emphasis on studies published between 1995 and 2000.

4.6.1. Approach

4.6.1.1. Predictands

Although mean temperature and precipitation (seasonal, monthly, or daily) are the most commonly used local predictands, statistical downscaling has also been applied to generate local scenarios of cloud cover, daily temperature range, extreme temperatures, relative humidity, sunshine duration, snow-cover duration, and sea-level anomalies (Enke and Spekat, 1997; Heyden et al., 1996; Kaas and Frich, 1995; Martin et al., 1997; Schubert, 1998; Solman and Nuñez, 1999). Even sea ice (Omstedt and Chen, 2001), ocean salinity and oxygen concentrations (Zorita and Laine, 2000), zooplankton (Heyden et al., 1998), and phytoplankton spring bloom in a Swedish lake (Blenckner and Chen, 2003) have been used as predictands.

4.6.1.2. Predictors

The large-scale predictors should satisfy certain conditions: they should be reproduced realistically by the particular global model; they should (alone or combined) be able to account for most of the observed variations in the predictand; the statistical relationships should be physically interpretable and temporally stationary; and, when applied to a changing climate, predictors that "carry the climate change signal" should be included (Giorgi et al., 2001).

The optimal choice of predictors depends upon the predictand. For downscaling local temperature, large-scale fields of geopotential height or air temperature might be used as the "signal-carrying" predictors (e.g., Huth, 1999). For precipitation, absolute or specific humidity may be used (Crane and Hewitson, 1998; Hellström et al., 2001; Wilby and Wigley, 2000). In maritime regions, air temperature can sometimes serve as a proxy for humidity (Wilby and Wigley, 2000). In addition, some indicator of atmospheric circulation (e.g., sea-level pressure or a geopotential height field) is usually included (e.g., Chen and Chen, 2003).

4.6.1.3. Methods

Surveys of methods for establishing links between large-scale predictors and local predictands are provided by Hewitson and Crane (1996), Zorita and von Storch (1997), Wilby and Wigley (1997), Xu (1999), Giorgi et al. (2001), and Mearns et al. (2001). The choice of

method should depend on predictand, time resolution, and also on the application of the scenario. Linear methods such as canonical correlation analysis (CCA), singular value decomposition (SVD), and multiple linear regression analysis (MLR) can, in most cases, be used to generate scenarios of monthly or seasonal values (e.g., Busuioc et al., 1999; Corte-Real et al., 1995; Huth and Kysely, 2000; Sailor and Li, 1999). To generate scenarios for variables such as daily precipitation, however, nonlinear techniques such as weather classification (e.g., Conway and Jones, 1998; Enke and Spekat, 1997; Goodess and Palutikof, 1998, Palutikof et al., 2002; Schnur and Lettenmaier, 1997), neural nets (Cavazoz, 1999; Clair and Ehrman, 1998; Crane and Hewitson, 1998; Schoof and Pryor, 2001), or analogues (Zorita and von Storch, 1999) are most useful. Weather generators (e.g., Semenov and Barrow, 1997; Semenov et al., 1998; Wilby et al., 1998; Wilks, 1999) can also be applied for generating scenarios with daily resolution, starting from monthly climate-change scenarios generated by one of the above methods.

4.6.1.4. Comparison of statistical downscaling and regional modeling

Several studies have compared results from statistical and regional modeling (Cubasch et al., 1996; Hellström et al., 2001; Kidson and Thompson, 1998; Murphy, 1999, 2000). The main impression from these studies is that results from the two downscaling techniques are usually quite similar for present-day climate, while differences in future climate projections are found more frequently. These differences can, to a large degree, be explained by the unwise choice of predictors in the statistical downscaling, for example, predictors that carry the climate signal (Murphy, 2000). It has also been suggested that results from statistical downscaling may be misleading because the projected climate change exceeds the range of data used to develop the model (Mearns et al., 2001). However, differences between results from statistical downscaling and regional modeling may also result from the ability of statistical downscaling to reproduce local features that are not resolved in the regional models (Hanssen-Bauer et al., 2003).

Some disadvantages of statistical downscaling versus regional modeling are as follows.

- The major weakness of statistical downscaling is the assumption that observed links between large-scale predictors and local predictands will persist in a changed climate.
- A problem when applying statistical downscaling techniques to daily values is that the observed autocorrelation between the weather at consecutive time steps is not necessarily reproduced. If it is essential to reproduce this, a suitable method (e.g., weather generators; Katz and Parlange, 1996; Wilks, 1999) should be used.
- Statistical downscaling does not necessarily reproduce a physically sound relationship between different climate elements. Using a downscaling

method based on weather classification for several predictands (e.g., Enke and Spekat, 1997) can minimize this problem.

- Successful statistical downscaling depends on long, reliable observational series of predictors and predictands.

Some advantages of statistical downscaling versus regional modeling are as follows.

- Statistical downscaling is less technically demanding than regional modeling. It is thus possible to downscale from several GCMs and several different emissions scenarios relatively quickly and inexpensively (Benestad, 2002).
- It is possible to tailor scenarios for specific localities, scales, and problems. The spatial resolution applied in regional climate modeling is still too coarse for many impact studies, and some variables are either not available or not realistically reproduced by regional models. For example, Omstedt and Chen (2001) applied statistical downscaling to infer sea-ice extent in the Baltic Sea.
- In most cases, the development of statistical downscaling models includes an evaluation of AOGCM performance in simulating the climate of a specific region (Busuioc et al., 1999, 2001a). Methods applied in statistical downscaling have been used to evaluate large-scale fields of single variables as well as the links between different fields (Busuioc et al., 2001b; Hanssen-Bauer and Førland, 2001; Wilby and Wigley, 2000). The stability of these links under global change has also been investigated (e.g., Chen and Hellström, 1999). Such analyses can indicate which variables serve as the best predictors.

4.6.2. Statistical downscaling of AOGCM climate change projections in the Arctic

A survey of statistical downscaling studies up to 2000 is provided by the IPCC (Giorgi et al., 2001). However, very few of these studies considered arctic sites. During the 1990s, a few statistical downscaling studies in the Atlantic/European sector of the Arctic were performed at the Danish Meteorological Institute. Kaas and Frich (1995) downscaled monthly means of diurnal temperature range (DTR) and cloud cover at ten synoptic stations from Greenland in the west to Finland in the east. The 500 hPa height and the 500/1000 hPa thickness anomaly fields were used as predictors in an MLR-based model. The model predictors were taken from the final 30 years of a control simulation of the 20th century and the final 30 years of a scenario "A" (business as usual) simulation of the 21st century generated by the ECHAM1 model (Cubasch et al., 1992). Kaas and Frich (1995) found that statistically significant negative trends in DTR were projected for Fennoscandia, especially in central and eastern areas, and especially during winter. For Greenland and Iceland, only minor trends in DTR were projected. Positive trends in cloud cover were pro-

jected over most of the area; these were most significant in northeastern areas of Fennoscandia.

In Canada, artificial neural networks (ANNs) have been applied to model hydrological variables (Clair and Ehrman, 1998; Clair et al., 1998; Ehrman et al., 2000). Clair et al. (1998) present a scenario for changed runoff from different Canadian ecozones (including arctic areas) under conditions of doubled atmospheric CO_2 concentrations. A doubled-CO_2 equilibrium climate change scenario produced by the Canadian climate model CCC (Boer et al., 1992) was used to generate scenarios for individual basins. Temperature and precipitation scenarios were fed into the ANN to produce scenarios of changes in runoff. In the arctic ecozones that were investigated in the study, the projected changes in annual runoff were between 0 and +10%, the spring melt advanced by between a couple of weeks and one month, and there was a tendency for reduced runoff during summer. Qualitatively similar findings are reported in section 6.8, where annual discharge from various North American rivers to the Arctic Ocean is projected to increase by 10 to 25% during the 21st century.

Recently, most of the statistical downscaling studies for the Arctic have been performed for the European sector as part of the Norwegian Regional Climate Development Under Global Warming (RegClim) project or the Swedish Regional Climate Modelling Programme (SWECLIM), both of which use regional modeling and statistical downscaling to generate climate scenarios. Statistical downscaling using results from several global models and for various emissions scenarios has been completed (Benestad, 2002, 2004; Chen et al., 2001). The primary global model used in the RegClim project was ECHAM4/OPYC3 (Roeckner et al., 1996, 1999), forced with the IS92a emissions scenario. The primary case studied was GSDIO, which included changes in GHGs, tropospheric ozone, and direct as well as indirect sulfur aerosol forcing (Roeckner et al., 1999). In SWECLIM, the main global models were HadCM2 (Johns, 1996; Johns et al., 1997) and ECHAM4/OPYC3. Hanssen-Bauer and Førland (2001) evaluated the ECHAM4/OPYC3 simulation of present-day climate over Norway and Svalbard, while Räisänen and Döscher (1999) evaluated the HadCM2 simulation of the present-day climate of northern Europe.

Sea-level pressure has proven to be a good indicator for the Scandinavian climate (Busuioc et al., 2001b; Chen, 2000; Chen and Hellström, 1999; Hanssen-Bauer and Førland, 2001), and was therefore used as a large-scale predictor in the statistical downscaling models. Depending on predictands, additional predictors included air temperature at 2 m height, humidity, and precipitation. The models were developed by linear techniques: CCA, SVD, or MLR. Monthly precipitation and temperatures at selected stations were the main predictands (Benestad, 2002, 2004; Busuioc et al., 2001a; Chen and Chen, 1999; Hanssen-Bauer et al., 2003; Hellström et al., 2001). Although not used for scenario estimation, some non-standard climate variables such as annual max-
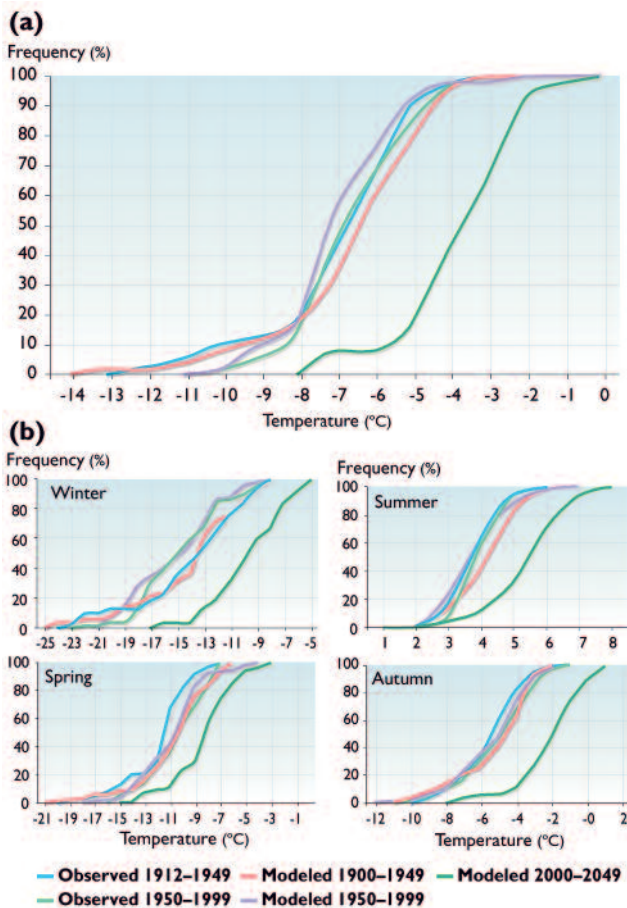
Fig. 4.32. Cumulative frequency plots of observed and modeled (a) mean annual temperature and (b) mean seasonal temperature at Svalbard Airport for various time slices (Hanssen-Bauer, 2002).

imum sea ice extent over the Baltic Sea (Chen and Li, 2004; Omstedt and Chen, 2001), sea level near Stockholm (Chen and Omstedt, 2002), and spring phytoplankton blooms in a Swedish lake (Blenckner and Chen, 2003) were also linked to atmospheric circulation and may thus be projected by statistical downscaling.

The statistically downscaled temperature scenario based upon the GSDIO integration projects increases in mean annual temperature of 0.2 to 0.5 °C per decade in Norway up to 2050 (Hanssen-Bauer et al., 2003), and 0.6 °C per decade in Svalbard (Hanssen-Bauer, 2002). Cumulative frequency (relative number of years that temperatures go below a certain threshold given as a function of the threshold value) plots of annual and seasonal mean temperatures based on this study (Fig. 4.32) show good correspondence between observations and model output for time slices within the 20th century. The smallest warming rates were simulated in southern Norway along the coast; the rates increase when moving inland and northward. Along the coast of southern Norway, the modeled warming rates are similar in all seasons. Farther north and in the interior, considerably larger warming rates are projected for winter than for summer. Comparing these results to the results from dynamic downscaling of the same integration (Bjørge et al., 2000) shows only minor differences in summer and autumn. In winter and spring, on the other hand, the statistical downscaling projects greater warming rates for

locations that are exposed to temperature inversions. Hanssen-Bauer et al. (2003) argue that it is reasonable to expect weaker winter inversions in the future, and that greater winter warming rates should be expected in valleys compared to mountains.

Benestad (2002, 2004) shows that statistical downscaling from several different climate models gives different local warming rates over Fennoscandia. Still, the temperature signal is robust in some respects: all models simulate warming; the warming is larger inland than along the coast; and the seasonal patterns are similar. A comparison of statistically downscaled temperature scenarios for Svalbard based on the GSDIO integration and HadCM3, both forced with the IS92a emissions scenario, and NCAR's CSM forced with a 1% per year increase in atmospheric CO_2 concentration, revealed differences (Fig. 4.33) that to a large degree can be explained in terms of different descriptions of sea-ice extent (Benestad et al., 2002). The HadCM3 model, which projects significantly stronger warming in this area than the other simulations, projects a substantial retreat of sea ice in the Barents Sea. The CSM model, which projects the most moderate warming rates, shows no melting of sea ice this area. Local temperature scenarios in the high Arctic are thus closely related to the projected changes in regional sea-ice cover. If the AOGCM fails to reproduce either the present sea-ice border or future melting in the region, the local temperature projections will be suspect.

Hellström et al. (2001) compared two dynamically and statistically downscaled precipitation scenarios for Sweden. The precipitation climates of the GCMs, dynamic models (i.e., RCMs), and statistical models from the control runs were also compared with respect to their ability to reproduce the observed seasonal cycle (Fig. 4.34). Improvements in the representation of the seasonal cycle by the downscaling models compared to the GCMs significantly increase the credibility of the downscaling models.
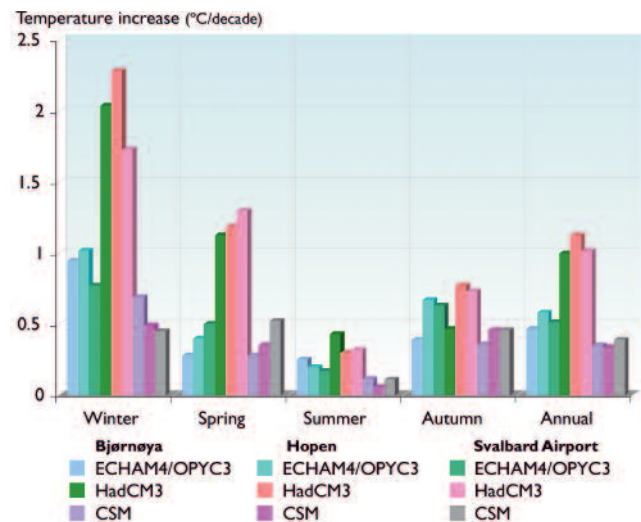
Fig. 4.33. Projections of seasonal and annual temperature increases between 1981–2000 and 2030–2050 for the arctic stations Bjørnøya, Hopen, and Svalbard Airport, based on statistical downscaling of three different general circulation models: ECHAM4/OPYC3, HadCM3, and CSM (Benestad et al., 2002).
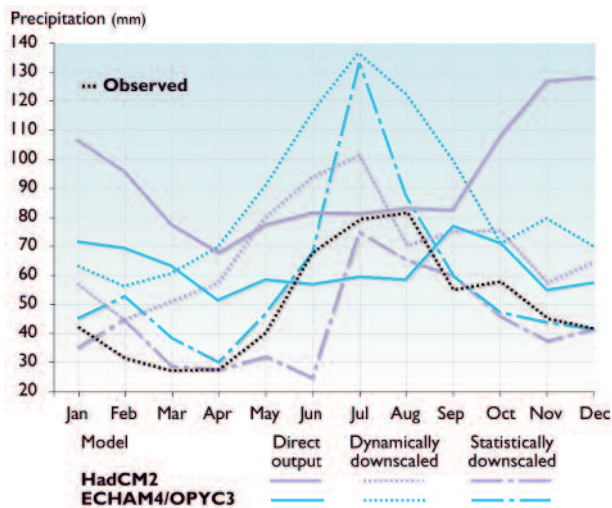
Fig. 4.34. Seasonal cycle of observed and modeled control period (1921–1950) precipitation for Kvikkjokk in northern Sweden (Hellström et al., 2001).

Chen et al. (2001) applied statistically downscaled scenarios from 17 CMIP2 AOGCMs to quantify AOGCM-related uncertainty in the estimation of precipitation scenarios. The result shows that there is an overall projected increase in annual precipitation over the 21st century throughout Sweden. The projected increase is greater in northern than southern Sweden. The precipitation in autumn, winter, and spring is projected to increase throughout the country, whereas decreasing summer precipitation is projected for the southern part of the country. The estimates for winter have a higher level of confidence than the estimates for summer. A statistically downscaled precipitation scenario based upon the GSDIO integration (Hanssen-Bauer et al., 2003) also projects increased annual precipitation in Norway. The projected rates of increase are smallest in southeastern Norway, where they are not statistically significant, and greatest along the northwestern and western coast, where they are highly significant (Fig. 4.35). In winter and autumn, statistically significant positive trends are projected for most of Norway, while most of the modeled changes in spring and summer precipitation are not statistically significant.

To date, statistical downscaling has primarily concentrated on monthly and annual scales. However, Linderson et al. (2004) developed downscaling models for daily statistics based upon monthly precipitation values for southern Sweden. Future scenarios of selected daily precipitation statistics were downscaled from a GCM developed at the Canadian Centre for Climate Modelling and Analysis (CGCM1; e.g., Flato et al., 2000). The downscaling models use large-scale precipitation, relative humidity, and circulation indices as predictors. The models are skillful in reproducing the variability of mean precipitation and the frequency of days with no precipitation, but less skillful concerning extremes and statistics of days with precipitation. By the time that atmospheric CO_2 doubles in the model, the CGCM1 projects an increase of 10% in annual mean precipitation (statistically significant at the 95% level), and an insignificant

reduction in the annual frequency of days with precipitation of 1.4%. An increase in precipitation intensity is projected throughout most of the year, especially during winter. The major changes include a substantial increase in winter precipitation, a delay in the timing of the summer maximum, and prolonged duration of the winter maximum relative to present-day climate. This indicates a more maritime precipitation climate in the scenario climate compared to the control climate.

Statistically downscaled climate scenarios for the North American and Russian parts of the Arctic have not yet been published. However, the Canadian Climate Impacts Scenarios (CCIS) Project has validated a downscaling tool, the Statistical DownScaling Model (SDSM; Wilby et al., 2002). The CCIS Project is providing predictor variable data to support the SDSM.

4.6.3. Summary

Although only a few statistical downscaling studies have been performed for arctic localities so far, results from the available studies indicate that these methods are able to resolve projected changes in temperature gradients between the coast and inland, and changes in valley temperature inversions. They also generate a more realistic representation of the annual precipitation cycle than the AOGCMs. If careful attention is given to the choice of predictors, scenarios from statistical downscaling and regional modeling seem to be consistent. However, statis-
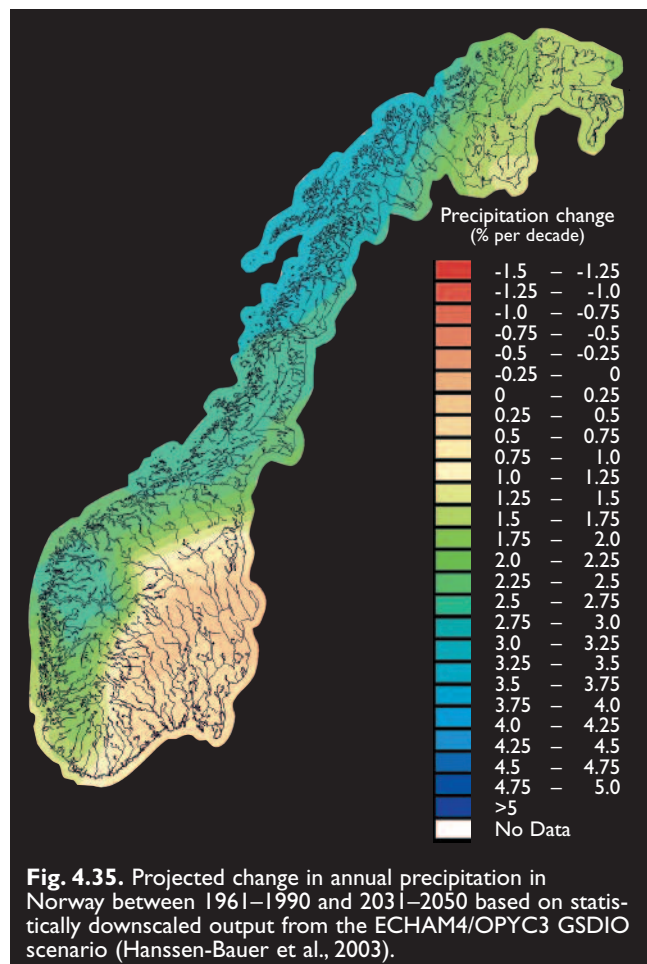
Fig. 4.35. Projected change in annual precipitation in Norway between 1961–1990 and 2031–2050 based on statistically downscaled output from the ECHAM4/OPYC3 GSDIO scenario (Hanssen-Bauer et al., 2003).

tical downscaling does not necessarily reproduce a physically based relationship between different climate elements. Conversely, the ability to downscale from several models and integrations is useful for assessing uncertainty. Results from downscaling temperature scenarios from several models underscore that the local temperature projections in the high Arctic depend on how well changes in sea-ice extent are represented in the AOGCMs.

4.7. Outlook for improving climate change projections for the Arctic

To provide more reliable climate change scenarios for the Arctic, several aspects of numerical climate models need further development. The most challenging aspects of model development are the physical parameterization schemes: much of the uncertainty in Arctic climate change projections can be attributed to an insufficient knowledge of many of the physical processes active in the Arctic domain. There is also substantial natural variability in the arctic climate system and this part of the uncertainty cannot be eliminated simply by model development and a refinement of the descriptions of physical processes. The large-scale flow is dominated by variability patterns such as the AO and the NAO (see section 2.2.2). In climate change simulations, both the frequency and nature of these flow patterns may be altered. To assess changes in the flow patterns, there must be a greater focus on the climate predictability problem to probe the inevitable natural uncertainty through a systematic search in probability space. To do this, ensemble projections are required where both initial states and uncertain model parameters are varied within a realistic range associated with a probability distribution. The development of more sophisticated physical parameterization schemes and the introduction of ensemble climate-change scenarios will both require considerable computing resources.

Historically, physical parameterization schemes have primarily been based on process descriptions and measurements from mid- and low latitudes (e.g., Randall et al., 1998). Assuming that the same physical processes are relevant to the Arctic, the developments have "propagated" from lower to higher latitudes in global models, and from AOGCMs to RCMs. In recent years, the Arctic has received particular attention from the climate modeling community, motivated by the strong arctic response to an increased GHG forcing in climate models. This has been demonstrated in the northern high latitudes along with a tremendous inter-model scatter, both in sensitivity to the forcing and in simulating the observed climate in this region. In particular, the amplification of global-model systematic errors in regional arctic models presents a serious challenge to future regional model developments.

In this section, research and model development priorities are summarized, aimed at an improvement of AOGCM performance in the Arctic and, particularly, at an increase in the credibility of AOGCM-based projections of future climate.

4.7.1. The Arctic part of the climate system — a key focus in developing AOGCMs

Surface air temperature and precipitation are variables of central interest from the viewpoint of AOGCM-based climate change scenarios. The level of confidence that can be placed on the projected changes depends on the accuracy and adequacy of the representations of many physical processes, particularly boundary-layer fluxes of heat, moisture, and momentum; clouds; and radiative fluxes.

Sea ice plays a dominant role in determining the intensity of these fluxes in the Arctic and to a large extent determines the climate sensitivity of the Arctic, in particular to GHG forcing. Description of sea ice is thus of central importance in the arctic climate system, and there is a considerable scope for improvement of the sea-ice components of current AOGCMs. More sophisticated treatments of sea-ice dynamics and thermodynamics can be included – up to the level of stand-alone regional Arctic Ocean/sea-ice models. However, even in the most comprehensive present-day sea-ice models, some important processes are not properly represented, including heat distribution between concurrent lateral and vertical melt or growth of the ice and convective processes inherent in sea ice (melt-pond and brine convection).

Improvements in the performance of AOGCM sea-ice components are hampered by errors in the forcing fields that determine sea-ice distribution. For example, the systematic bias in the arctic surface atmospheric pressure and the associated bias in the wind forcing of sea-ice as simulated by atmospheric components of AOGCMs (and stand-alone AGCMs) prevents even sea-ice models with advanced dynamics from properly simulating spatial distributions of sea ice (Bitz et al., 2002). The causes of the atmospheric pressure biases are not clear. Possible linkages include topographic (resolution) effects on atmospheric dynamics, lower boundary fluxes, as well as atmospheric chemistry and dynamics of the upper atmosphere (Walsh, in press).

The atmospheric boundary layer in the Arctic is poorly represented in current AOGCMs. It is unlikely that the representation can be improved just by increasing model vertical resolution. Insufficient understanding of the physics of the atmospheric boundary layer in the Arctic and the inappropriate parameterizations used in the current generation of AOGCMs call for further research in this field. To a certain extent, the same can be said about radiative transfer parameterizations, which should account for specific features of the arctic atmosphere and the underlying surface, including both the vertical and the horizontal heterogeneity of this complex system (Randall et al., 1998).

From a global perspective, clouds have been identified as the most serious source of uncertainty in present-day climate models (McAvaney et al., 2001). This is also true for the Arctic. In particular, the multilayer arctic clouds with their specific complexities associated with mixed

phases and low temperatures need to be represented better. Other uncertain aspects of clouds involve the radiative properties of ice crystals and the concentration of various types of crystals, which have very different properties with respect to their interaction with electromagnetic radiation.

Present climate-change modeling efforts largely focus upon effects in the atmosphere, including effects on air temperatures and precipitation. Modeling potential climate change in the marine Arctic has received less attention, although changes in the thermohaline circulation have been extensively studied, primarily with low resolution, uncoupled models. Due to the lack of coordination among modeling studies, few definitive projections can be made about changes to such variables as Arctic Ocean temperatures and salinities, stratification, and circulation (including the thermohaline circulation). In light of this, future modeling efforts should attempt to more fully address changes in the ocean. This will require better resolution in the ocean models and improved coupling between the dynamic atmosphere and dynamic ocean components, particularly in the presence of sea ice.

The freshwater budget of the Arctic Ocean (and its possible link to the intermittency of North Atlantic deep-water formation) is affected by the hydrological cycle not only in the region, but also far beyond it, including the vast terrestrial watersheds of the Arctic Ocean. For satisfactory simulations, river discharge into the Arctic Ocean needs to be properly represented in order to maintain the observed stratification and sea-ice distribution and transport. It is not clear whether the simple river discharge schemes used in current AOGCMs are sufficient, although it appears that incorporating more comprehensive river routing schemes will help ensure proper seasonality of the discharge and result in an improvement in the representation of Arctic Ocean general circulation. Accounting for the freshwater influx into the ocean from glaciers and the Greenland Ice Sheet will require more advanced parameterizations than those employed today and, ideally, require introducing dynamics into the ice-sheet components.

Processes and feedbacks associated with vegetation may also play an important role in the terrestrial Arctic, affecting heat, water, and momentum fluxes. The effects of vegetation on terrestrial snow cover and surface albedo, evapotranspiration processes, and the possible expansion of boreal forests into regions currently occupied by tundra are among many processes that may potentially be crucial in the context of climate change. Developing comprehensive interactive dynamic vegetation components of AOGCMs should eventually increase confidence in AOGCM-based projections of future climate.

Climatic changes of special concern for indigenous communities include weather variability and predictability; the extent, thickness, and quality of sea ice; the extent, duration, and hardness of snow cover; freeze-thaw cycles (particularly in autumn, when a layer of ice on the ground may be produced and last all winter, blocking access to forage for grazing animals); sudden changes in wind direction; and changes in the strength and frequency of winds and storms (Chapter 3). While most of these quantities are either directly available, or easily derivable from standard model outputs, representation of a few of these variables will require additional efforts from the modeling community in the future.

4.7.2. Improved resolution of arctic processes

To model climatically important processes in the Arctic, models with a high spatial resolution are required. To achieve this with present-day computing resources, regional models are required. In the future, global models may also have adequate resolution, but for the foreseeable future regional models will be required to complement the global simulations, because their results are closer to actual local climatic conditions and can more easily be translated into impacts than global model results.

When nested within a GCM, the large-scale circulation is imposed by the lateral boundaries of the RCM. Regional models are not able to, nor intended to, correct large-scale errors made by the global model from which conditions are drawn. The role of the regional model is to add regional detail and fine spatial and temporal scales to the simulation, not to improve the large-scale simulation. An alternative to regional models is presented by the evolving global variable-resolution stretched-grid approach that provides additional spatial detail over a region of interest (e.g., Giorgi et al., 2001). This technique allows for a feedback to the global scale from the region with high resolution. While this may seem appealing at first, it raises the question of whether this feedback is preferable when similar feedbacks from other regions are represented at a lower resolution.

The need for high resolution is not restricted to the atmospheric model component. To simulate the coupled atmosphere–ice–ocean system in the Arctic, a high-resolution ocean component is also required. In particular, the coupling processes occur on small horizontal and vertical scales, thus a high-resolution regional coupled atmosphere-ocean model is needed. Some early versions of such coupled models already exist, but much additional development work is required.

A further increase in atmospheric resolution (to <10 km horizontally) will require the use of non-hydrostatic model equations. New parameterizations of physical processes such as cloud formation and turbulence are also necessary at these scales. With a very high resolution (<1 km), non-hydrostatic models start to resolve individual clouds, thus necessitating further changes in cloud parameterizations. A special emphasis needs to be put on cloud microphysics, including the ice crystals and aerosols that provide nuclei for the condensation process.

The arctic climate depends on the unique high-latitude characteristics of processes such as ice dynamics and persistent low-level clouds. Simulation deficiencies are partly due to coarse model resolution and partly due to inadequate model process descriptions. As mentioned previously, most model formulations are based on low-latitude observations that do not cover the extreme conditions occurring in the Arctic. To validate coupled high-resolution models in the Arctic, improved and extended observational datasets are required. *In situ* observations exist for a few locations and restricted time periods, but more such datasets are needed. To obtain better coverage in space and time, remote sensing instruments are necessary. Several satellite missions are planned that hopefully will provide observational datasets with a much better coverage.

4.7.3. Better representation of the stratosphere in AGCMs

Most current AGCMs are aimed at simulating tropospheric processes, and the stratosphere is only included with a limited resolution. On the other hand, many of the middle atmosphere three-dimensional circulation models describe only the stratosphere and the mesosphere, having a lower boundary at the tropopause (IPCC, 2001). Such models are primarily intended to simulate processes that are internal to the stratosphere, and it is assumed that the interaction with the troposphere can be neglected.

To model current arctic climate and stratospheric and tropospheric ozone concentrations, as well as to project their future changes, AGCMs must describe the troposphere and the stratosphere in comparable detail. Most models assume that all ozone-related processes are located in the stratosphere: ozone and ozone-related species, as well as their photochemical sources and sinks and air transport in the ozone layer (20–30 km average height). However, some of the stratospheric transport features have a tropospheric origin. Two important processes in this regard are planetary wave propagation in the northern mid-latitudes and gravitational wave destruction in the middle and upper stratosphere. While the planetary waves are well-resolved by climate models, gravity-wave drag occurs at small scales and is therefore difficult to simulate with the coarse grids of most current AGCMs. In many AGCMs, these dynamic factors are roughly parameterized by Rayleigh friction at upper model levels. This parameterization also serves the purpose of preventing spurious reflection of vertically propagating gravity waves at the upper boundary. This feature is necessary in a climate model, but in order to resolve vertically propagating waves realistically, more resolution is needed in the middle and upper stratosphere. Austin et al. (1997) demonstrated that the shift from 19 to 49 levels in an AGCM with coupled chemistry considerably improved the ozone and temperature simulation in the winter stratosphere.

The AO is another important feature affecting the stratosphere (Wallace, 2000). The AO is a naturally occurring phenomenon but difficult to project with current GCMs. A gradual increase in the AO positive phase persistence has been observed in recent years (Hoerling et al., 2001; Shindell et al., 2001). While the change may be a natural fluctuation in the AO, it may also be a result of increased atmospheric GHG concentrations. A better resolution of the stratosphere in models is required to determine whether this is the case, and, if it is, whether further increases in GHG concentrations are likely to exert a greater influence on the AO. A change in the AO would also influence the ozone distribution in the arctic stratosphere, giving rise to additional climate-relevant feedbacks in the Arctic. One example could be a change in the latitudinal heating gradient in the stratosphere caused by a change in the ozone distribution. An altered heating gradient would result in a changed temperature gradient, which in turn would change the zonal wind distribution. The zonal wind distribution determines the vertical planetary wave propagation characteristics that in turn affect ozone distribution.

4.7.4. Coupling chemical components to GCMs

Ozone is an important GHG and moderates fluxes of ultraviolet radiation at ground level. In addition to an adequate description of dynamic processes, GCMs must incorporate detailed photochemical components for better simulation of ozone formation and destruction in the atmosphere. Due to the complicated character of ozone photochemistry in the arctic stratosphere, which has significant input from heterogeneous reactions on polar stratospheric cloud (PSC) particle surfaces, the inclusion of the microphysics of particle formation and destruction must be considered. This is omitted in the photochemical components of most present-day GCMs. Instead, the observed spectra of PSC particles is assumed to appear immediately when the air temperature drops below a certain threshold temperature and to disappear at once when the temperature rises above the threshold. The actual delay in the observed PSC effects compared to those modeled indicates the importance of considering PSC microphysics in models, especially in the simulation of arctic ozone "mini-holes" and their rapid evolution in space and time (Austin et al., 2003).

The denitrification of cold polar air in winter is another process in the microphysics of PSC formation and the chemistry that activates ozone-depleting chlorine radicals and repartitioning of bromine species. Polar stratospheric cloud particles that contain liquid nitric acid are supercooled ternary solutions of nitric acid, sulfuric acid, and water. They grow in the stratosphere to nitric acid dihydrate (NAD) and nitric acid trihydrate (NAT) large particles, which remove nitric acid from the stratosphere by gravitational sedimentation and contribute to the denoxification (removal of nitric acid) of the arctic stratosphere. Both NAD and NAT particles are formed intensively at temperatures of 190 to 192 K – the "nucleation window" (Tabazadeh et al., 2001). These

"window temperature" belts are persistent at the periphery of winter polar vortices in the Antarctic for several months, and in the Arctic for about a month, and produce significant denitrified stratospheric layers (Tabazadeh et al., 2001).

This phenomenon as well as the PSC microphysics and chemistry have spatial and temporal scales finer than current GCM and CTM grids can resolve. A suitable parameterization of these effects is needed in addition to an elaboration of the whole photochemical computation scheme. Together with the necessary refinement of the simulation of dynamic processes, these requirements make the problem of arctic ozone modeling computationally demanding and scientifically challenging.

Another atmospheric chemistry aspect of the Arctic is the production of cloud condensation nuclei near the surface and the possible involvement of naturally occurring dimethyl sulfide (DMS) in this process. Dimethyl sulfide particles originate from arctic seawater, and the flux to the atmosphere is thus strongly coupled to the existence of sea ice. It may be that the local arctic production of DMS is a determining factor for droplet size distributions in low clouds and thus may have a significant effect on low-cloud radiative properties. If this is the case, cloud properties would be sensitive to the occurrence of sea ice and a dramatic change in sea-ice distribution would affect the arctic radiative balance. This type of effect, as well as arctic haze effects, whose radiative forcing has been estimated from observations (e.g., Herber et al., 2002; Quinn et al., 2002), need to be included in AGCMs.

4.7.5. Ensemble simulations

A more ambitious strategy for ensemble climate simulations is needed in order to better understand natural climate variability in the Arctic and how it may be affected by global climate change. In discussing the impacts of climate change, changes in the distribution of climatic events are as interesting as changes in the mean. The ACIA used the results of five climate models to study future changes in arctic climate. In order to increase the accuracy of the different error estimates, a larger scenario sample is needed. In numerical weather prediction, experience has shown that a sample involving 50 to 100 simulations with identical models but different initial states gives a reasonable estimate of forecast uncertainties. For arctic climate change, error estimates based on a sample of this size could be adequate. In addition, it would be advantageous to increase model resolution to better capture physical processes and to better describe sharp spatial gradients (fronts), which are often the regions where extreme events occur. Both types of improvement require large additional computing resources. Further research is needed to find a reasonable balance between ensemble size, model resolution, and the complexity of physical process descriptions. For climate simulation ensembles, it is also necessary to perturb model parameters and external forcings. The uncertainty aspects to be addressed thus include natural variability, uncertainties in model sensitivity to prescribed forcings, and uncertainties in the forcings.

Estimates of extreme events and their frequency of occurrence also require ensemble simulations. For precipitation in particular, extreme events are often more interesting than changes in the mean (Palmer and Räisänen, 2002). To obtain reliable estimates of changes in the frequency of extreme events, ensemble simulations are necessary. This is thus an added benefit of climate-change projection ensembles and is required to make projections of changes in storm frequencies or other extreme events. It has recently been shown that an increased GHG forcing could contribute to an increase in intense storm events in particular areas of the North Atlantic Ocean and Western Europe (Van den Brink et al., 2003). At the same time, a decrease in storm frequencies is projected for other regions of the North Atlantic. To arrive at this result, a very large ensemble was used, and in order to achieve that, a simplified atmospheric model (quasi-geostrophic, three vertical levels, and a coarse horizontal resolution) had to be utilized. The drawback of using such a simplified model is that storm dynamics are not described in full detail and storm characteristics have to be derived from empirically based, statistical methods similar to the downscaling technique discussed in section 4.6. Other studies using more advanced model tools but smaller ensembles have not been able to simulate significant increases in storm frequencies (Carnell and Senior, 1998; Knippetz et al., 2000; Lunkeit et al., 1996; Ulbrich and Christoph, 1999).

4.7.6. Conclusions

The general increase in computing resources that have become available for climate system modeling in recent years favors progress in developing new generations of AOGCMs – mostly by adding new components, increasing resolution, and extending ensembles of simulations. Conversely, the Arctic is one of the regions of the world with limited availability of observational data necessary for model validation and evaluation (e.g., Walsh, in press). Nevertheless, it has been shown that model performance can be improved with systematic model improvements and better resolution. For the Arctic, it is necessary to perform climate change simulations involving the entire globe; however, spatial resolution in the Arctic could be improved with the use of regional models driven by global simulations. The ultimate goal is to use as high a resolution as possible over the entire globe. In simulating arctic climate change, sea-ice processes are of primary importance. Boundary-layer fluxes and clouds are closely linked with sea-ice processes. All components require improvements to increase confidence in climate change projections. Expectations for model improvement are increasing because of increasing international activity in the field of model intercomparison exercises (e.g., Puri, 2002; Box 4.2), allowing the iden-

tification of model errors, their causes, and how they may be reduced.

Some scientists doubt that AOGCMs can provide realistic scenarios of future climate change. However, even if present day models have major shortcomings and need to be improved, they still provide useful information about possible changes in the future climate. The models are based on a physical understanding of the climate system and, as such, provide a physically coherent picture of likely climate change. There are very few other methods, if any, which can be used to provide such credible climate change estimates. Statistical methods, other than simple extrapolation of present trends, require a physical model in the background to provide a basis to generate statistically representative estimates of variables that cannot be deduced directly from the physical model. The authors of this chapter are thus confident that future model improvements will provide better estimates of the arctic climate change that may occur as a result of increasing atmospheric GHG concentrations.

There will always be uncertainties in the estimates and some of these uncertainties cannot be reduced below a certain level. These include, for example, uncertainties associated with the lack of observations to provide an accurate initial state for a model simulation, model parameter uncertainties, and the inherent limited predictability of any atmospheric/oceanic simulation (Lorenz, 1963). While the level of uncertainty can be lowered, it will never be certain that all physical processes relevant to climate change have been included in a model simulation. There could still be surprises to come in the understanding of climate change. Solar variability, the effects of cosmic rays, and volcanic eruptions may all contribute more to arctic climate change than is presently thought, but this remains to be seen. As climate change science progresses there will always be new results that could significantly change understanding of how the arctic climate system works; however, the present estimates are based on the best knowledge available today about climate change.

References

Austin, J., N. Butchart and R. Swinbank, 1997. Sensitivity of ozone and temperature to vertical resolution in a GCM with coupled stratospheric chemistry. Quarterly Journal of the Royal Meteorological Society, 123:1405-1431.

Austin, J., D. Shindell, S.R. Beagley, C. Bruhl, M. Damers, E. Manzini, T. Nagashima, P. Newman, S. Pawson, G. Pitari, E. Rozanov, C. Schnadt and T.A. Shepherd, 2003. Uncertainties and assessments of chemistry-climate models of the stratosphere. Atmospheric Chemistry and Physics, 3:1-27.

Bailey, D.A. and A.H. Lynch, 2000a. Development of an Antarctic Regional Climate System Model: Part 1. Sea ice and large-scale circulation. Journal of Climate, 13:1337-1350.

Bailey, D.A. and A.H. Lynch, 2000b. Development of an Antarctic Regional Climate System Model: Part 2. Station validation and surface energy balance. Journal of Climate, 13:1351-1361.

Bailey, D.A., A.H. Lynch and K.S. Hedström, 1997. The impact of ocean circulation on regional polar climate simulations using the Arctic Region Climate System Model. Annals of Glaciology, 25:203-207.

Barthelet, P., L. Terray and S. Valcke, 1998. Transient CO_2 experiment using the ARPEGE/OPAICE non flux corrected coupled model. Geophysical Research Letters, 25:2277-2280.

Benestad, R., 2002. Empirically downscaled multi-model ensemble temperature and precipitation scenarios for Norway. Journal of Climate, 15:3008-3027.

Benestad, R., 2004. Tentative probabilistic temperature scenarios for northern Europe. Tellus A: Dynamic Meteorology and Oceanography, 56:89-101.

Benestad, R., E.J. Forland and I. Hanssen-Bauer, 2002. Empirically downscaled temperature scenarios for Svalbard. Atmospheric Science Letters, 3(2-4):71-93.

Bengtsson, L., V.A. Semenov and O. Johannessen, 2003. The Early Century Warming in the Arctic – A Possible Mechanism. Rep. 345. Max Planck Institute for Meteorology, Hamburg, Germany, 31pp.

Bitz, C., G. Flato and J. Fyfe, 2002. Sea ice response to wind forcing from AMIP models. Journal of Climate, 15:523-535.

Bjørge, D., J.E. Haugen and T.E. Nordeng, 2000. Future Climate in Norway. Dynamical downscaling experiments within the RegClim project. Research Report 103, Norwegian Meteorological Institute, Oslo.

Blenckner, T. and D. Chen, 2003. Comparison of the impact of regional and north-Atlantic atmospheric circulation on an aquatic ecosystem. Climatic Research, 23:131-136.

Boer, G.J., 2000a. Analysis and verification of model climate. In: P. Mote and A. O'Neill (eds.). Numerical Modeling of the Global Atmosphere in the Climate System. NATO Science Series C-550. Kluwer Academic Publishers.

Boer, G.J., 2000b. Climate model intercomparison. In: P. Mote and A. O'Neill (eds.). Numerical Modeling of the Global Atmosphere in the Climate System. NATO Science Series C-550. Kluwer Academic Publishers.

Boer, G.J., N.A. McFarlane and M. Lazare, 1992. Greenhouse gas-induced climate change simulated with the CCC second-generation general circulation model. Journal of Climate, 5:1045-1077.

Boville, B.A. and P.R. Gent, 1998. The NCAR Climate System Model, Version One. Journal of Climate, 11:1115-1130.

Boville, B.A., J.T. Kiehl, P.J. Rasch and F.O. Bryan, 2001. Improvements to the NCAR CSM-1 for transient climate simulations. Journal of Climate, 14:164-179.

Braconnot, P. (ed.), 2000. Paleoclimate Modeling Intercomparison Project (PMIP): Proceedings of the Third PMIP Workshop, La Huardière, Canada, 4-8 October 1999. ICPO Publications Series No. 34, PAGES 2000-1, WMO/TD No. 1007, WCRP Series Report No. 111, 271pp.

Braconnot, P., O. Marti and S. Joussaume, 1997. Adjustment and feedbacks in a global coupled ocean-atmosphere model. Climate Dynamics, 13:507-519.

Broecker, W.S., 1997. Thermohaline circulation, the achilles heel of our climate system: will man-made CO_2 upset the current balance? Science, 278:1582-1588.

Bromwich, D., J. Cassano, T. Klein, G. Heinemann, K. Hines, K. Steffen and J. Box, 2001. Mesoscale modeling of katabatic winds over Greenland with the Polar MM5. Monthly Weather Review, 129(9):2290-2309.

Bryan, K., S. Manabe and R.C. Pacanowski, 1975. A global ocean-atmosphere climate model. II: the oceanic circulation. Journal of Physical Oceanography, 5:30-46.

Bryazgin, N.N., 1976. Yearly mean precipitation in the Arctic region accounting for measurement errors. Proceedings of the Arctic and Antarctic Research Institute, 323:40-74. (In Russian)

Busuioc, A., H. von Storch and R. Schnur, 1999. Verification of GCM-generated regional seasonal precipitation for current climate and of statistical downscaling estimates under changing climate conditions. Journal of Climate, 12:258-272.

Busuioc, A., D. Chen and C. Hellström, 2001a. Performance of statistical downscaling models in GCM validation and regional climate estimates: application for Swedish precipitation. International Journal of Climatology, 21:557-578.

Busuioc, A., D. Chen and C. Hellström, 2001b. Temporal and spatial variability of precipitation in Sweden and its link with the large scale atmospheric circulation. Tellus, 53A(3):348-367.

Carnell, R.E. and C.A. Senior, 1998. Changes in mid-latitude variability due to increasing greenhouse gases and sulphate aerosols. Climate Dynamics, 14:369-383.

Carter, T.R., M.L. Parry, H. Harasawa and S. Nishioka, 1994. IPCC Technical Guidelines for Assessing Climate Change Impacts and Adaptations. Department of Geography, University College, London.

Carter, T.R., M. Hulme, J.F. Crossley, S. Malyshev, M.G. New, M.E. Schlesinger and H. Tuomenvirta, 2000. Climate Change in the 21st Century – Interim Characterizations based on the New IPCC Emissions Scenarios. The Finnish Environment 433, Finnish Environment Institute, Helsinki, 148pp.

Carter, T.R., E.L. La Rovere, R.N. Jones, R. Leemans, L.O. Mearns, N. Nakićenović, A.B. Pittock, S.M. Semenov and J. Skea, 2001. Developing and applying scenarios. In: J.J. McCarthy, O.F. Canziani, N.A. Leary, D.J. Dokken and K.S. White (eds.). Climate Change 2001: Impacts, Adaptation, and Vulnerability. Pp. 145-190. Contribution of Working Group II to the Third Assessment Report of the Intergovernmental Panel on Climate Change. Cambridge University Press.

Cassano, J.J., T.R. Parish and J. King, 2001. Evaluation of turbulent surface flux parameterizations for the stable boundary layer over Halley, Antarctica. Monthly Weather Review, 129:26-46.

Cavazos, T., 1999: Large-scale circulation anomalies conductive to extreme precipitation events and derivation of daily rainfall in northeastern Mexico and southeastern Texas. Journal of Climate, 12:1506-1523.

Chen, D., 2000. A monthly circulation climatology for Sweden and its application to a winter temperature case study. International Journal of Climatology, 20:1067-1076.

Chen, D. and Y. Chen, 1999. Development and verification of a multiple regression downscaling model for monthly temperature in Sweden. In: D. Chen, C. Hellström, Y. Chen (eds.). Preliminary Analysis and Statistical Downscaling of Monthly Temperature in Sweden, pp. 41-55. Report C16, Earth Sciences Centre, University of Gothenburg, Sweden.

Chen, D., and Y. Chen, 2003. Association between winter temperature in China and upper air circulation over East Asia revealed by Canonical Correlation Analysis. Global and Planetary Change, 37:315-325.

Chen, D. and C. Hellström, 1999. The influence of the North Atlantic Oscillation on the regional temperature variability in Sweden: spatial and temporal variations. Tellus, 51A(4):505-516.

Chen, D. and X. Li, 2004. Scale dependent relationship between maximum ice extent in the Baltic Sea and atmospheric circulation. Global and Planetary Change, 41:275-283.

Chen, D. and A. Omstedt, 2002. Using statistical downscaling to quantify the GCM-related uncertainty in regional climate change scenarios: A case study of Swedish precipitation. SWECLIM Newsletter, Swedish Meteorological and Hydrological Institute, Norrköping, Sweden.

Chen, D., C. Achberger, J. Räisänen and C. Hellström, 2001. Using statistical downscaling to quantify the GCM-related uncertainty in regional climate change scenarios: A case study of Swedish precipitation. SWECLIM Newsletter, Swedish Meteorological and Hydrological Institute, Norrköping, Sweden.

Christensen, J.H. and O.B. Christensen, 2003. Severe summer flooding in Europe. Nature, 421:805-806.

Christensen, J.H. and P. Kuhry, 2000. High resolution regional climate model validation and permafrost simulation for the East-European Russian Arctic. Journal of Geophysical Research, 105:29647-29658.

Christensen, J.H., O.B. Christensen, P. Lopez, E. van Meijgaard and M. Botzet, 1996. The HIRHAM4 Regional Atmospheric Climate Model. Danish Meteorological Institute, Scientific Report 96-4.

Christensen, J.H., B. Machenhauer, R.G. Jones, C. Schär, P.M. Ruti, M. Castro and G. Visconti, 1997. Validation of present-day regional climate simulations over Europe: LAM simulations with observed boundary conditions. Climate Dynamics, 13:489-506.

Christensen, J.H., T.R. Carter and F. Giorgi, 2002. PRUDENCE employs new methods to assess European climate change. Eos, Transactions, American Geophysical Union, 83(13):147.

Christensen, O.B., 1999. Relaxation of soil variables in a Regional Climate Model. Tellus, 51A:674-685.

Clair, T.A. and J. Ehrman, 1998. Using neural networks to assess the influence of changing seasonal climates in modifying discharge, dissolved organic carbon, and nitrogen export in eastern Canadian rivers. Water Resources Research, 34(3):447-455.

Clair, T.A., J. Ehrman and K. Higuchi, 1998. Changes to the runoff of Canadian ecozones under a doubled CO_2 atmosphere. Canadian Journal of Fisheries and Aquatic Sciences, 55(11):2464-2477.

Claussen, M., L.A. Mysak, A.J. Weaver, M. Crucifix, T. Fichefet, M.-F. Loutre, S.L. Weber, J. Alcamo, V.A. Alexeev, A. Berger, R. Calov, A. Ganopolski, H. Goosse, G. Lohmann, F. Lunkeit, I.I. Mokhov, V. Petoukhov, P. Stone and Z. Wang, 2002. Earth system models of intermediate complexity: closing the gap in the spectrum of climate system models. Climate Dynamics, 18:579-586.

Conway, D. and P.D. Jones, 1998. The use of weather types and air flow indices for GCM downscaling. Journal of Hydrology, 212:348-361.

Corte-Real, J., X. Zhang and X. Wang, 1995. Large-scale circulation regimes and surface climate anomalies over the Mediterranean. International Journal of Climatology, 15:1135-1150.

Crane, R.G. and B.C. Hewitson, 1998. Doubled CO_2 precipitation changes for the Susquehanna Basin: downscaling from the genesis General Circulation Model. International Journal of Climatology, 18:65-76.

Cubasch, U., K. Hasselmann, H. Höck, E. Maier-Raimer, U. Mikolajewicz, B.D. Santer and R. Sausen, 1992. Time-dependent greenhouse warming computations with a coupled ocean-atmosphere model. Climate Dynamics, 9:55-69.

Cubasch, U., H. von Storch, J. Waszkewitz and E. Zorita, 1996. Estimates of climate change on southern Europe derived from dynamical climate model output. Climate Research, 7:129-149.

Cubasch, U., G.A. Meehl, G.J. Boer, R.J. Stouffer, M. Dix, A. Noda, C.A. Senior, S. Raper and K.S. Yap, 2001. Projections of future climate change. In: J.T. Houghton, Y. Ding, D.J. Griggs, M. Noguer, P.J. van der Linden, X. Dai, K. Maskell and C.A. Johnson (eds.). Climate Change 2001: The Scientific Basis, pp. 526-582. Contribution of Working Group I to the Third Assessment Report of the Intergovernmental Panel on Climate Change. Cambridge University Press.

Curry, J.A. and A.H. Lynch, 2002. Comparing Arctic Regional Climate Models. Eos, Transactions, American Geophysical Union, 83:87.

Curry R., B. Dickson and I. Yashayaev, 2003. A change in the freshwater balance of the Atlantic Ocean over the past four decades. Nature, 426:826-829.

Delworth, T.L. and T.R. Knutson, 2000. Simulation of early 20th century global warming. Science, 287:2246-2250.

Delworth, T.L., R.J. Stouffer, K.W. Dixon, M.J. Spelman, T.R. Knutson, A.J. Broccoli, P.J. Kushner and R.T. Wetherald, 2002. Simulation of climate variability and change by the GFDL R30 coupled climate model. Climate Dynamics, 19(7):555-574.

Denis, B., R. Laprise and D. Cava, 2002. Downscaling ability of one-way nested regional climate models: the big-brother experiment. Climate Dynamics, 18:627-646.

Dethloff, K., A. Rinke, R. Lehmann, J.H. Christensen, M. Botzet and B. Machenhauer, 1996. A regional climate model of the Arctic atmosphere. Journal of Geophysical Research, 101:23401-23422.

Dethloff, K., C. Abegg, A. Rinke, I. Hebestadt and V.F. Romanov, 2001. Sensitivity of Arctic climate simulations to different boundary-layer parameterizations in a regional climate model. Tellus, 53A:1-26.

Dethloff, K., M. Schwager, J.H. Christensen, S. Kiilsholm, A. Rinke, W. Dorn, F. Jung-Rothenhäusler, H. Fischer, S. Kipfstuhl and H. Miller, 2002. Greenland precipitation from ice core estimates and regional climate model simulations. Journal of Climate, 15:2821-2832.

Dickson, B., I. Yashayaev, J. Meincke, B. Turrell, S. Dye and J. Holfort, 2002. Rapid freshening of the deep North Atlantic Ocean over the past four decades. Nature, 416:832-837.

Dorn, W., K. Dethloff, A. Rinke and E. Roeckner, 2003. Competition of NAO regime changes and increasing greenhouse gases and aerosols with respect to Arctic climate projections. Climate Dynamics, 21(5-6): 447-458.

Ehrman, J., K. Higuchi and T.A. Clair, 2000. Backcasting to test the use of neural networks for predicting runoff in Canadian rivers. Canadian Water Resources Journal, 25(3):279-291.

Emori, S., T. Nozawa, A. Abe-Ouchi, A. Numaguti, M. Kimoto and T. Nakajima, 1999. Coupled ocean-atmosphere model experiments of future climate change with an explicit representation of sulfate aerosol scattering. Journal of the Meteorological Society of Japan, 77:1299-1307.

Enke, W. and A. Spekat, 1997. Downscaling climate model outputs into local and regional weather elements by classification and regression. Climate Research, 8:195-207.

Etchevers, P., E. Martin, R. Brown, C. Fierz, Y. Lejeune, E. Bazile, A. Boon, Y.-J. Dai, R. Essery, A. Fernandez, Y. Gusev, R. Jordan, V. Koren, E. Kowalczyck, R. Nasonova, D. Pyles, A. Schlosser, A. Shmakin, T.G. Smirnova, U. Strasser, D. Verseghy, T. Yamazaki and Z.-L. Yang, 2002. SnowMIP, an intercomparison of snow models: first results. In: Proceedings of the International Snow Science Workshop, Penticton, Canada, 29 September - 4 October 2002, 8pp.

Flato, G.M. and G.J. Boer, 2001. Warming asymmetry in climate change experiments. Geophysical Research Letters, 28:195-198.

Flato, G.M., G.J. Boer, W.G. Lee, N.A. McFarlane, D. Ramsden, M.C. Reader and A.J. Weaver, 2000. The Canadian Centre for Climate Modelling and Analysis global coupled model and its climate. Climate Dynamics, 16:451-467.

Folland, C., J. Shukla, J. Kinter and M. Rodwell, 2002. The climate of the twentieth century project. Exchanges (Newsletter of CLIVAR), 7(2):37-39.

Frei, A., J.A. Miller and D.A. Robinson, 2003a. Improved simulations of snow extent in the second phase of the Atmospheric Model Intercomparison Project (AMIP-2). Journal of Geophysical Research, 108:(D12), 4369, doi:10.1029/2002JD003030.

Frei, C., J.H. Christensen, M. Deque, D. Jacob, R.G. Jones and P.L. Vidale, 2003b. Daily precipitation statistics in regional climate models: evaluation and intercomparison for the European Alps. Journal of Geophysical Research, 108: 10.1029/2002JD002287.

Furevik, T., M. Bentsen, H. Drange, I.K.T. Kindem, N.G. Kvamstø and A. Sorteberg, 2003. Description and validation of the Bergen Climate Model: ARPEGE coupled with MICOM. Climate Dynamics, 21:27-51.

Ganopolski, A. and S. Rahmstorf, 2001. Rapid changes of glacial climate simulated in a coupled climate model. Nature, 409:153-158.

Gates, W.L., 1992. AMIP: The Atmospheric Model Intercomparison Project. Bulletin of the American Meteorological Society, 73:1962-1970.

Gates, W.L., J.S. Boyle, C.C. Covey, C.G. Dease, C.M. Doutriaux, R.S. Drach, M. Fiorino, P.J. Gleckler, J.J. Hnilo, S.M. Marlais, T.J. Phillips, G.L. Potter, B.D. Santer, K.R. Sperber, K.E. Taylor and D.N. Williams, 1998. An overview of the results of the Atmospheric Model Intercomparison Project (AMIP). PCMDI Rep. No. 45, UCRL-JC-129928. Program for Climate Model Diagnosis and Intercomparison, Lawrence Livermore National Laboratory, Livermore, CA, 29 pp. + figs.

Gibson, J.K., P. Kållberg, S. Uppala, A. Hernandez, A. Nomura and E. Serrano, 1997. ERA description. ECMWF Reanalysis Project Rep. Series 1. European Centre for Medium Range Weather Forecasts, Reading, UK, 66pp.

Giorgi, F. and L.O. Mearns, 1999. Introduction to special section: Regional climate modeling revisited. Journal of Geophysical Research, 104:6335-6352.

Giorgi, F. and L.O. Mearns, 2003. Probability of regional climate change calculated using the Reliability Ensemble Averaging (REA) method. Geophysical Research Letters, 30(12):311-314.

Giorgi, F., B. Hewitson, J. Christensen, M. Hulme, H. von Storch, P. Whetton, R. Jones, L. Mearns and C. Fu, 2001. Regional climate information – evaluation and projections. In: J.T. Houghton, Y. Ding, D.J. Griggs, M. Noguer, P.J. van der Linden, X. Dai, K. Maskell and C.A. Johnson (eds.). pp. 583-638. Climate Change 2001: The Scientific Basis. Contribution of Working Group I to the Third Assessment Report of the Intergovernmental Panel on Climate Change. Cambridge University Press.

Goodess, C.M. and J.P. Palutikof, 1998. Development of daily rainfall scenarios for southeast Spain using a circulation-type approach to downscaling. International Journal of Climatology, 10:1051-1083.

Gordon, C., C. Cooper, C.A. Senior, H. Banks, J.M. Gregory, T.C. Johns, J.F.B. Mitchell and R.A. Wood, 2000. The simulation of SST, sea ice extents and ocean heat transports in a version of the Hadley Centre coupled model without flux adjustments. Climate Dynamics, 16:147-168.

Hagemann, S. and L. Dümenil, 1998. A parameterization of the lateral water flow for the global scale. Climate Dynamics, 14:17-31.

Hahn, C.J., S.G. Warren and J. London, 1995. The effect of moonlight on observations of cloud cover at night, and applications to cloud climatology. Journal of Climate, 8:1429-1466.

Hanna, E. and P. Valdes, 2001. Validation of ECMWF (re)analysis surface climate data, 1979-1998 for Greenland and implications for mass balance modelling of the ice sheet. International Journal of Climatology, 21(2):171-195.

Hanssen-Bauer, I., 2002. Temperature and precipitation at Svalbard 1900-2050: measurements and scenarios. Polar Record, 38(206):225-232.

Hanssen-Bauer, I. and E.J. Førland, 2001. Verification and analysis of a climate simulation of temperature and pressure fields over Norway and Svalbard. Climate Research, 16:225-235.

Hanssen-Bauer, I., E.J. Førland, J.E. Haugen and O.E. Tveito, 2003. Temperature and precipitation scenarios for Norway: Comparison of results from dynamical and empirical downscaling. Climate Research, 25:15-27.

Harding, R.J., S.-E. Gryning, S. Halldin and C.R. Lloyd, 2001. Progress in understanding of land surface/atmosphere exchanges at high latitudes. Theoretical and Applied Climatology, 70:5-18.

Haugen, J.E., D. Bjørge and T.E. Nordeng, 2000. Dynamic downscaling: further results. RegClim General Technical Report, No.4. Available from the Norwegian Institute for Air Research.

Hellström, C., D. Chen, C. Achberger and J. Räisänen, 2001. Comparison of climate change scenarios for Sweden based on statistical and dynamical downscaling of monthly precipitation. Climate Research, 19:45-55.

Herber, A., L. Thomason, H. Gernandt, U. Leiterer, D. Nagel, K.-H. Schulz, J. Kaptur, T. Albrecht and J. Notholt, 2002. Continuous day and night aerosol optical depth observations in the Arctic between 1991 and 1999. Journal of Geophysical Research, 107(D10):4097, doi: 10.1029/2001JD000536.

Hewitson, B.C. and R.G. Crane, 1996. Climate downscaling: techniques and application. Climate Research, 7:85-95.

Heyden, H., E. Zorita and H. Von Storch, 1996. Statistical downscaling of monthly mean North Atlantic air-pressure to sea level anomalies in the Baltic Sea. Tellus, 48A:312-323.

Heyden, H., H. Fock and W. Greve, 1998. Detecting relationships between interannual variability in ecological time series and climate using a multivariate statistical approach – a case study on Helgoland Road zooplankton. Climate Research, 10:179-191.

Hirst, A., S.P. O'Farrell and H.B. Gordon, 2000. Comparison of a coupled ocean-atmosphere model with and without oceanic eddy-induced advection. Part I: Ocean spinup and control integrations. Journal of Climate, 13:139-163.

Hoerling, M.P., J.W. Hurrell and T. Xu, 2001. Tropical origin for recent North Atlantic climate change. Science, 292:90-92.

Hostetler, S.W., F. Giorgi, G.T. Bates and P.J. Bartlein, 1994. Lake-atmosphere feedbacks associated with paleolakes Bonneville and Lahontan. Science, 263:665-668.

Hunke, E.C. and J.K. Dukowicz, 1997. An elastic-viscous-plastic model for sea ice dynamics. Journal of Physical Oceanography, 27:1849-1867.

Huntingford, C., R.G. Jones, C. Prudhomme, R. Lamb and J.H.C. Gash, 2003. Regional climate model predictions of extreme rainfall for a changing climate. Quarterly Journal of the Royal Meteorological Society, 129:1607-1621.

Huth, R., 1999. Statistical downscaling in central Europe: Evaluation of methods and potential predictors. Climate Research, 13:91-101.

Huth, R. and J. Kysely, 2000. Constructing site-specific climate change scenarios on a monthly scale using statistical downscaling. Theoretical and Applied Climatology, 66:13-27.

IGPO, 2000. GEWEX Cloud System Study (GCSS) Second Science and Implementation Plan. Global Energy and Water Cycle Experiment (GEWEX). International GEWEX Project Office, Document No. 34, 52pp.

IPCC, 1994. IPCC Technical Guidelines for Assessing Climate Change Impacts and Adaptations. Prepared by Working Group II. T.R. Carter, M.L. Parry, H. Harasawa and S. Nishioka (eds.). WMO/UNEP, CGER-IO15-94. Intergovernmental Panel on Climate Change, 59pp.

IPCC, 1996. Climate Change 1995: The Science of Climate Change. Contribution of Working Group I to the Second Assessment Report of the Intergovernmental Panel on Climate Change. J.T. Houghton, L.G. Meira Filho, B.A. Callander, N. Harris, A. Kattenberg and K. Maskell (eds.). Intergovernmental Panel on Climate Change. Cambridge University Press, 572pp.

IPCC, 2001. Climate Change 2001: The Scientific Basis. Contribution of Working Group I to the Third Assessment Report of the Intergovernmental Panel on Climate Change. J.T. Houghton, Y. Ding, D.J. Griggs, M. Noguer, P.J. van der Linden, X. Dai, K. Maskell and C.A. Johnson (eds.). Intergovernmental Panel on Climate Change. Cambridge University Press, 881pp.

IPCC-TGCIA, 1999. Guidelines on the Use of Scenario Data for Climate Impact and Adaptation Assessment. Version 1. Prepared by T.R. Carter, M. Hulme and M. Lal. Intergovernmental Panel on Climate Change, Task Group on Scenarios for Climate and Impact Assessment, 69pp.

Jacob, D. and R. Podzun, 1997. Sensitivity studies with the Regional Climate Model REMO. Meteorology and Atmospheric Physics, 63:119-129.

Johns, T.C., 1996. A description of the second Hadley Centre coupled model (HADCM2). Report No. 71. Hadley Centre for Climate Prediction and Research, UK.

Johns, T.C., R.E. Carnell, J.F. Crossley, J.M. Gregory, J.F.B. Mitchell, C.A. Senior, S.F.B. Tett and R.A. Wood, 1997. The second Hadley Centre coupled atmosphere-ocean GCM: model description, spinup and validation. Climate Dynamics, 13:103-134.

Jones, R.G., J.M. Murphy and M. Noguer, 1995. Simulation of climate change over Europe using a nested regional climate model. I: Assessment of control climate, including sensitivity to location of lateral boundaries. Quarterly Journal of the Royal Meteorological Society, 121:1413-1449.

Jones, R.G., J.M. Murphy, M. Noguer and A.B. Keen, 1997. Simulation of climate change over Europe using a nested regional-climate model. II: comparison of driving and regional model responses to a doubling of carbon dioxide. Quarterly Journal of the Royal Meteorological Society, 123:265-292.

Kaas, E. and P. Frich, 1995. Diurnal temperature range and cloud cover in the Nordic countries: observed trends and estimates for the future. Atmospheric Research, 37:211-228.

Kalnay, E., 2003. Atmospheric Modeling, Data Assimilation and Predictability. Cambridge University Press, 341pp.

Kattsov, V.M. and V.P. Meleshko, 2004. Evaluation of atmosphere-ocean general circulation models used for projecting future climate change. Izvestia, Russian Academy of Sciences – Atmospheric and Oceanic Physics, 40(6):647-658.

Kattsov, V.M. and J.E. Walsh, 2002. Reply to comments on 'Twentieth-century trends of Arctic precipitation from observational data and a climate model simulation' by H. Paeth, A. Hense, and R. Hagenbrock. Journal of Climate, 15:804-805.

Kattsov, V.M., V.P. Meleshko, V.M. Gavrilina, V.A. Govorkova and T.V. Pavlova, 1998. Freshwater budget of the polar regions as simulated with current atmospheric general circulation models. Izvestia Russian Academy of Sciences Phys. Atmos. Ocean, 34:479-489.

Kattsov, V.M., J.E. Walsh, A. Rinke and K. Dethloff, 2000. Atmospheric climate models: simulations of the Arctic Ocean fresh water budget components. In: E.L. Lewis, E.P. Jones, P. Lemke, T.D. Prowse and P. Wadhams (eds.). The Freshwater Budget of the Arctic Ocean, pp. 209-247. Kluwer Academic Publishers.

Kattsov, V.M., S.V. Vavulin, V.A. Govorkova and T.V. Pavlova, 2003. Scenarios of the Arctic climate change in the 21st century. Russian Meteorology and Hydrology, 10:5-19.

Katz, R.W. and M.B. Parlange, 1996. Mixtures of stochastic processes: applications to statistical downscaling. Climate Research, 7:185-193.

Källén, E., V. Kattsov, J. Walsh and E. Weatherhead, 2001. Report from the Arctic Climate Impact Assessment Modeling and Scenarios Workshop. Stockholm, January 29-31 2001. 35pp.

Khrol, V.P. (ed.), 1996. Atlas of Water Balance of the Northern Polar Area. Gidrometeoizdat, St. Petersburg, 81pp.

Kidson, J.W. and C.S. Thompson, 1998. Comparison of statistical and model-based downscaling techniques for estimating local climate variations. Journal of Climate, 11:735-753.

Kiilsholm, S., J.H. Christensen, K. Dethloff and A. Rinke, 2003. Net accumulation of the Greenland Ice Sheet: Modelling Arctic regional climate change. Geophysical Research Letters, 30, 10.1029/2002GL015742.

Kistler, R., E. Kalnay, W. Collins, S. Saha, G. White, J. Woollen, M. Chelliah, W. Ebisuzaki, M. Kanamitsu, V. Kousky, H. van den Dool, R. Jenne and M. Fiorino, 2001. The NCEP-NCAR 50-year reanalysis: Monthly means CD-ROM and documentation. Bulletin of the American Meteorological Society, 82:247-268.

Knippetz, P., U. Ulbrich and P. Speth, 2000. Changing cyclones and surface wind speeds over the North Atlantic and Europe in a transient GHG experiment. Climate Research, 15:109-122.

Knutson, T.R., T.L. Delworth, K.W. Dixon and R.J. Stouffer, 1999. Model assessment of regional surface temperature trends (1949-1997). Journal of Geophysical Research, 104:30981-30996.

Langley Atmospheric Sciences Data Center, 1983-1991. Langley Eight-Year Shortwave and Longwave Surface Radiation Budget Dataset, July 1983-June 1991. NASA. (CD-ROM)

Laprise, R., D. Caya, M. Giguère, G. Bergeron, H. Côte, J.-P. Blanchet, G.J. Boer and N.A. McFarlane, 1998. Climate and climate change in western Canada as simulated by the Canadian regional climate model. Atmosphere-Ocean, 36:119-167.

Legates, D.R. and C.L. Willmott, 1990. Mean seasonal and spatial variability in gauge-corrected global precipitation. International Journal of Climatology, 10:111-133.

Leggett, J.W., J. Pepper and R.J. Swart, 1992. Emission scenarios for the IPCC: an update. In: J.T. Houghton, B.A. Callander and S.K. Varney (eds.). Climate Change 1992. The Supplementary Report to the IPCC Scientific Assessment, pp. 69-95. Cambridge University Press.

Lemke, P., W.D. Hibler III, G.M. Flato, M. Harder and M. Kreyscher, 1997. On the improvement of sea-ice models for climate simulations: The sea-ice model intercomparison project. Annals of Glaciology, 25:183-187.

Linderson, M-L., C. Achberger and D. Chen, 2004. Statistical downscaling and scenario construction of precipitation in Scania, southern Sweden. Nordic Hydrology, 35(3):261-278.

Lorenz, E.N., 1963. The predictability of hydrodynamic flow. Transactions of the New York Academy of Sciences, Series II, 25:409-432.

Lunkeit, F., M. Ponater, R. Sausen, M. Sogalla, U. Ulbrich and M. Windelband, 1996. Cyclonic activity in a warmer climate. Beitrage zur Physik der Atmosphare, 69:393-407.

Lynch, A.H., W.L. Chapman, J.E. Walsh and G. Weller, 1995. Development of a regional climate model of the western Arctic. Journal of Climate, 8:1555-1570.

Lynch, A.H., M.F. Glück, W.L. Chapman, D.A. Bailey and J.E. Walsh, 1997. Remote sensing and climate modeling of the St. Lawrence Is. Polynya. Tellus, 49A:277-297.

Lynch, A.H., D.L. McGinnes and D.A. Bailey, 1998. Snow-albedo and the spring transition in a regional climate system model: influence of land surface model. Journal of Geophysical Research, 103:29037-29049.

Lynch, A.H., J.A. Maslanik and W. Wu, 2001. Mechanisms in the development of anomalous sea ice extent in the western Arctic: A case study. Journal of Geophysical Research, 106:28097-28105.

Mabuchi, K., Y. Sato and H. Kida, 2000. Numerical study of the relationships between climate and the carbon dioxide cycle on a regional scale. Journal of the Meteorological Society of Japan, 78:25-46.

Machenhauer, B., M. Windelband, M. Botzet, R. Jones and M. Deque, 1996. Validation of present-day regional climate simulations over Europe: Nested LAM and variable resolution global model simulations with observed or mixed layer ocean boundary conditions. MPI Report 191. Max Planck Institute for meteorology, Hamburg.

Machenhauer, B., J. Windelband, M. Botzet, J.H. Christensen, M. Deque, R. Jones, P.M. Ruti and G. Visconti, 1998. Validation and analysis of regional present-day climate and climate change simulations over Europe. MPI Report 275. Max Planck Institute for meteorology, Hamburg.

Majewski, D., D. Liermann, P. Prohl, B. Ritter, M. Buchhold, T. Hanisch, G. Paul, W. Wergen and J. Baumgardner, 2002. The operational global Icosahedral-Hexagonal Gridpoint Model GME: description and high-resolution tests. Monthly Weather Review, 130:319-338.

Mahrt, L., 1998: Stratified atmospheric boundary layers and breakdown of models. Theoretical and Computational Fluid Dynamics, 11:263-279.

Manabe, S. and R.J. Stouffer, 1997. Coupled ocean-atmosphere model response to freshwater input: comparision to Younger Dryas event. Paleoceanography, 12:321-336.

Manabe, S. and R.T. Wetherald, 1975. The effects of doubling the CO_2 concentration on the climate of a general circulation model. Journal of Atmospheric Sciences, 32:3-15.

Manabe, S., R.J. Stouffer, M.J. Spelman and K. Bryan, 1991. Transient responses of a coupled ocean-atmosphere model to gradual changes of atmospheric CO_2. Part I: Annual mean response. Journal of Climate, 4:785-818.

Martin, E., B. Timbal and E. Brun, 1997. Downscaling of general circulation model output: simulation of snow climatology of the French Alps and sensitivity to climate change. Climate Dynamics, 13:45-56.

Maslanik, J.A., M.C. Serreze and R.G. Barry, 1996: Recent decreases in Arctic summer ice cover and linkage to atmospheric circulation anomalies. Geophysical research Letters, 23:1677-1680.

Maslanik, J.A., A.H. Lynch, M.C. Serreze and W. Wu, 2000. A case study of regional climate anomalies in the Arctic: performance requirements for a coupled model. Journal of Climate, 13:383-401.

McAvaney, B.J., C. Covey, S. Joussaume, V. Kattsov, A. Kitoh, W. Ogana, A.J. Pitman, A.J. Weaver, R.A. Wood and Z.-C. Zhao, 2001. Model evaluation. In: J.T. Houghton, Y. Ding, D.J. Griggs, M. Noguer, P.J. van der Linden, X. Dai, K. Maskell and C.A. Johnson (eds.). pp. 471-524. Climate Change 2001: The Scientific Basis. Contribution of Working Group I to the Third Assessment Report of the Intergovernmental Panel on Climate Change. Cambridge University Press.

McGregor, J.L., J.J. Katzfey and K.C. Nguyen, 1999. Recent regional climate modelling experiments at CSIRO. In: H. Ritchie (ed.). Research Activities in Atmospheric and Oceanic Modelling, pp. 7.37-7.38. CAS/JSC Working Group on Numerical Experimentation Report 28. WMO/TD - No. 942. World Meteorological Organization, Geneva.

Mearns, L.O., M. Hulme, T.R. Carter, R. Leemans, M. Lal and P. Whetton, 2001. Climate scenario development. In: J.T. Houghton, Y. Ding, D.J. Griggs, M. Noguer, P.J. van der Linden, X. Dai, K. Maskell and C.A. Johnson (eds.). pp. 739-768. Climate Change 2001: The Scientific Basis. Contribution of Working Group I to the Third Assessment Report of the Intergovernmental Panel on Climate Change. Cambridge University Press.

Meehl, G.A., G.J. Boer, C. Covey, M. Latif and R.J. Stouffer, 2000. The Coupled Model Intercomparison Project (CMIP). Bulletin of the American Meteorological Society, 81:313-318.

Meleshko, V.P., V.M. Kattsov, V.A. Govorkova, S.P. Malevsky-Malevich, E.D. Nadyozhina and P.V. Sporyshev, 2004. Anthropogenic climate changes in the 21st century in Northern Eurasia. Russian Meteorology and Hydrology, 7:5-26.

Murphy, J., 1999. An evaluation of statistical and dynamical techniques for downscaling local climate. Journal of Climate, 12:2256-2284.

Murphy, J., 2000. Predictions of climate change over Europe using statistical and dynamical downscaling techniques. International Journal of Climatology, 20:489-501.

Murray, R.J., 1996. Explicit generation of orthogonal grids for ocean models. Journal of Computational Physics, 126:251-273.

Nakićenović, N. and R. Swart (eds.), 2000. Intergovernmental Panel on Climate Change, Special Report on Emissions Scenarios. Cambridge University Press, 599pp.

NAST, 2001. Climate Change Impacts on the United States: The Potential Consequences of Climate Variability and Change. National Assessment Synthesis Team, Report for the US Global Change Research Program. Cambridge University Press, 620pp.

Nelson, F.E. and S.I. Outcalt, 1987. A computational method for prediction and regionalization of permafrost. Arctic and Alpine Research, 19:279-288.

New, M., M. Hulme and P. Jones, 1999. Representing twentieth-century space-time climate variability. Part I: Development of a 1961-90 mean monthly terrestrial climatology. Journal of Climate, 12:829-856.

New, M., M. Hulme and P. Jones, 2000. Representing twentieth-century space-time climate variability. Part II: Development of 1901-96 monthly grids of terrestrial surface climate. Journal of Climate, 13:2217-2238.

Noguer, M., R. Jones and J. Murphy, 1998. Sources of systematic errors in the climatology of a regional climate model over Europe. Climate Dynamics, 14:691-712.

Nozawa, T., S. Emori, T. Takemura, T. Nakajima, A. Numaguti, A. Abe-Ouchi and M. Kimoto, 2000. Coupled ocean-atmosphere model experiments of future climate change based on IPCC SRES scenarios. Preprints, Eleventh Symposium on Global Change Studies, 9-14 January 2000, Long Beach, California, pp. 352-355.

Omstedt, A. and D. Chen, 2001. Influence of atmospheric circulation on the maximum ice extent in the Baltic Sea. Journal of Geophysical Research, 106(C3):4493-4500.

Otterå, O.H., H. Drange, M. Bentsen, N.G. Kvamstø and D. Jiang, 2003: The sensitivity of the present day Atlantic meridional overturning circulation to freshwater forcing. Geophysical Research Letters, 30: 1898, doi:101029/2003GL017578.

Pacanowski, R.C. and S.M. Griffies, 1999. The MOM 3 Manual. Geophysical Fluid Dynamics Laboratory/NOAA, Princeton, New Jersey, 680pp.

Palmer, T.N. and J. Räisänen, 2002. Quantifying the risk of extreme seasonal precipitation events in a changing climate. Nature, 415:512-514.

Palutikof, J.P., C.M. Goodess, S.J. Watkins and T. Holt, 2002. Generating daily rainfall and temperature scenarios at multiple sites: Examples from the Mediterranean. Journal of Climate, 15:3529-3548.

Paterson, A.B. and N. Reeh, 2001. Thinning of the ice sheet in north-west Greenland over the past forty years. Nature, 414:60-62.

Peterson, B.J., R.M. Holmes, J.W. McClelland, C.J. Vörösmarty, R.B. Lammers, A.I. Shiklomanov, I.A. Shiklomanov and S. Rahmstorf, 2002. Increasing river discharge to the Arctic Ocean. Science, 298:2171-2173.

Polyakov, I. and M. Johnson, 2000. Arctic decadal and interdecadal variability. Geophysical Research Letters, 24:4097-4100.

Polyakov, I., S.-I. Akasofu, U. Bhatt, R. Colony, M. Ikeda, A. Makshtas, C. Swingley, D. Walsh and J. Walsh, 2002a. Trends and variations in Arctic climate system. Eos, Transactions, American Geophysical Union, 83(47):547-548.

Polyakov, I., G. Alekseev, R. Bekryaev, U. Bhatt, R. Colony, M. Johnson, V. Karklin, A. Makshtas, D. Walsh and A. Yulin, 2002b. Observationally based assessment of polar amplification of global warming. Geophysical Research Letters, 29(18):1878-1881.

Poulus, G.S., and S.P. Burns, 2003. An evaluation of bulk Ri-based surface layer flux formulas for stable and very stable conditions with intermittent turbulence. Journal of Atmospheric Science, 60:2523-2537.

Power, S.B., R.A. Colman, B.J. McAvaney, R.R. Dahni, A.M. Moore and N.R. Smith, 1993. The BMRC coupled atmosphere/ocean/sea-ice model. Bureau of Meteorology Research Centre, Research Rep. 37. Melbourne, 58pp.

Proshutinsky, A., M. Steele, J. Zhang, G. Holloway, N. Steiner, S. Hakkinen, D. Holland, R. Gerdes, C. Koeberle, M. Karcher, M. Johnson, W. Maslowski, W. Walczowski, W. Hibler and J. Wang, 2001. Multinational effort studies differences among Arctic Ocean models. Eos, Transactions, American Geophysical Union, 82(637):643-644.

Puri, K., 2002. Activities of the CAS/JSC Working Group on Numerical Experimentation (WGNE). In: H. Ritchie (ed.). Research Activities in Atmospheric and Oceanic Modelling. Report No. 32, WMO/TD-No. 1105.

Qian, Y. and F. Giorgi, 1999. Interactive coupling of regional climate and sulfate aerosol models over East Asia. Journal of Geophysical Research, 104:6501-6514.

Quinn, P.K., T.L. Miller, T.S. Bates, J.A. Ogren, E. Andrews and G.E. Shaw, 2002. A 3-year record of simultaneously measured aerosol chemical and optical properties at Barrow, Alaska. Journal of Geophysical Research, 107(D11):4130, doi:10.1029/2001JD001248.

Randall, D., J. Curry, D. Battisti, G. Flato, R. Grumbine, S. Hakkinen, D. Martinson, R. Preller, J. Walsh and J. Weatherly, 1998. Status of and outlook for large-scale modeling of atmosphere-ice-ocean interactions in the Arctic. Bulletin of the American Meteorological Society, 79:197-219.

Räisänen, J., 2001. CO_2-induced climate change in the Arctic area in the CMIP2 experiments. SWECLIM Newsletter, 11:23-28.

Räisänen, J. and R. Döscher, 1999. Simulation of present-day climate in Northern Europe in the HadCM2 GCM. Reports on Meteorology and Climatology, No. 48. Swedish Meteorological and Hydrological Institute.

Räisänen, J. and T.N. Palmer, 2001. A probability and decision-model analysis of a multi-model ensemble of climate change simulations. Journal of Climate, 14:3212-3226.

Räisänen, J., M. Rummukainen, A. Ullerstig, B. Bringfelt, U. Hansson and U. Willén, 1999. The first Rossby Centre regional climate scenario – dynamical downscaling of CO_2-induced climate change in the HadCM2 GCM. Reports on Meteorology and Climatology, No. 85, Swedish Meteorological and Hydrological Institute, 56pp.

Räisänen, J., U. Hansson, A. Ullerstig, R. Döscher, L.P. Graham, C. Jones, M. Meier, P. Samuelsson and U. Willén, 2003. GCM driven simulations of recent and future climate with the Rossby Centre coupled atmosphere Baltic Sea regional climate model RCAO. Reports on Meteorology and Climatology, No. 101, Swedish Meteorological and Hydrological Institute, 61pp.

Rind, D., P. deMenocal, G. Russell, S. Sheth, D. Collins, G. Schmidt and J. Teller, 2001. Effects of glacial meltwater in the GISS coupled atmosphere-ocean model 1. North Atlantic Deep Water response. Journal of Geophysical Research, 16:27335-27353.

Rinke, A., A.H. Lynch and K. Dethloff, 2000. Intercomparison of Arctic regional climate simulations: case studies of January and June 1990. Journal of Geophysical Research, 105:29669-29683.

Rinke, A., R. Gerdes, K. Dethloff, T. Kandlbinder, M. Karcher, F. Kauker, S. Frickenhaus, C. Köberle and W. Hiller, 2003. A case study of the anomalous Arctic sea ice conditions during 1990: insight from coupled and uncoupled regional climate model simulations. Journal of Geophysical Research, 108 (D9),4275, doi:10.1029/2002JD003146.

Roeckner, E., J.M. Oberhuber, A. Bacher, M. Christoph and I. Kirchner, 1996. ENSO variability and atmospheric response in a global coupled atmosphere-ocean GCM. Climate Dynamics, 12:737-754.

Roeckner, E., L. Bengtsson, J. Feichter, J. Lelieveld and H. Rodhe, 1999. Transient climate change simulations with a coupled atmosphere-ocean GCM including the tropospheric sulfur cycle. Journal of Climate, 12:3004-3032.

Roed, L.P., X.B. Shi and B. Hackett, 2000. The Importance of Allowing Turbulent and Diffusive Diapycnal Mixing in Isopycnic Coordinate Ocean Models. RegClim General Tech. Rep. 4, 139-148. Available from the Norwegian Institute for Air Research.

Rummukainen, M., J. Räisänen, B. Bringfelt, A. Ullerstig, A. Omstedt, U. Willén, U. Hansson and C. Jones, 2001. A regional climate model for northern Europe: model description and results from the downscaling of two GCM control simulations. Climate Dynamics, 17:339-359.

Ruosteenoja, K., T.R. Carter, K. Jylhä and H. Tuomenvirta, 2003. Future climate in world regions: an intercomparison of model-based projections for the new IPCC emissions scenarios. The Finnish Environment 644, Finnish Environment Institute.

Russell, G.L. and D. Rind, 1999. Response to CO_2 transient increase in the GISS coupled model: regional coolings in a warmer climate. Journal of Climate, 12:531-539.

Rysgaard, S., T. Vang, M. Stjernholm, B. Rasmussen, A. Windelin and S. Kiilsholm, 2003. Physical conditions, carbon transport and climate change impacts in a NE Greenland fjord. Arctic, Antarctic and Alpine Research, 35(3):301-312.

Sadourny, R., A. Arakawa and Y. Mintz, 1968. Integration of the nondivergent barotropic equation with an icosahedral hexagonal grid on the sphere. Monthly Weather Review, 96:351-356.

Sailor, D.J. and X. Li, 1999. A semiempirical downscaling approach for predicting regional temperature impacts associated with climatic change. Journal of Climate, 12:103-114.

Santer, B.D., T.M.L. Wigley, M.E. Schlesinger and J.F.B. Mitchell, 1990. Developing climate scenarios from equilibrium GCM results. MPI Rep. 47, Max Planck Institute for Meteorology, Hamburg, 29pp.

Sausen, R., K. Barthel and K. Hasselmann, 1987. A flux correction method for removing the climate drift of climate models. Report No. 1. Max Planck Institute for Meteorology, 39pp.

Schiller, A., U. Mikolajewicz and R. Voss, 1997. The stability of the North Atlantic thermohaline circulation in a coupled ocean-atmosphere general circulation model. Climate Dynamics, 13:325-347.

Schnur, R. and D. Lettenmaier, 1997. A case study of statistical downscaling in Australia using weather classification by recursive partitioning. Journal of Hydrology, 211:362-379.

Schoof, J.T. and S.C. Pryor, 2001. Downscaling temperature and precipitation: A comparison of regression-based methods and artificial neural networks. International Journal of Climatology, 21:773-790.

Schrum, C., U. Huebner, D. Jacob and R. Podzun, 2001. A coupled atmosphere/ice/ocean model for the North Sea and the Baltic Sea. Berichte aus dem Zentrum für Meeres- und Klimaforschung Nr. 41, Reihe B: Ozeanographie. Inst. Meereskunde, Hamburg.

Schubert, S., 1998. Downscaling local extreme temperature changes in south-eastern Australia from the CSIRO MARK2 GCM. International Journal of Climatology, 18:1419-1439.

Schweiger, A.J., R.W. Lindsay, J.R. Key and J.A. Francis, 1999. Arctic clouds in multiyear satellite data sets. Geophysical Research Letters, 26:1845-1848.

Semenov, M.A. and E. Barrow, 1997. Use of stochastic weather generator in the development of climate change scenarios. Climatic Change, 35:397-414.

Semenov, M.A., R.J. Brooks, E.M. Barrow and C.W. Richardson, 1998. Comparison of the WGEN and LARS-WG stochastic weather generators for diverse climates. Climate Research, 10:95-107.

Shindell, D.T., G.A. Schmidt, R.L. Miller and D. Rind, 2001. Northern Hemisphere winter climate response to greenhouse gas, ozone, solar, and volcanic forcing. Journal of Geophysical Research, 106:7193-7210.

Small, E.E., F. Giorgi and L.C. Sloan, 1999a. Regional climate model simulation of precipitation in central Asia: Mean and interannual variability. Journal of Geophysical Research, 104:6563-6582.

Small, E.E., L.C. Sloan, S. Hostetler and F. Giorgi, 1999b. Simulating the water balance of the Aral Sea with a coupled regional climate-lake model. Journal of Geophysical Research, 104:6583-6602.

Smith, J.B., M. Hulme, J. Jaagus, S. Keevallik, A. Mekonnen and K. Hailemariam, 1998. Climate change scenarios. In: J.F. Feenstra, I. Burton, J. Smith and R.S.J. Tol (eds.). Handbook on Methods for Climate Change Impact Assessment and Adaptation Strategies, pp. 3-1 - 3-40. Version 2.0. United Nations Environment Programme and Institute for Environmental Studies, Vrije Universiteit, Amsterdam.

Solman, S.A. and M.N. Nuñez, 1999. Local estimates of global climate change: A statistical downscaling approach. International Journal of Climatology, 19:835-861.

Stendel, M., T. Schmith, E. Roeckner and U. Cubasch, 2000. The climate of the 21st century: transient simulations with a coupled atmosphere-ocean general circulation model. Danish Climate Centre Report 00-6, 51pp.

Stocker, T.F., G.K.C. Clarke, H. Le Treut, R.S. Lindzen, V.P. Meleshko, R.K. Mugara, T.N. Palmer, R.T. Pierrehumbert, P.J. Sellers, K.E. Trenberth and J. Willebrand, 2001. Physical climate processes and feedbacks. In: J.T. Houghton, Y. Ding, D.J. Griggs, M. Noguer, P.J. van der Linden, X. Dai, K. Maskell and C.A. Johnson (eds.), pp. 418-470. Climate Change 2001: The Scientific Basis. Contribution of Working Group I to the Third Assessment Report of the Intergovernmental Panel on Climate Change. Cambridge University Press.

Stott, P., 2003: Attribution of regional-scale temperature changes to anthropogenic and natural causes. Geophysical Research Letters, 30(14): 1728, doi:10.1029/2003GL017324.

Stott, P.A., S.F.B. Tett, G.S. Jones, M.R. Allen, J.F.B. Mitchell and G.J. Jenkins, 2000. External control of twentieth century temperature variations by natural and anthropogenic forcings. Science, 15:2133-2137.

Stouffer, R.J. and K.W. Dixon, 1998. Initialization of coupled models for use in climate studies. In: A. Staniforth (ed.). Research Activities in Atmospheric and Oceanic Modelling, pp. I.1-I.15. Rep. 27, WMO/TD-No. 865.

Tabazadeh, A., E.J. Jensen, O.B. Toon, K. Drdla and M.R. Schoeberl, 2001. Role of the stratospheric polar freezing belt in denitrification. Science, 291:2591-2594.

Takahashi, M., 1999. Simulation of the quasibiannial oscillation in a general circulation model. Geophysical Research Letters, 26, 1307-1310.

Takle, E.S., W.J. Gutowski, R.W. Arritt, Z. Pan, C.J. Anderson, R.S. da Silva, D. Caya, S.-C. Chen, F. Giorgi, J.H. Christensen, S.-Y. Hong, H.-M.H. Juang, J. Katzfey, W.M. Lapenta, R. Laprise, P. Lopez, G.E. Liston, J. McGregor, A. Pielke and J.O. Roads, 1999. Project to intercompare regional climate simulation (PIRCS): Description and initial results. Journal of Geophysical Research, 104:19443-19461.

Tao, X., J.E. Walsh and W.L. Chapman, 1996. An assessment of global climate model simulations of Arctic air temperatures. Journal of Climate, 9:1060-1076.

Tett, S.F.B., G.S. Jones, P.A. Stott, D.C. Hill, J.F.B. Mitchell, M.A. Allen, W.J. Ingram, T.C. Johns, C.E. Johnson, A. Jones, D.L. Roberts, D.M.H. Sexton and M.J. Woodage, 2000. Estimation of Natural and Anthropogenic Contributions to 20th Century. Hadley Centre Tech Note 19. Hadley Centre for Climate Prediction and Response, UK, 52pp.

Tokioka, T., A. Noda, A. Kitoh, Y. Nikaidou, S. Nakagawa, T. Motoi, S. Yukimoto and K. Takata, 1995. A transient CO_2 experiment with the MRI CGCM. Quick Report. Journal of the Meteorological Society of Japan, 73(4):817-826.

Trenberth, K. (ed.), 1992. Climate System Modelling. Cambridge University Press, 788pp.

Tsvetsinskaya, E., L.O. Mearns and W.E. Easterling, 2000. Effects of plant growth and development on interannual variability in mesoscale atmospheric simulations. In: Proceedings of the Tenth International Offshore and Polar Engineering Conference. Vol. I, pp. 729-736. International Society of Offshore and Polar Engineers, Cupertino, California.

Ulbrich, U. and M. Christoph, 1999. A shift of the NAO and increasing storm track activity over Europe due to anthropogenic greenhouse gas forcing. Climate Dynamics, 15:551-559.

Van den Brink, H.W., G.P. Konnen and J.D. Opsteegh, 2003. The reliability of extreme surge levels, estimated from observational records of order of hundred years. Journal of Coastal Research, 19:376-388.

Vellinga, M., R.A. Wood and J.M. Gregory, 2002. Processes governing the recovery of a perturbed thermohaline circulation in HadCM3. Journal of Climate, 15:764-780.

von Storch, H., 1999. The global and regional climate system. In: H. von Storch and G. Flöser (eds.). Anthropogenic Climate Change, pp. 3-36. Springer Verlag.

Voss, R., R. Sausen and U. Cubasch, 1998. Periodically synchronously coupled integrations with the atmosphere-ocean general circulation model ECHAM3/LSG. Climate Dynamics, 14:249-266.

Wallace, J.M., 2000. North Atlantic Oscillation/annular mode: Two paradigms – one phenomenon. Quarterly Journal of the Royal Meteorological Society, 126:729-805.

Walsh, J.E., in press. Summary of a workshop on modeling the Arctic atmosphere, Madison, Wisconsin, 20-22 May 2002. Bulletin of the American Meteorological Society.

Walsh, J.E., V. Kattsov, D. Portis and V. Meleshko, 1998. Arctic precipitation and evaporation: model results and observational estimates. Journal of Climate, 11:72-87.

Walsh, J.E., V. Kattsov, W. Chapman, V. Govorkova and T. Pavlova, 2002. Comparison of Arctic climate simulations by uncoupled and coupled global models. Journal of Climate, 15:1429-1446.

Washington, W.M., J.W. Weatherly, G.A. Meehl, A.J. Semtner Jr., T.W. Bettge, A.P. Graig, W.G. Strand Jr., J. Arblaster, V.B. Wayland, R. James and Y. Zhang, 2000. Parallel climate model (PCM) control and transient simulations. Climate Dynamics, 16:755-774.

WCRP, 2002. WOCE/CLIVAR, 2002: WOCE/CLIVAR Working Group on Ocean Model Development. Report of the Third Session. World Climate Research Programme, Informal Rep. No. 14/2002.

Weisse, R., H. Heyen and H. von Storch, 2000. Sensitivity of a regional atmospheric model to a sea state-dependent roughness and the need for ensemble calculations. Monthly Weather Review, 128:3631-3642.

Wilby, R.L. and T.M.L. Wigley, 1997. Downscaling general circulation model output: a review of methods and limitations. Progress in Physical Geography, 21:530-548.

Wilby, R.L. and T.M.L. Wigley, 2000. Precipitation predictors for downscaling: observed and general circulation model relationships. International Journal of Climatology, 20:641-661.

Wilby, R.L., T.M.L. Wigley, D. Conway, P.D. Jones, B.C. Hewitson, J. Main and D.S. Wilks, 1998. Statistical downscaling of general circulation model output: A comparison of methods. Water Resources Research, 34:2995-3008.

Wilby, R.L., C.W. Dawson and E.M. Barrow, 2002. SDSM – a decision support tool for the assessment of regional climate change impacts. Environmental Modelling and Software, 17:145-157.

Wilks, D., 1999. Multisite downscaling of daily precipitation with a stochastic weather generator. Climate Research, 11:125-136.

Yukimoto, S., M. Endoh, Y. Kitamura, A. Kitoh, T. Motoi and A. Noda, 2000. ENSO-like interdecadal variability in the Pacific Ocean as simulated in a coupled GCM. Journal of Geophysical Research, 105(D10):13945-13963.